

RENEWABLE ENERGY
POWER SYSTEM
MODULAR
SIMULATOR

RPM-SIM _____
User's Guide

By

Jan T. Białasiewicz, Ph.D., P.E.
Eduard Muljadi, Ph.D.
R. Gerald Nix, Ph.D., P.E.
Stephen Drouilhet, P.E.



NREL

National Renewable Energy Laboratory

1617 Cole Boulevard
Golden, Colorado 80401-3393

NREL is a U.S. Department of Energy Laboratory
Operated by Midwest Research Institute • Battelle • Bechtel

Contract No. DE-AC36-98-GO10337

RENEWABLE ENERGY
POWER SYSTEM
MODULAR
SIMULATOR

RPM-SIM

User's Guide

By

Jan T. Białasiewicz, Ph.D., P.E.
Eduard Muljadi, Ph.D.
R. Gerald Nix, Ph.D., P.E.
Stephen Drouilhet, P.E.



NREL

National Renewable Energy Laboratory

1617 Cole Boulevard
Golden, Colorado 80401-3393

NREL is a U.S. Department of Energy Laboratory
Operated by Midwest Research Institute • Battelle • Bechtel

Contract No. DE-AC36-98-GO10337

DISCLAIMER, COPYRIGHT, AND USER NOTICE

COPYRIGHT STATUS: The National Renewable Energy Laboratory (NREL) is operated for the U.S. Department of Energy by the Midwest Research Institute (MRI). MRI-authored software is sponsored by the U.S. Department of Energy under Contract DE-AC36-99-GO10337. Accordingly, with respect to such software, the U.S. Government and others acting on its behalf retain a paid-up, nonexclusive, irrevocable, worldwide license to reproduce, prepare derivative works, distribute copies to the public, and perform publicly and display publicly, by or on behalf of the U.S. Government.

USER: This software, including any modules and subprograms, data, and information are provided as a service to the public free of charge. Although the software was created with care, the User assumes full responsibility for its use and uses the software at the User's risk. MRI may make changes to the software provided herein, but has no obligation to modify the software, to continue future development of the software, or to support and maintain the software.

DISCLAIMER OF ENDORSEMENT: Reference herein to any specific commercial products, process, or service by trade name, trademark, manufacturer, or otherwise, does not necessarily constitute or imply its endorsement, recommendation, or favoring by the U.S. Government or MRI. The views and opinions of authors expressed in the information and data involving the software do not necessarily state or reflect those of the U.S. Government or MRI.

DISCLAIMER OF LIABILITY: THE SOFTWARE, DATA AND INFORMATION ARE PROVIDED "AS IS." NEITHER THE U.S. GOVERNMENT NOR MRI NOR ANY OF THEIR EMPLOYEES, MAKES ANY WARRANTY, EXPRESS OR IMPLIED, INCLUDING THE WARRANTIES OF MERCHANTABILITY AND FITNESS FOR PARTICULAR PURPOSE, OR ASSUMES ANY LEGAL LIABILITY OR RESPONSIBILITY FOR THE ACCURACY, COMPLETENESS, OR USEFULNESS OF ANY SUCH SOFTWARE, OR OF ANY INFORMATION, APPARATUS, PRODUCT, OR PROCESS DISCLOSED, OR REPRESENTS THAT ITS USE WOULD NOT INFRINGE PRIVATELY OWNED RIGHTS.

NOTICE

This report was prepared as an account of work sponsored by an agency of the United States government. Neither the United States government nor any agency thereof, nor any of their employees, makes any warranty, express or implied, or assumes any legal liability or responsibility for the accuracy, completeness, or usefulness of any information, apparatus, product, or process disclosed, or represents that its use would not infringe privately owned rights. Reference herein to any specific commercial product, process, or service by trade name, trademark, manufacturer, or otherwise does not necessarily constitute or imply its endorsement, recommendation, or favoring by the United States government or any agency thereof. The views and opinions of authors expressed herein do not necessarily state or reflect those of the United States government or any agency thereof.

Available to DOE and DOE contractors from:
Office of Scientific and Technical Information (OSTI)
P.O. Box 62
Oak Ridge, TN 37831
Prices available by calling 423-576-8401

Available to the public from:
National Technical Information Service (NTIS)
U.S. Department of Commerce
5285 Port Royal Road
Springfield, VA 22161
703-605-6000 or 800-553-6847
or
DOE Information Bridge
<http://www.doe.gov/bridge/home.html>



Printed on paper containing at least 50% wastepaper, including 20% postconsumer waste

CONTENTS

Part I: Simulator Description

Chapter 1: Purpose and General Characteristics	1
Chapter 2: Point of Common Coupling.....	6
Chapter 3: Diesel Generator	11
Chapter 4: AC Wind Turbine	18
Chapter 5: Rotary Converter	28
Chapter 6: Village Load	40
Chapter 7: Dump Load	45

Part II: Case Studies and Validation Tests

Chapter 8: Case Studies.....	50
Chapter 9: Validation Tests at the Component Level.....	87
Chapter 10: Validation Tests at the System Level	118

Appendix 1: How to Set-up and Run the Simulation.....	133
Appendix 2: Synchronous Generator Model E7201L1 Data Sheet	137
Appendix 3: Wales Control System Dump Load Dispatch at the HPTB.....	141
Appendix 4: Documentation for RPM-SIM on CD-ROM	145

PART I

SIMULATOR DESCRIPTION

Purpose and General Characteristics

The advantage of hybrid power systems is the combination of the continuously available diesel power and locally available, pollution-free wind energy. With the hybrid power system, annual diesel fuel consumption can be reduced and, at the same time, pollution can be minimized. A proper control strategy has to be developed to take full advantage of the wind energy during the periods of time it is available and to minimize diesel fuel consumption. The control system is subject to the specific constraints of a particular application. It has to maintain power quality, measured by the quality of electrical performance, i.e., both the voltage and the frequency have to be controlled. This results in a need for a simulation study of each new system to confirm that a control strategy results in desired system performance.

Using the VisSimTM¹ visual environment, we developed a modular simulation system to facilitate an application-specific and low-cost study of the system dynamics for wind-diesel hybrid power systems. The simulation study can help in the development of control strategies to balance the system power flows under different generation/load conditions. Using the typical modules provided, it is easy to set up a particular system configuration.

In this manual, we present the principal modules of the simulator and, using case studies of a hybrid system, we demonstrate some of the benefits that can be gained from understanding the effects of the designer's modifications to these complex dynamic systems. In these systems, the diesel generator, working as a master, controls the voltage and the frequency. The wind speed varies with time and so does the village load. Therefore, we regard the diesel generator as a controlled energy source, whereas the wind is an uncontrolled energy source and the village load is an uncontrolled energy sink. The diesel generator balances the difference between the power consumed by the village load and the power generated by the wind turbine. On occasion, the wind speed can be very high, resulting in energy generation that exceeds the energy demand of the village load. Under such circumstances, the power from the diesel becomes very low, and the wind may try to drive the diesel engine. Should the wind turbine override the diesel, the frequency control could be lost, and the system would become unstable. To avoid this condition, the dump load is controlled so that the power generated by the diesel will always be higher than a minimum value. In addition, the energy surplus can be saved for future use by utilizing the rotary converter/battery assembly. Therefore, the dump load should be regarded as a controlled energy sink. When the battery is being discharged the rotary converter/battery assembly should be regarded as a controlled energy source. On the other hand, when the battery is being charged, it should be regarded as a controlled energy sink. By properly choosing the sequence of events programmed for our case studies, we demonstrate that all operation aspects of the hybrid power system, briefly

¹ VisSim is the trademark of Visual Solutions.

discussed above, can be easily taken into consideration. The single-line diagram of a typical hybrid power system, which involves all modules available in the simulator, is shown in Figure 1.1. The user must include the point of common coupling (PCC) module, as a node where all power sources and power sinks are connected, in every simulation diagram. The other principal modules shown in Fig. 1.1 are the diesel generator (DG), the AC wind turbine (WT) with the induction generator and the wind speed time series as the input, the rotary converter (RC) with the battery bank (BB), the village load (VL), and the dump load (DL). In addition, $R+jX$ represents the transmission-line impedance and PFC represents the power factor-correcting capacitors. In all electrical simulations, we use the d-q axis convention and synchronous reference frame. In particular, in the PCC module, the q-axis and d-axis components v_{qs1} and v_{ds1} of the line voltage V_s are defined.

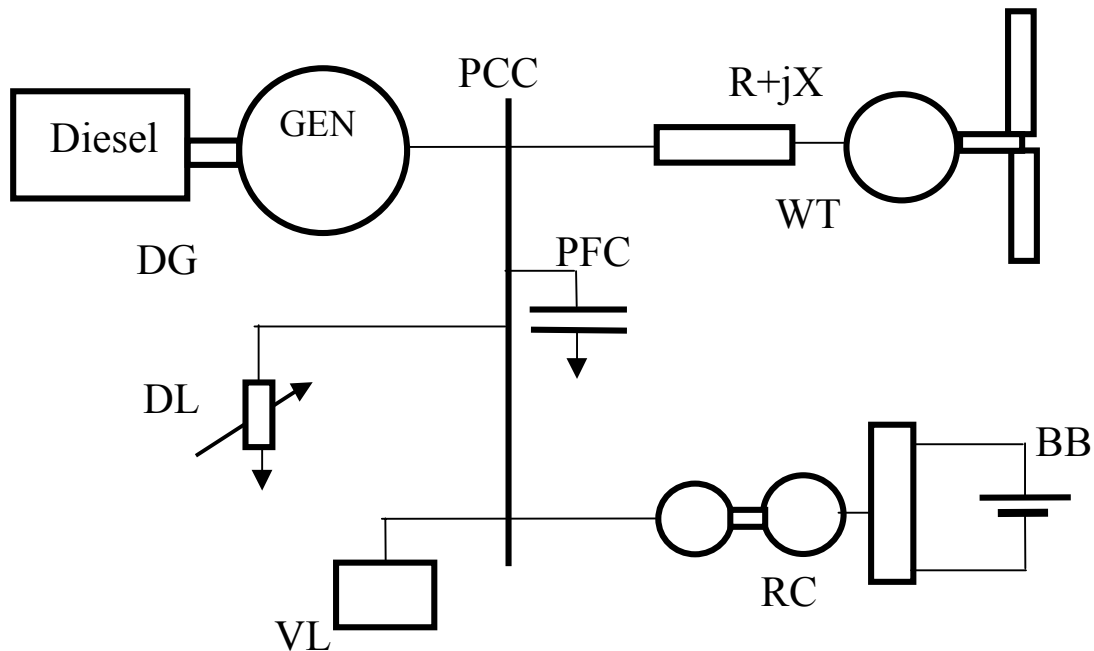


Figure 1.1 A typical hybrid power system

Using the typical modules provided, it is easy to set up a system of a desired configuration. The **Add** command of the File menu is used to place all the required modules (provided in the RPMSim_DST subdirectory of VisSim) on the simulation screen. The VisSim's multilevel programming concept, along with the ability of creating compound blocks, facilitates presentation of simulation modules, their submodules, or both at different levels of "resolution."

Clicking the mouse on the block which represents a module reveals, where appropriate, its block diagram. This reveals the submodules with their connections, inputs and outputs, and possibly a short explanation note. This note lists parameters to be declared by the user, system variables generated by this particular module, and gives a general description of the module. Clicking on any submodule of a given block diagram results in obtaining a screen that contains blocks SIMULATION DIAGRAM and PARAMETER

MODULE, as well as an explanation note. The parameter module contains application-specific parameters to be declared by the user. The simulation diagram shows the equation-level representation of a particular device using the simulation blocks available in VisSim menus. An explanation note can also be attached if appropriate.

The user can attach a display block to any simulation variable to obtain its numerical value or attach a plot block to obtain its graphical representation as a function of time. These blocks are available under the Signal Consumer menu and can be used at any level of the simulation diagram. VisSim menus list commands that automate many tasks and blocks that correspond to numerous linear and nonlinear functions.

General Characteristics of Principal Modules

The following are the principal modules and their file names currently available in the simulator subdirectory:

- Point of common coupling, file PCC.vsm
- Diesel generator, file DG.vsm
- AC wind turbine/wind speed, file wtg_base.vsm (used to represent a single or the first of multiple wind turbines; includes the wind speed module), file WTG.vsm (used to represent additional wind turbines; does not include the wind speed module), and file WIND_SPEED.vsm (represents wind speed)
- Rotary converter/battery bank assembly, file BB_RC.vsm
- Village load, file VL.vsm
- Dump load, file DL.vsm.

The PCC module must be included in every simulation diagram. This module is a node where all power sources and power sinks are connected. The top simulation diagram of the PCC module displays a button used to turn the village load on or off by clicking the mouse. This switching can also be performed while the simulation is running.

The diesel generator module includes a model of a diesel engine, a synchronous generator, an engine speed control block (that generates a fuel/air ratio (represented by the $\%_{FUEL}$ variable)) required to keep the frequency constant, and a voltage regulator, that determines the field current to keep the line voltage constant.

The AC wind turbine module simulates the two-step conversion of wind power to electrical power. In the first step, the wind power is converted to mechanical power represented by the torque developed by the wind turbine rotor and transmitted to the induction generator through the gearbox. In the second step, the electrical power is obtained. This module includes a model of a transmission line connecting the induction generator with the synchronous generator at the point of common coupling. The power

factor-correction capacitors, located at the induction generator are also included. For the designer's convenience, the AC wind turbine module is included in two files. The file `wtg_base.vsm` consists of the AC wind turbine module, the PCC WT-GEN block (included to enable simulation of multiple wind turbine systems) and the wind speed module. The file `WTG.vsm` contains the wind turbine module and is used to represent additional wind turbines in simulation diagrams of power systems with multiple wind turbines. If the multiple wind turbines with different wind profiles are simulated, the wind speed module (or modules) must be added (with **Add** command) to the simulation screen, as illustrated in Figure 1.2. The user must connect (click and drag) its output to the input of the AC wind turbine module on the top-view simulation diagram of a hybrid power system. If, in the multiple wind turbine simulation, the same wind profile is used for all wind turbines, then the variable V_{wind} must be added and connected to the input of each additional wind turbine, as illustrated in Figure 1.3.

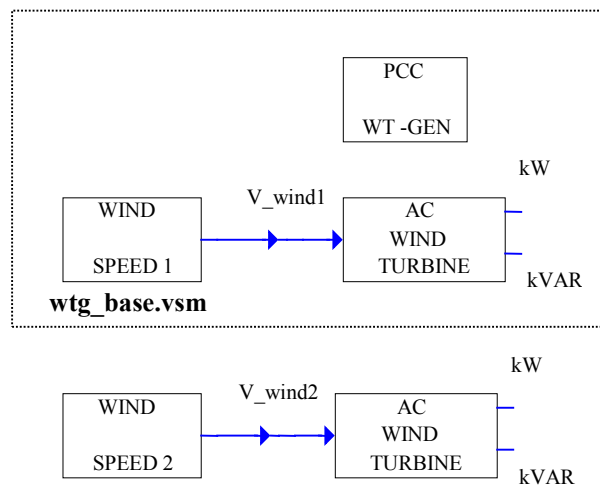


Figure 1.2 Multiple wind turbines with different wind profiles

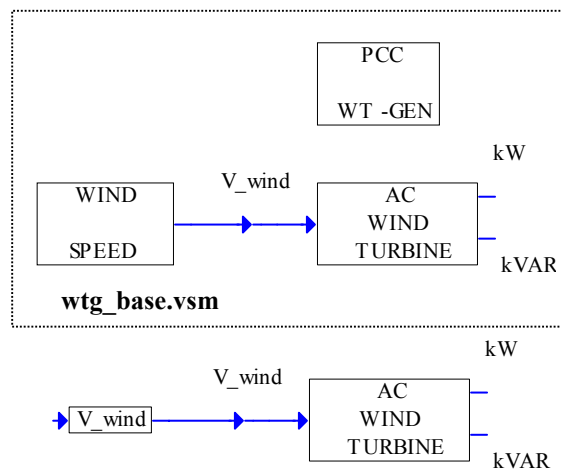


Figure 1.3 Multiple wind turbines with the same wind profile

The wind speed module is implemented with the import data file block provided in VisSim. It imports data points from a specified wind speed file and translates them into the output wind speed signal. The user can change the wind speed file. It is a two-column ASCII file, in which the first column is the time data column and the second is the wind speed column.

The rotary converter/battery bank assembly consists of a battery bank block and rotary converter block. The rotary converter consists of two machines: the DC motor and the synchronous generator. It performs the AC/DC conversion while charging the battery and performs the DC/AC conversion while discharging the battery. It can also be set up to work as a synchronous condenser while the user controls the level of reactive power generated or absorbed. The battery bank block represents energy storage designed to work with the rotary converter. It can be either charged or discharged depending on the sign of the reference power P_{BAT_ref} . If this sign is negative, the DC motor of the rotary converter works as a generator and charges the battery. If the sign of P_{BAT_ref} is positive, the battery is discharged and, through the rotary converter, provides power to the system.

The village load module represents the load specified by the real power consumption and the village load power factor. The village load profile is programmed and stored in a file. The file must be available before running the program.

The dump load is an adjustable resistive load controlled in the steps of dissipated power to be declared by the user. The dump load module is used to load the diesel engine by selecting the number of load elements active, i.e., the number of power steps applied. This selection is done automatically by one of the following control strategies chosen by the user:

- The diesel power control strategy that maintains the minimum diesel load so that the power delivered by the diesel engine is greater than a certain percentage of its rated power.
- The frequency control strategy that controls the number of the load elements active to keep the frequency within the limits set by the user.

The user has the choice to activate either one of these control strategies by clicking on a button (available in the VisSim's signal producers menu) that, when activated, turns red and generates the signal 1.

For all modules included in the simulator, we assumed (for both real and reactive power) the following general power sign convention: the power absorbed is displayed as negative and the power generated is displayed as positive. A village load (as an inductive load) always absorbs both the real and the reactive power and both powers are always negative. The real power of a diesel generator always remains positive and its reactive power may be positive or negative. The real power of the wind turbine generator is negative during motoring and is positive during generation. Its reactive power is always absorbed, i.e., it is displayed as a negative quantity.

Point of Common Coupling

The point of common coupling (PCC) module, the node where all power sources and power sinks are connected, must be included in every simulated power system. In Figure 2.1, we show a single-line diagram (as in Figure 1.1) of a hybrid power system where we dot-framed the PCC part of the diagram.

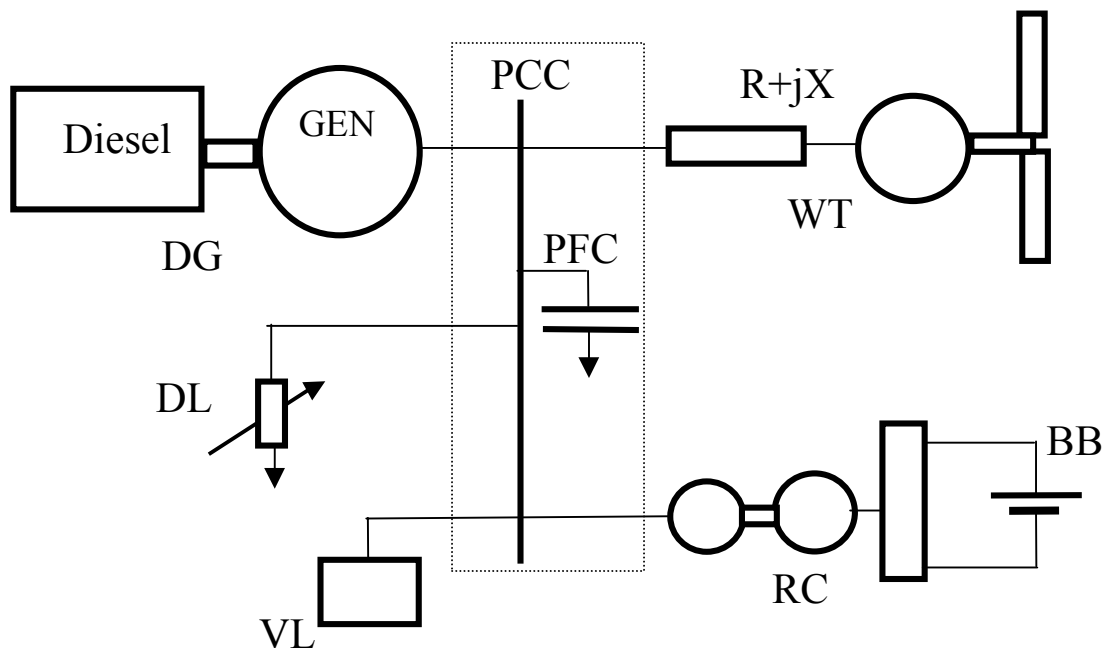


Figure 2.1 A single-line hybrid power system diagram with the PCC part dot-framed

The user brings the PCC module to the simulation screen using the **Add** command and selecting file PCC.vsm. Then, the user obtains top-view diagram of the PCC module (shown in Figure 2.2) by clicking the mouse on the rectangle representing this module. This view features three elements: (1) the mouse-controlled button used to turn on (red button, variable *VillageLoad* = value logic 1) and off (white button, variable *VillageLoad* = value logic 0) the village load, (2) the parameter module compound block, and (3) the simulation diagram compound block. Figure 2.3, which is the expansion of the parameter module, shows the parameters to be declared by the user. Figure 2.4 represents the expansion of the simulation diagram compound block. Recall that in all simulations we use the d-q axis convention. Therefore, each voltage and current has two components. Consequently, Figure 2.4(a) represents the relationship between the d-axis components of the currents of all system modules, and it shows how the d-axis component of the line voltage is obtained. The same is repeated in Figure 2.4(b) for the q-axis components. To

make the relationships between the currents and voltages involved obvious, the circuit diagrams (corresponding to the simulation diagrams of Figure 2.4) are shown in Figure 2.5.

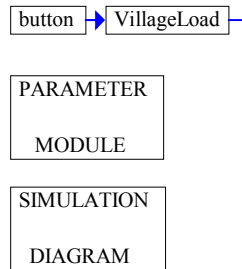


Figure 2.2 Top-view diagram of the PCC module

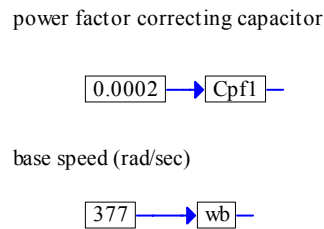


Figure 2.3 Parameter module of the PCC

The following are the denotations for q-axis and d-axis components of the currents involved:

- i_{qSD}, i_{dSD} - current provided by synchronous generator/diesel module,
- i_{qRC}, i_{dRC} - current provided by rotary converter,
- i_{qs}, i_{ds} - transmission line current (to asynchronous machine/wind turbine),
- i_{qDL}, i_{dDL} - dump load current,
- i_{qV}, i_{dV} - village load current.

Note that if the current representing a given module enters the top node in the circuit diagram of Figure 2.5 (or is added at the summing junction in Figure 2.4), then its power is positive when it is generating power and negative when it is absorbing power. On the other hand, if the current representing a given module leaves the top node in the circuit diagram of Figure 2.5 (or is subtracted at the summing junction in Figure 2.4), then its calculated power is positive when it is absorbing power and negative when it is generating power. To follow the general convention that the power generated is positive and the power absorbed is negative, we invert the sign of the power calculated for the modules represented by the currents leaving the top node in the diagram of Figure 2.5.

Let us consider some examples. The diesel generator always generates the real power. Therefore, its real power is always positive, or we say that it follows the assumed current sign convention. On the contrary, the diesel generator may generate or absorb the reactive power, i.e., the diesel reactive power may be positive or negative, depending on the load demand. The wind turbine generator during the motoring period absorbs real power, i.e., it draws the current from the PCC junction. The direction, in which this current flows, is the same as the direction assumed. Therefore, the calculated (absorbed) real power is positive. It requires the change of sign to follow the general convention. For the same reason, we must change sign of the real power calculated when the wind turbine is generating. According to the circuit diagrams shown in Figure 2.5 we define the following currents:

$$i_{qPFC1} = i_{qSD} + i_{qRC} - i_{qs} - i_{qDL} - i_{qV},$$

$$i_{dPFC1} = i_{dSD} + i_{dRC} - i_{ds} - i_{dDL} - i_{dV}.$$

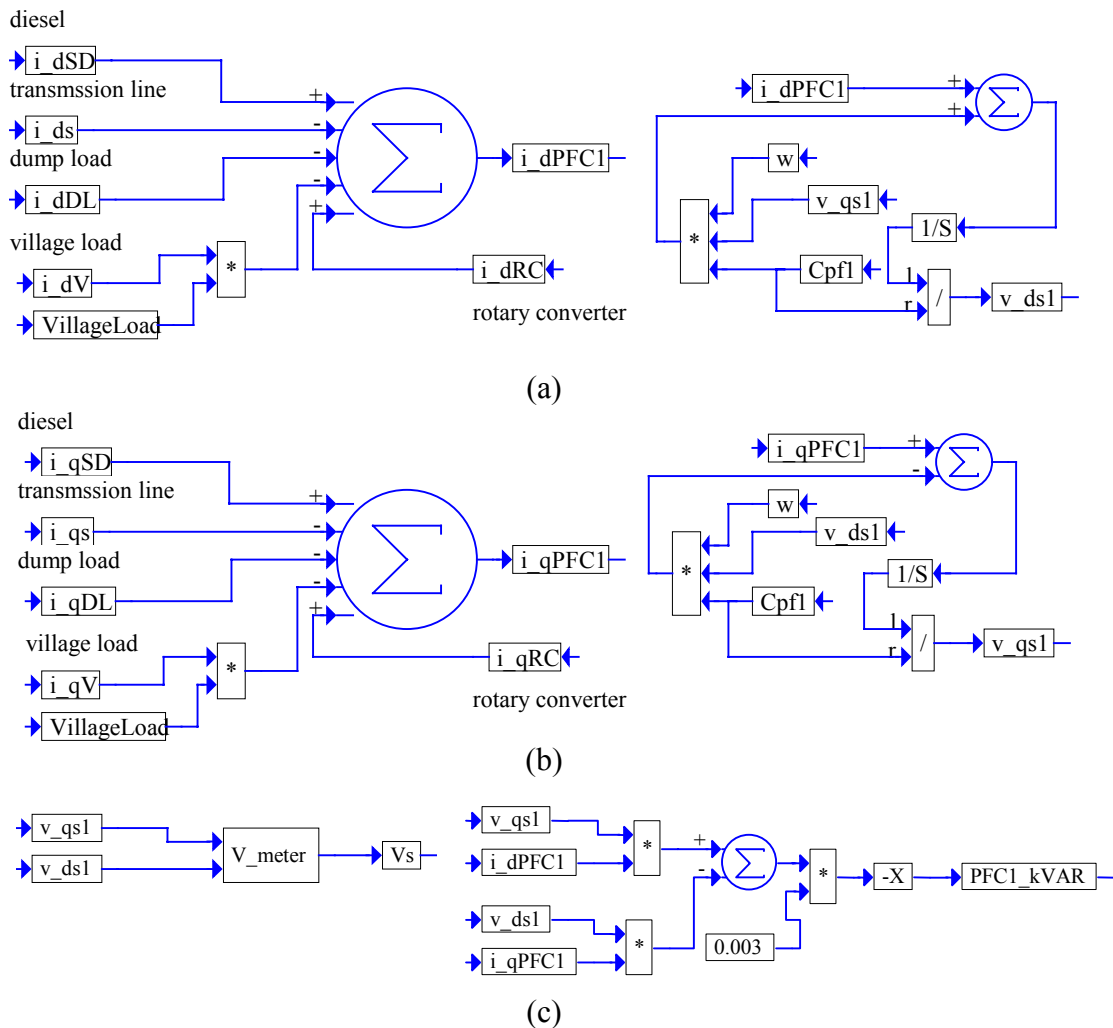


Figure 2.4 PCC module simulation diagram: (a) d-axis diagram, (b) q-axis diagram and (c) calculation of the system voltage and the reactive power generated by the power factor correcting capacitor

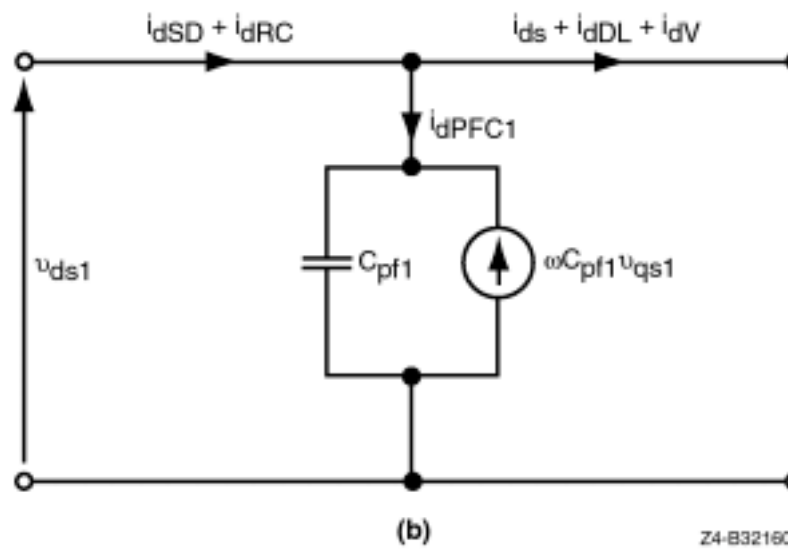
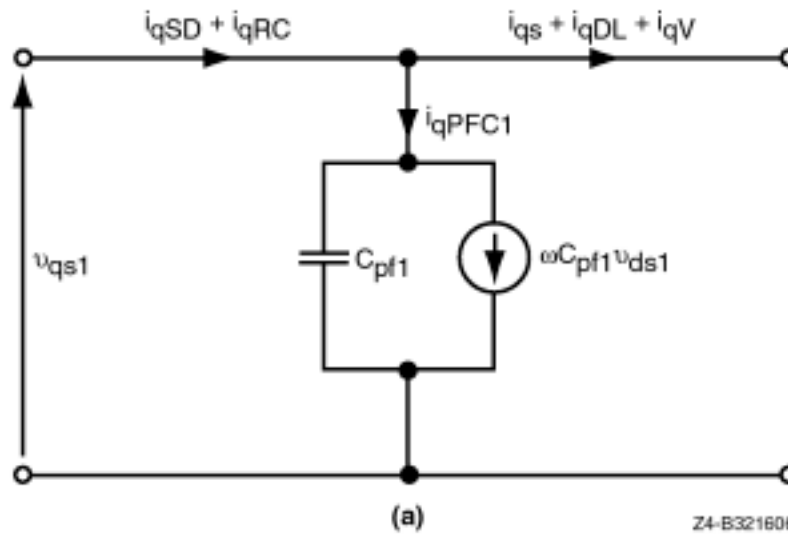


Figure 2.5 PCC module circuit diagram: (a) q-axis diagram and (b) d-axis diagram

Using the same circuit diagram, we write the following equations defining q-axis and d-axis components v_{qs1} and v_{ds1} of the line voltage (V_s):

$$v_{qs1} = \frac{1}{C_{pf1}} (i_{qPFC1} - \omega C_{pf1} v_{ds1}) dt ,$$

$$v_{ds1} = \frac{1}{C_{pf1}} (i_{dPFC1} + \omega C_{pf1} v_{qs1}) dt ,$$

where C_{pf1} is the power factor-correcting capacitor of the value to be declared by the user in the parameter module shown in Figure 2.3, and ω is the real system frequency calculated in the diesel generator module that must be a part of every simulated power system. These equations are implemented in the right-side parts of Figure 2.4(a) and Figure 2.4(b).

V_s is calculated in the compound block V_meter , shown in Figure 2.4(c), according to the following equation:

$$V_s = \sqrt{v_{qs1}^2 + v_{ds1}^2} .$$

The calculation of the reactive power generated by the power factor-correcting capacitor is also shown in Figure 2.4 (c). According to our convention, the reactive power generated must be positive. If the power is generated, the currents i_{qPFC1} and i_{dPFC1} should be entering the summing junction. The user can check and see that the currents are leaving the junction. In other words, the calculated reactive power is negative. Thus, we introduce the inversion of sign in the calculation of the reactive power shown in Figure 2.4(c).

Diesel Generator

In Figure 3.1, we show a single-line diagram (as in Figure 1.1) of a hybrid power system where we dot-framed the part of the diagram representing the diesel generator (DG). As shown in this figure, it consists of two machines: (1) a diesel engine and (2) a synchronous generator. The user brings the diesel generator module to the simulation screen using the **Add** command and selecting the file DG.vsm.

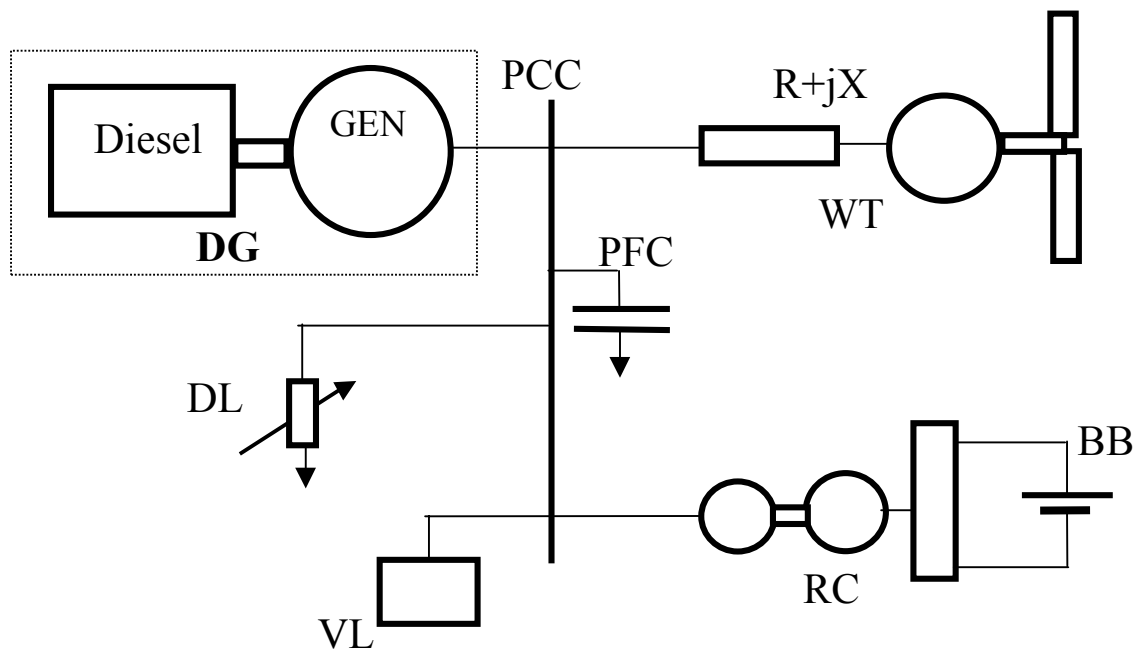


Figure 3.1 A single-line power system diagram with the DG part dot-framed

Figure 3.2(a) represents the top-view diagram of the diesel generator module. Two outputs SD_{kW} and SD_{kVAR} make the real and reactive power available for monitoring with either a display or plot block to be chosen and connected (click and drag) by the user. By clicking the mouse the user obtains the second-level block diagram, such as the one in Figure 3.2(b), that represents the principal functional blocks of the diesel generator with their interconnections and all inputs and outputs are clearly shown. At this level, the per phase voltage set point V_{s_ref} and the frequency set point f_b can easily be set at required values by typing the new value into the setup block. According to this block diagram, the speed control block generates a proper fuel/air ratio (represented by the variable $\%_{FUEL}$) for the diesel engine. This enables the engine to generate the proper torque to drive the synchronous generator. The voltage regulator (with the proper adjustment of the field current of the synchronous generator) controls the line voltage V_s .

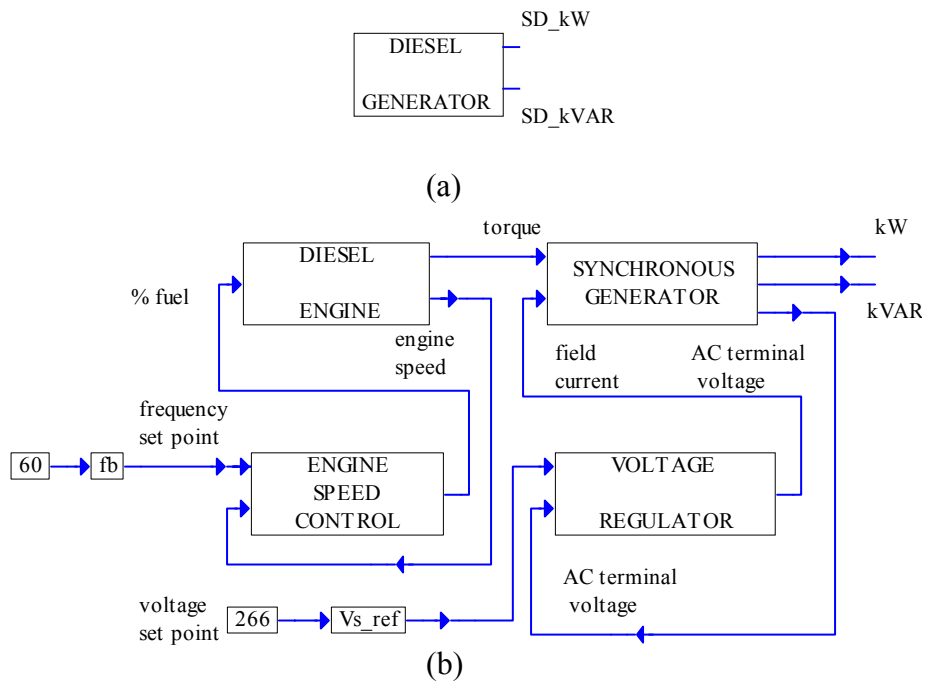


Figure 3.2 Block diagrams of the DG module: (a) top-view diagram and (b) second-level diagram showing principal functional modules and their interconnections

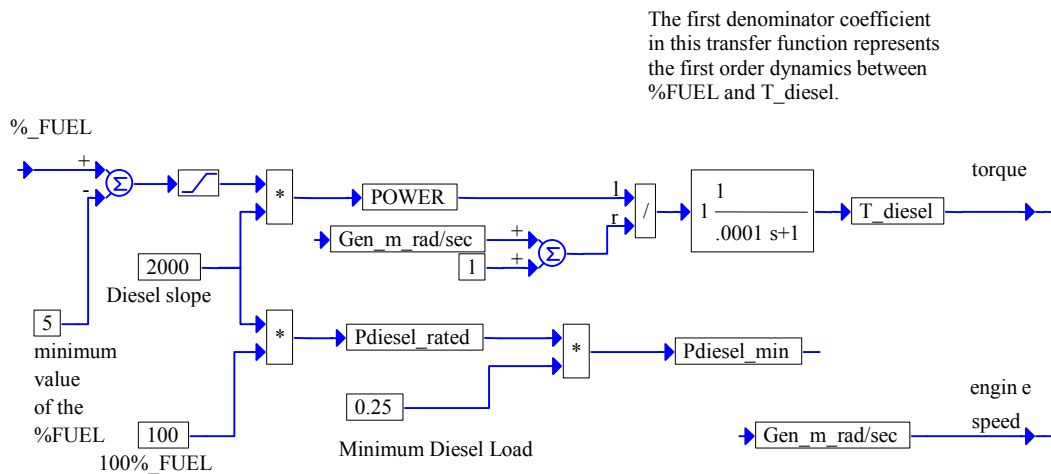


Figure 3.3 Simulation diagram of the diesel engine module

Figure 3.3 represents a simple simulation diagram of a diesel engine. Its $POWER=f(\%_{FUEL})$ characteristic is represented as a straight line with the slope and the minimum value of the $\%_{FUEL}$ (the dead zone) that is defined by the user based on the data from the diesel engine manufacturer, so that it will approximate the engine modeled. The user can see from Figure 3.3 that the rated power for the simulated diesel engine is 200

kW. Using the generated power and angular velocity $Gen_{m_rad/sec}$, the torque T_{diesel} is generated assuming the first-order dynamics¹. The time constant can be specified by the user. The minimum diesel load P_{diesel_min} (chosen in Figure 3.3 to be 25% of the rated power) is calculated. Diesel power is controlled to generate above minimum. This objective is accomplished by connecting the right number of dump load resistors (for more information see Chapter 7).

The first- and the second-level expansions of the synchronous generator module are shown in Figure 3.4. The first level, presented in Figure 3.4(a), consists of two compound blocks (parameter module and simulation diagram) and shows two control inputs T_{diesel} and the field current i_f and three outputs SD_{kW} , SD_{kVAR} , and V_s . Note that for clarity of presentation, the output V_s is calculated in the PCC module as shown in Figure 2.4(c). Figure 3.4(b) lists all machine parameters declared by the user. Figure 3.4(c) shows the first level expansion of the synchronous generator simulation diagram with the following compound blocks: torque equation, power calculations (where the outputs SD_{kW} and SD_{kVAR} are generated), and the Q-generator and D-generator. This block diagram also shows that the electromotive force generated is assumed as a reference, i.e., its phase is assumed to be zero. Consequently, its d-axis component is zero, which is symbolically shown as a zero input to the D-generator. Under this assumption, the input to the Q-generator is defined by the following equation:

$$E_{q_D} = K_{e_D} \omega \Phi = K_{e_D} \omega L_f i_f ,$$

where Φ is the flux proportional to the field current (i_f) and the other parameters are explained in Figure 3.4(b). The Q-generator and D-generator, shown in Figure 3.5(b), generate the current i_{qSD} and i_{dSD} respectively contributed by the diesel generator to the system at the PCC module. These currents are calculated according to the following equations:

$$i_{qSD} = \frac{1}{L_{qSD}} (E_{q_D} - v_{qs1} - R_{SD} i_{qSD} - \omega L_{dSD} i_{dSD}) dt ,$$

$$i_{dSD} = \frac{1}{L_{dSD}} (-v_{ds1} - R_{SD} i_{dSD} + \omega L_{qSD} i_{qSD}) dt .$$

The power calculation block is shown in an expanded form in Figure 3.5(c). The electrical power generated is calculated according to the following equation:

$$P_{Egen_D} = 3 i_{qSD} E_{q_D} .$$

Then, the real power provided to the system is calculated as

$$P_{gen} = 3(v_{qs1} i_{qSD} + v_{ds1} i_{dSD}) \text{ [W]} \quad \text{or} \quad SD_{kW} = 10^{-3} P_{gen} \text{ [kW]} .$$

¹ The first-order dynamics of the form $K/(sT+1)$ is implemented with the transfer function block provided by VisSim. In the dialog box of this block, the user declares the gain K and the coefficients of the numerator and the denominator polynomial of the transfer function.

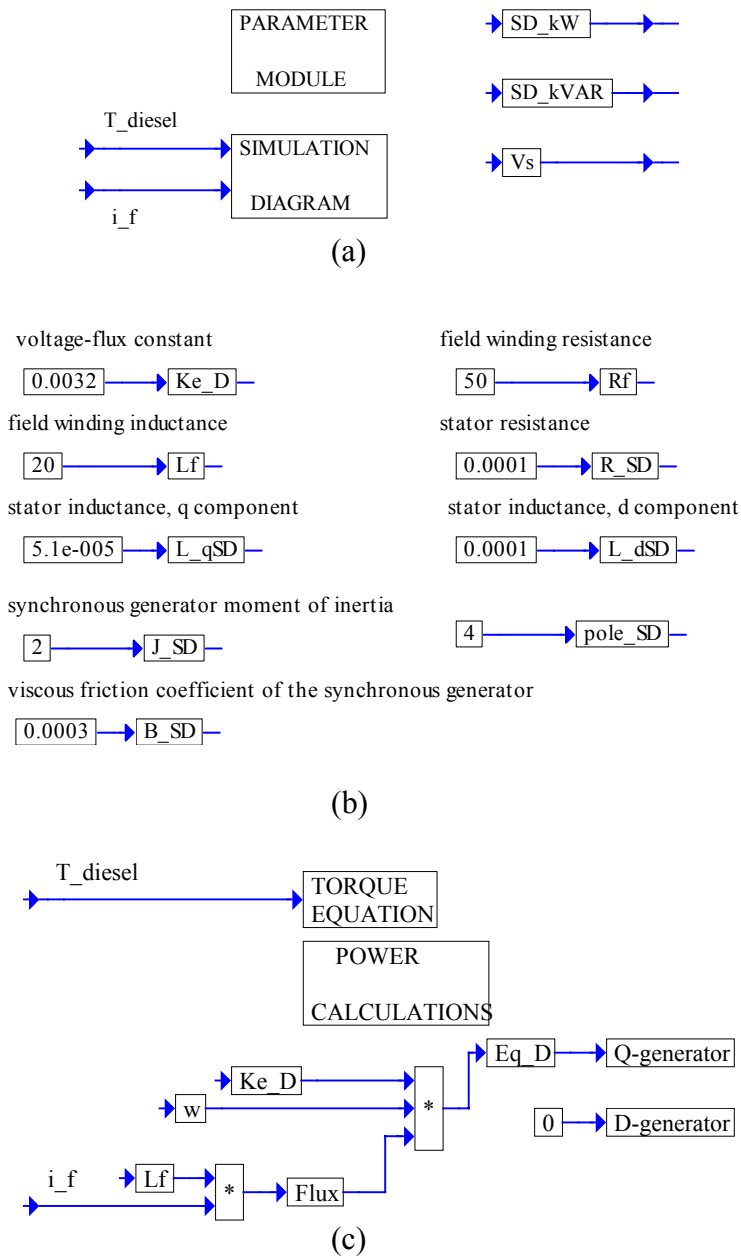


Figure 3.4 First- and second-level expansion of the synchronous generator module: (a) first level expansion, (b) parameter module expansion and (c) simulation diagram expansion

The apparent power SD_{kVA} and the reactive power SD_{kVAR} are also calculated in this block according to the following equations:

$$SD_{kVA} = 3 \times 10^{-3} \sqrt{v_{qs1}^2 + v_{ds1}^2} \sqrt{i_{qSD}^2 + i_{dSD}^2} ,$$

$$SD_{kVAR} = 3 \times 10^{-3} (v_{qs1} i_{dSD} + v_{ds1} i_{qSD}) .$$

Finally, in Figure 3.5(a) the torque equation is simulated in order to obtain the angular velocity of the diesel generator $Gen_{m_rad/sec}$. We have the following equation:

$$Gen_{m_rad/sec} = \frac{1}{J_{SD}} (T_{diesel} - T_{gen} - B_{SD} Gen_{m_rad/sec}) dt ,$$

where T_{gen} represents the generated electrical power P_{Egen_D} , i.e.,

$$T_{gen} = \frac{P_{Egen_D}}{Gen_{m_rad/sec}} .$$

There are two more blocks in the second-level simulation diagram of the diesel generator module shown in Figure 3.2(b): the engine speed control block and the voltage regulator. They are fully expanded in Figure 3.6 and Figure 3.7, respectively.

In Figure 3.6, using the angular velocity $Gen_{m_rad/sec}$, we find the value of the ratio f/f_b and an important system variable, the angular frequency $\omega = 2\pi f$. Then the frequency f is found.

The speed of the diesel engine is controlled by the control variable $\%_{FUEL}$ generated by the governor (represented in the simulation by the proportional + integral (PI) controller) so that the relative frequency error $1 - f/f_b$ is driven to zero.

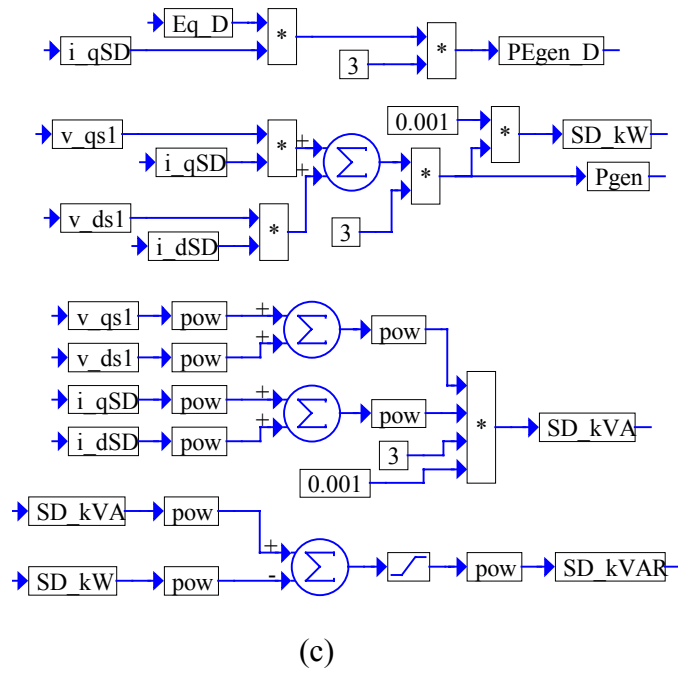
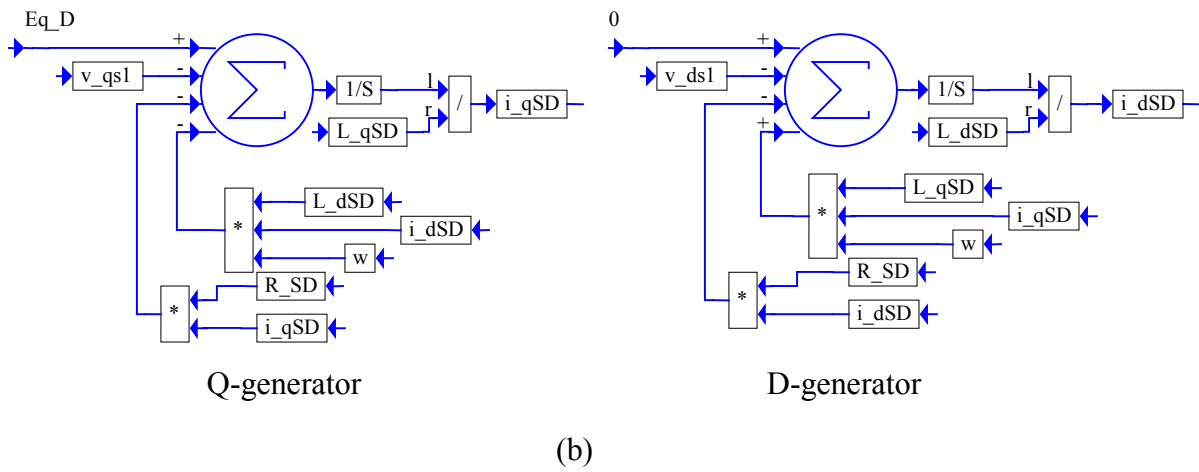
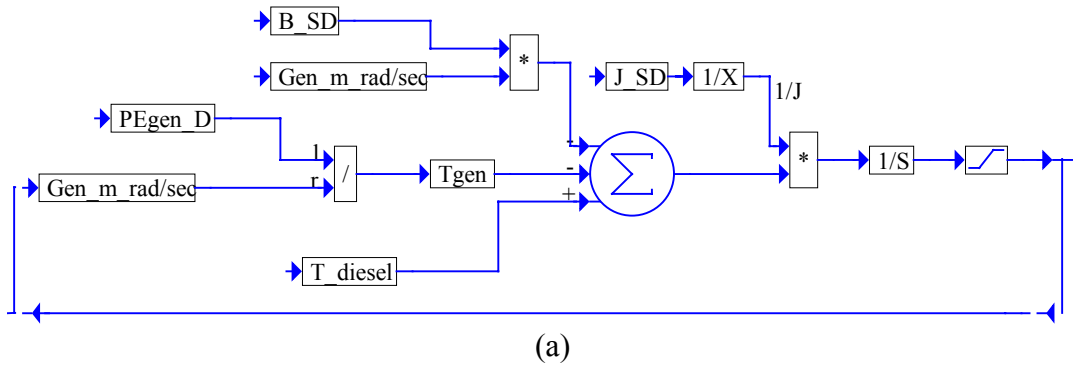


Figure 3.5 Simulation diagram of the synchronous generator (DG module):
 (a) torque equation, (b) Q-generator and D-generator and (c) power calculations

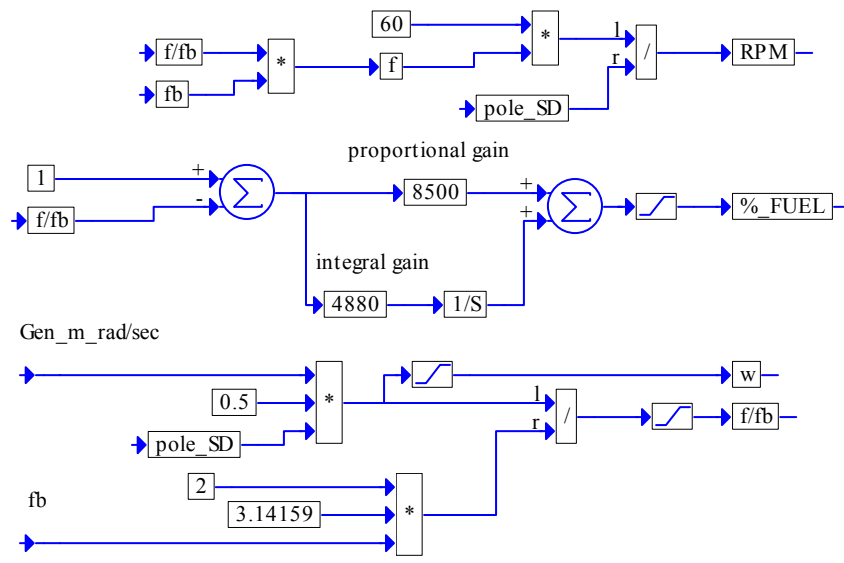


Figure 3.6 Simulation diagram of the engine speed control system

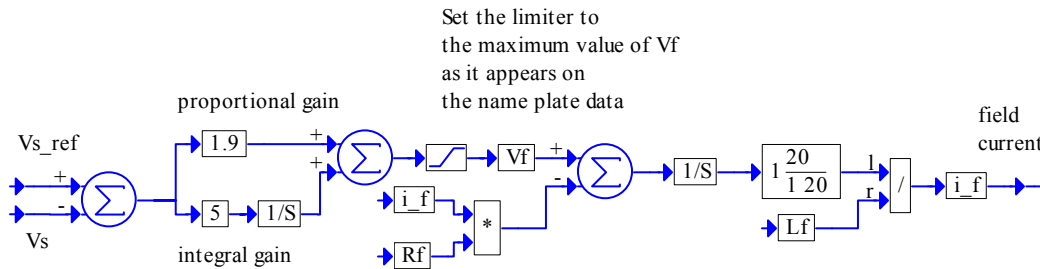


Figure 3.7 Simulation diagram of the voltage regulator

In Figure 3.7, the field current i_f of the synchronous generator is calculated according to the equation

$$i_f = \frac{1}{L_f} \int (V_f - R_f i_f) dt,$$

where the voltage V_f is defined as the output of PI controller, which is determined to drive the line voltage error $V_{s_ref} - V_s$ to zero. To smooth the field current the low-pass filter with the cut-off frequency of 20 rad/s is added. The limiter must be set to the value of V_f as it appears on the name plate data of the machine. The user should adjust proportional and integral gain to avoid saturation of the field current. The practical solution is to make proportional gain slightly smaller than $(V_f)/(V_{s_ref})$ and, then, to set the largest possible integral gain to avoid saturation.

AC Wind Turbine

In Figure 4.1, we show a single-line diagram (as in Figure 1.1) of a hybrid power system where we dot-framed the part of the diagram representing the AC wind turbine (WT). As shown in this figure, the WT consists of two machines: (1) a wind turbine and (2) an asynchronous generator. In addition, power factor-correcting capacitor (PFC) (not shown at this presentation level) and line impedance $R+jX$ is also included. The user brings the WT modules to the simulation screen using the **Add** command and selecting the file `wtg_base.vsm` and (if more than one AC wind turbine is on the system) `WTG.vsm` one for each additional WT on the system. In the multiple wind turbine system, the power factor-correcting capacitors are included in the PCC module and in every WT block.

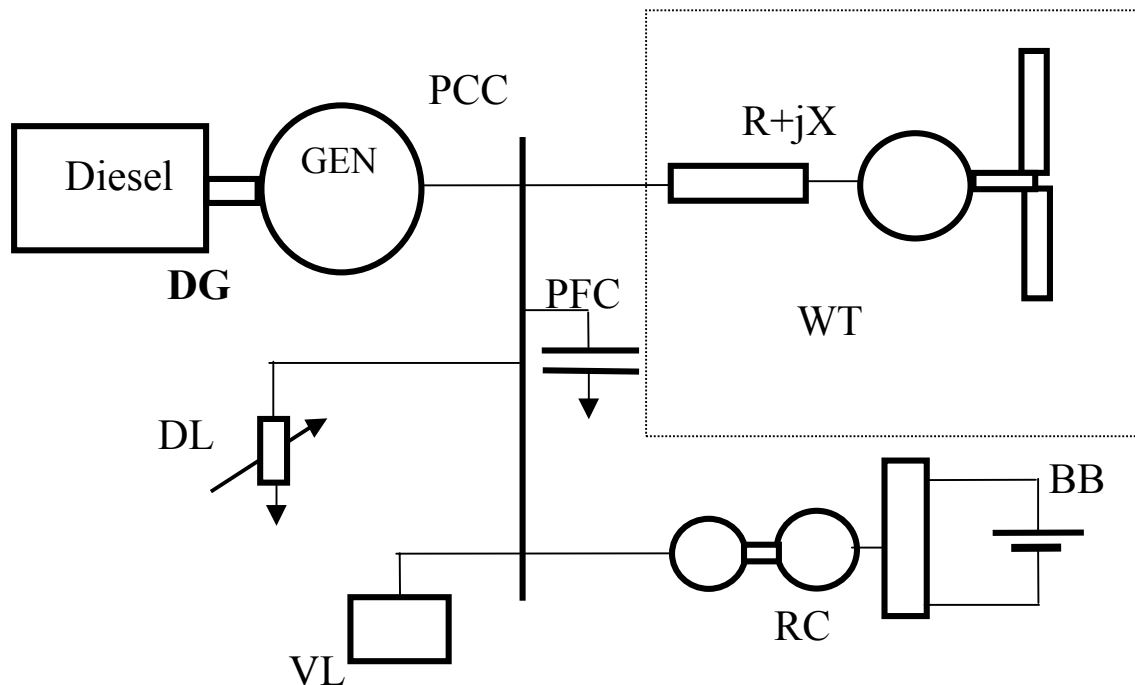


Figure 4.1 A single-line power system diagram with the WT module dot-framed

Figure 4.2 presents the top-view block diagram of the AC wind turbine module implemented by the file `wtg_base.vsm`. It consists of three blocks (shown in Figure 4.2(b)) which are WT, point of common coupling of the wind turbine generators (PCC WT-GEN) (included to enable simulation of multi-turbine systems) and wind speed. In this second-level simulation diagram, we included specific instructions for the user on how to append the simulation diagram of the PCC WT-GEN block (shown in Figure 4.2(d)) when multiple wind turbines are involved in the system. The WT module has two

outputs labeled kW and kVAR, which make the real and reactive power available for monitoring. In Figure 4.2(c), we present the expansion of the WT block, showing the interconnections of its principal components and their inputs and outputs. In this simulation, the reactive power has two components: (1) one absorbed by the induction generator and (2) one contributed by the power factor-correction capacitor block.

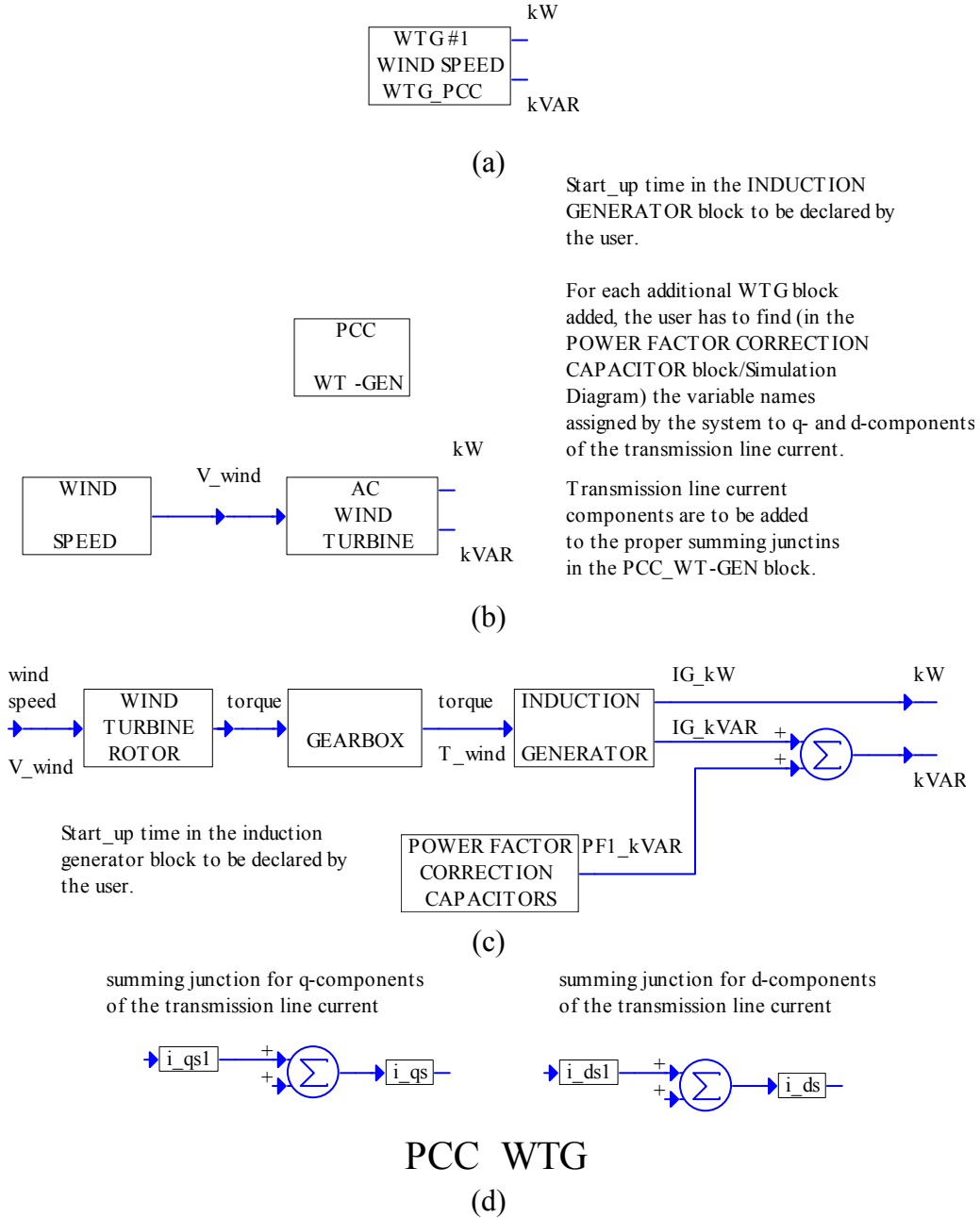


Figure 4.2 AC wind turbine module implemented by the file wtg_base.vsm: (a) top-view diagram, (b) second level diagram, (c) expansion of the AC wind turbine block and (d) expansion of the PCC WT-GEN block

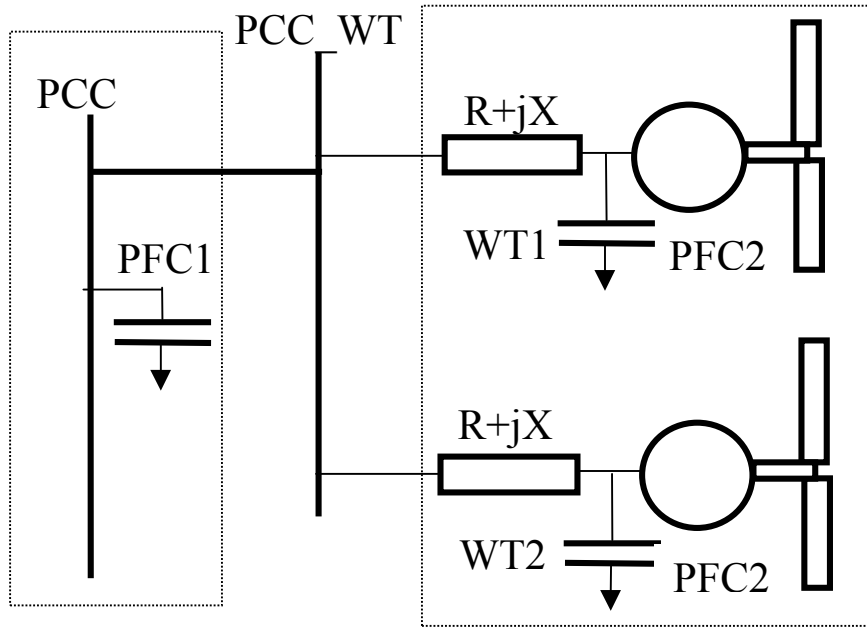


Figure 4.3 Two wind turbines connected to the power system

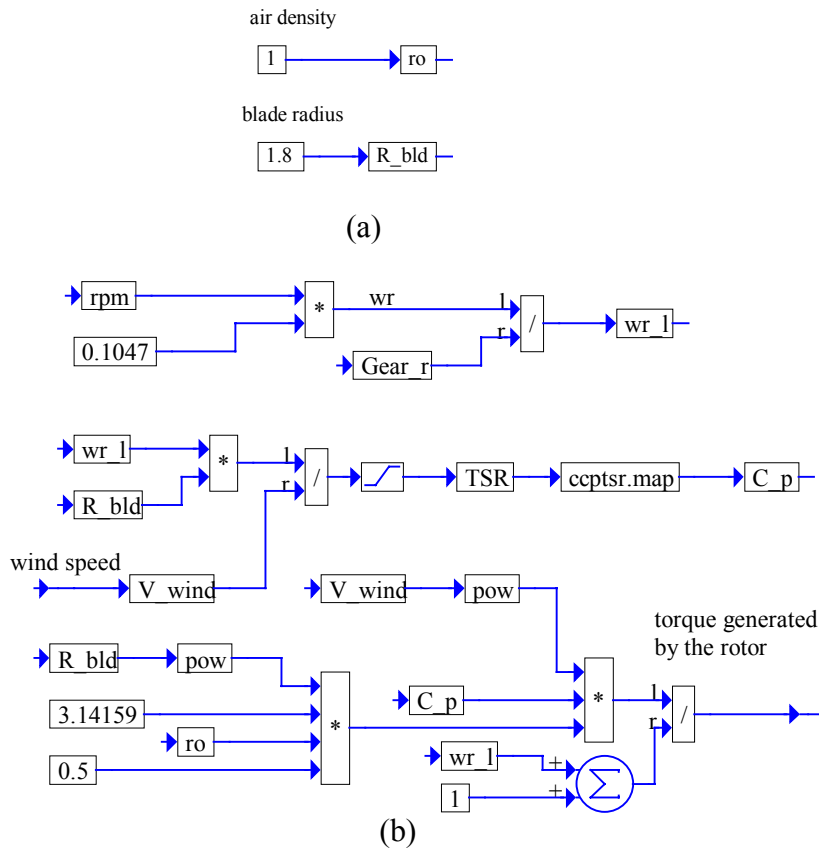


Figure 4.4 Wind turbine rotor: (a) parameter module expansion and (b) simulation diagram expansion

In Figure 4.3, we show a part of the power system with two wind turbines. In this figure, the wind turbine generators are connected to the PCC_WT, which is connected to the PCC of the system. Power factor correction capacitors PFC2 represent capacitors included in the WT1 and WT2 AC wind turbine blocks.

Clicking the mouse on any of the blocks shown in Figure 4.2(c), the user obtains its lower level expansion. Such expansion of the wind turbine rotor block consists of two blocks: (1) the parameter module and (2) the simulation diagram. These blocks can be expanded to another level by clicking the mouse on the respective blocks as shown in Figure 4.4(a) and (b). The parameter module contains two parameters: the air density ρ and the blade radius R_{bld} .

In the simulation diagram the velocity rpm of the induction machine is converted to the angular velocity ω_r in radians/second, which in turn is divided by the gear ratio $Gear_r$. This results in the angular velocity of the blade ω_{r-l} , i.e.,

$$\omega_{r-l} = \frac{\omega_r}{Gear_r} = \frac{0.1047rpm}{Gear_r}.$$

Then, the tip-speed ratio TSR is calculated using the relation

$$TSR = \frac{\omega_{r-l} R_{bld}}{V_{wind}}.$$

The nonlinear relation between TSR and the performance coefficient C_p is encapsulated in the map block, which performs piece-wise linear interpolated look-ups. ASCII data file is used for this mapping. The C_p , generated by the map block, is then used to calculate the wind power P_{wind} , from which the torque generated by the wind turbine T_{wt} is determined. These calculations, shown in Figure 4.4(b), are represented by the following equations:

$$P_{wind} = 0.5\rho\pi R_{bld}^2 C_p V_{wind}^3,$$

$$T_{wt} = \frac{P_{wind}}{\omega_{r-l}}.$$

In Figure 4.5, the expansion of the gearbox block is shown, in which the gear ratio is declared and the high-velocity torque is calculated, appended with a negative sign for future calculations, and denoted by T_{wind} .

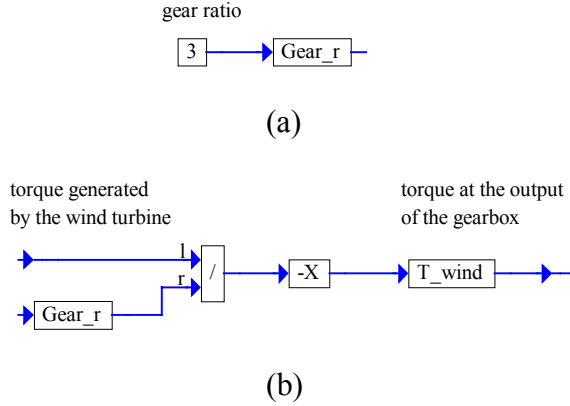


Figure 4.5 Gearbox: (a) parameter module expansion and (b) expansion of the simulation diagram

The first level expansion of the induction generator block is shown in Figure 4.6. The parameters of the machine, to be declared by the user, are listed in the parameter module as shown in Figure 4.6(a). In addition, the calculations of a set of constants in terms of these parameters, that simplify the simulation of induction generator, are also placed in the parameter module. This part of the parameter module is not shown in Figure 4.6(a). The following equations, implemented in the parameter module, specify these constants:

$$a^{-1} = 1 + X'_{lr} / (X_m + X_{ls}), \quad b^{-1} = 1 + X_{ls} / (X_m + X'_{lr}),$$

$$c = \frac{r_s \omega_b}{X_{ls}}, \quad d = \omega_b, \quad e = \frac{r'_r \omega_b}{X'_{lr} X}, \quad f^{-1} = X_{ls}, \quad g^{-1} = X'_{lr}, \quad h = \frac{P}{2J\omega_b}, \quad k = \frac{3P}{4\omega_b},$$

where $\omega_b=377$ [rad/s] is the base speed.

The first-level expansion of the simulation diagram of the induction machine is shown in Figure 4.6(b). Let us concentrate on the two main blocks labeled ds_axis and qs_axis. The expansions of these blocks can be obtained by clicking the mouse. They implement the following equations describing the induction machine:

$$\Psi_{qs} = \omega_b \left[v_{qs2} - \frac{\omega}{\omega_b} \Psi_{ds} + \frac{r_s}{X_{ls}} (\Psi_{mq} - \Psi_{qs}) \right] dt,$$

$$\Psi_{ds} = \omega_b \left[v_{ds2} - \frac{\omega}{\omega_b} \Psi_{qs} + \frac{r_s}{X_{ls}} (\Psi_{md} - \Psi_{ds}) \right] dt,$$

$$\Psi'_{qr} = \omega_b \left[v'_{qr} - \frac{\omega - \omega_r}{\omega_b} \Psi'_{dr} + \frac{r'_r}{X'_{lr}} (\Psi_{mq} - \Psi'_{dr}) \right] dt,$$

$$\Psi'_{dr} = \omega_b \left[v'_{dr} - \frac{\omega - \omega_r}{\omega_b} \Psi'_{qr} + \frac{r'_r}{X'_{lr}} (\Psi_{md} - \Psi'_{dr}) \right] dt,$$

$$\Psi_{mq} = a\Psi'_{qr} + b\Psi_{qs},$$

$$\Psi_{md} = a\Psi'_{dr} + b\Psi_{ds},$$

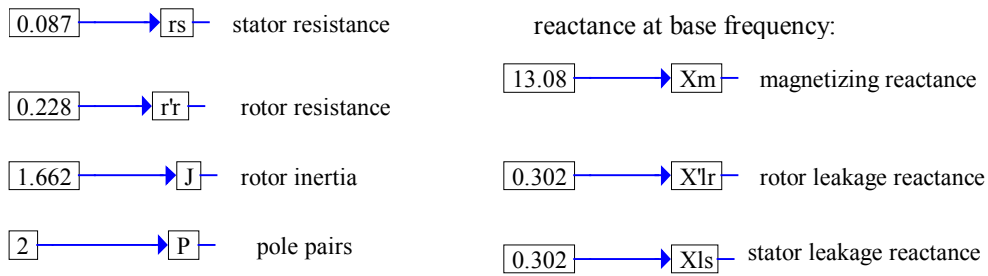
$$i_{qi} = f(\Psi_{qs} - \Psi_{mq}),$$

$$i_{di} = f(\Psi_{ds} - \Psi_{md}),$$

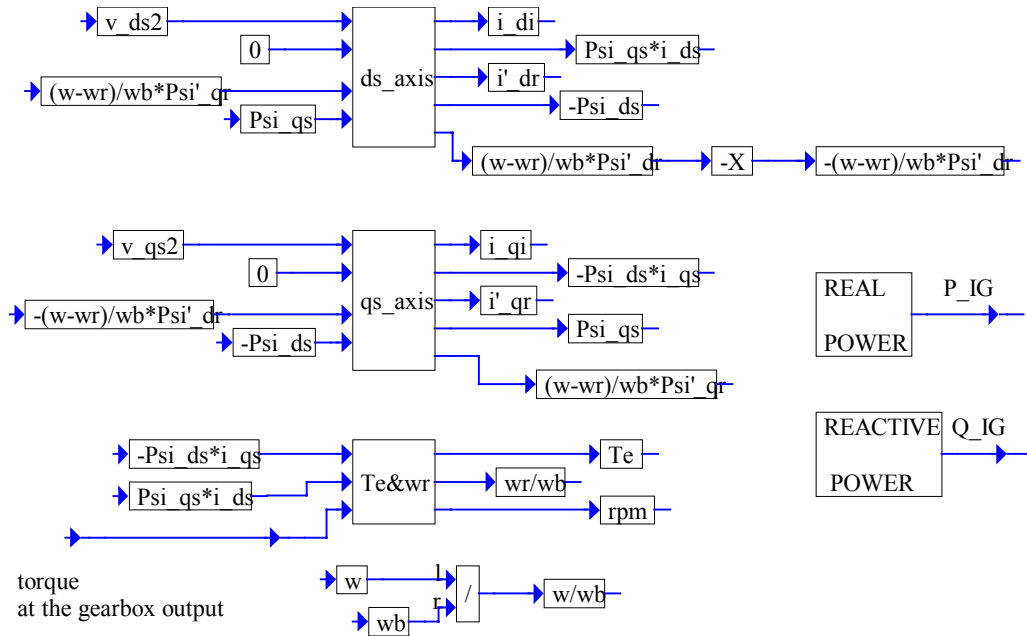
$$i'_{qr} = g(\Psi_{qr} - \Psi_{mq}),$$

$$i'_{dr} = g(\Psi_{dr} - \Psi_{md}),$$

where v_{qs2} and v_{ds2} are defined in the power factor-correction capacitor block described below.



(a)



(b)

Figure 4.6 First-level expansion of the induction generator block:
 (a) parameter module and (b) simulation diagram.

Note that according to the model assumed (as best seen in Figure 4.8) the induction generator current components, i_{di} and i_{qi} , equal to the respective transmission line currents, i_{ds} and i_{qs} , minus the respective components, i_{dPFC2} and i_{qPFC2} , of the power factor-correction capacitor current. The block labeled Te&wr implements the following equations:

$$T_e = k(\Psi_{ds}i_{qi} - \Psi_{qs}i_{di}),$$

$$\frac{\omega_r}{\omega_b} = h (T_e - T_{wind})dt,$$

$$rpm = 9.54929 \frac{\omega_r}{P}.$$

The equation implemented in the real power block is

$$P_{IG} = 3 \times 10^{-3} (v_{qs2}i_{qi} + v_{ds2}i_{di}) [\text{kW}].$$

The equations implemented in the reactive power block are

$$Q_{IG} = 3 \times 10^{-3} (v_{qs2}i_{di} + v_{ds2}i_{qi}) [\text{kVAR}],$$

$$S_{IG} = 3 \times 10^{-3} \sqrt{v_{qs2}^2 + v_{ds2}^2} \sqrt{i_{qi}^2 + i_{di}^2} [\text{kVA}].$$

Figure 4.7 presents power factor-correction capacitor and transmission line model block. Its parameter module is expanded in Figure 4.7(a) and shows the following parameters declared by the user:

- C_{pfc} - power factor correction capacitor at the wind turbine site,
- R_{LN} - transmission line resistance,
- L_{LN} - transmission line inductance.

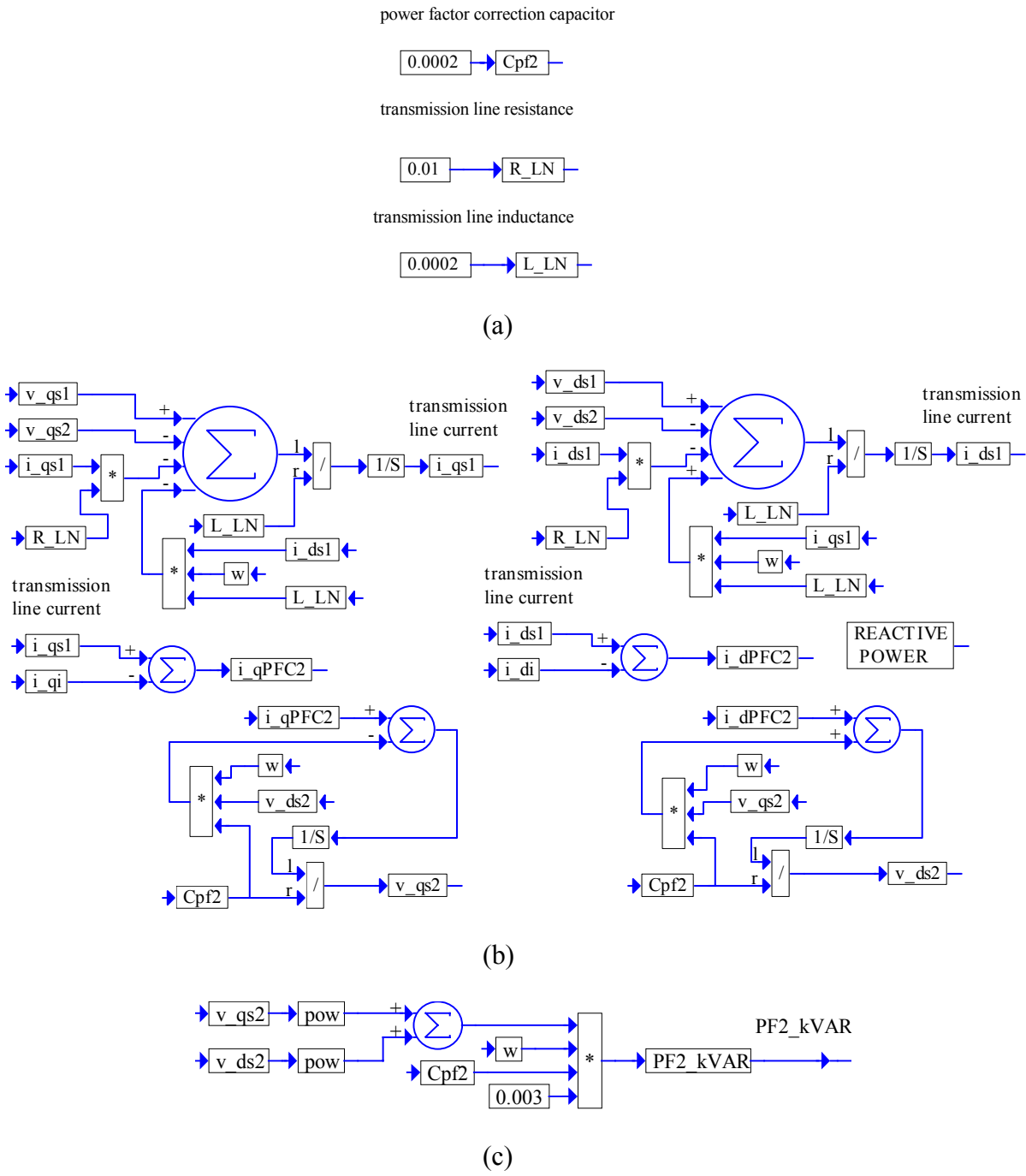
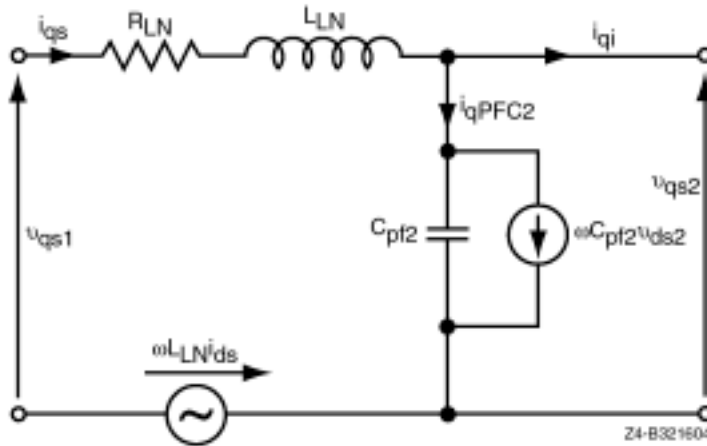
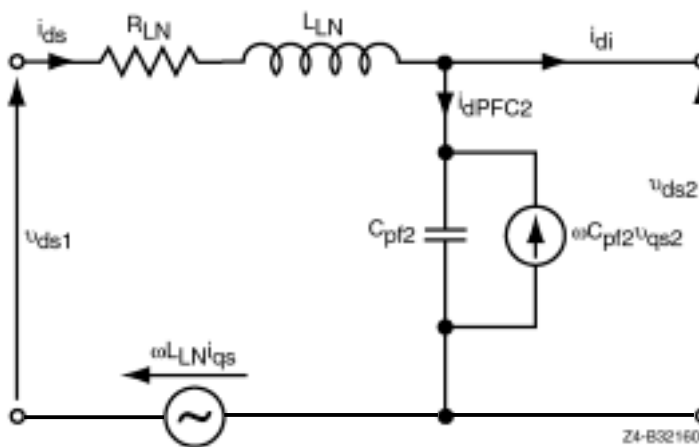


Figure 4.7 Power factor-correction capacitors and transmission line model block:
 (a) parameter module, (b) simulation diagram and
 (c) expansion of the reactive power block



(a)



(b)

Figure 4.8 Circuit diagram of the power factor-correction capacitors and transmission line model block: (a) q-axis circuit representation and (b) d-axis circuit representation

The simulation diagram is expanded in Figure 4.7(b) and its corresponding circuit diagram is shown in Figure 4.8. The transmission line connects the diesel generator with the induction generator. According to the circuit diagram, the d-q axis equations involved are the following:

$$i_{qPFC2} = i_{qs1} - i_{qi}$$

$$i_{dPFC2} = i_{ds1} - i_{di}$$

$$v_{qs2} = \frac{1}{C_{pf2}} (i_{qPFC2} - \omega C_{pf2} v_{ds2}) dt ,$$

$$v_{ds2} = \frac{1}{C_{pf2}} (i_{dPFC2} + \omega C_{pf2} v_{qs2}) dt ,$$

$$i_{qs1} = \frac{1}{L_{LN}} (v_{qs1} - v_{qs2} - \omega L_{LN} i_{ds1} - R_{LN} i_{qs1}) dt ,$$

$$i_{ds1} = \frac{1}{L_{LN}} (v_{ds1} - v_{ds2} + \omega L_{LN} i_{qs1} - R_{LN} i_{ds1}) dt .$$

The variables, i_{qs1} and i_{ds1} , used in these equations to account for a multiple wind turbine system (as explained in Figure 4.2(d)) correspond to the currents, i_{qs} and i_{ds} , in Figure 4.8.

Finally, Figure 4.7(c) shows the expansion of the reactive power block, which implements the equation

$$PF2_{kVAR} = 3 \times 10^{-3} \omega C_{pf2} (v_{qs2}^2 + v_{ds2}^2) .$$

The file WTG.vsm, used as we already mentioned for simulation of multiple wind turbine generators systems, is identical with the AC wind turbine block shown in Figure 4.2(b). However, when this file is added to the simulation screen to represent additional wind turbine, VisSim will automatically rename the variables generated in this simulation diagram. The user is, in particular, interested in the new names of the d and q component of the transmission line current for the added wind turbine generator. The components of this current must be added by the user at the summing junctions in the simulation diagram of the PCC WT-GEN block shown in Figure 4.2(d).

After addition of the file WTG.vsm the block AC WIND TURBINE appears in the simulation screen. Now, (as illustrated in Figure 1.2 and Figure 1.3) the user has to add and connect to its input the variable V_wind or has to generate a new WIND SPEED block and connect its output to the input of the newly added AC WIND TURBINE block. Then the user must click on the AC WIND TURBINE block, click on POWER FACTOR CORRECTION CAPACITORS block, and click on SIMULATION DIAGRAM block. The simulation diagram shown in Figure 4.7(b) will appear in the screen. The names of the transmission line current components for the added wind turbine generator will be visible. Now, the user has to open PCC WT_GEN block shown in Figure 4.2(d) and add these variables at the proper summing junctions. If more than two wind turbines are on the system, the user must first (with the click of the mouse) add connectors to the summing junctions in Figure 4.2(d) (as a default there are provided connectors for only one additional WTG).

Rotary Converter/Battery Bank Assembly

In Figure 5.1, we show a single-line diagram (as in Fig. 1.1) of a hybrid power system where we dot-framed the part of the diagram representing the rotary converter/battery bank assembly (RC). As shown in this figure, the RC consists of a battery bank and two machines: (1) a DC machine and (2) a synchronous machine. In this chapter, the DC machine will be presented in detail, while the synchronous machine will be briefly discussed. For a complete discussion of the synchronous machine, see Chapter 3. The user brings the RC to the simulation screen using the **Add** command and selecting the file `BB_RC.vsm`.

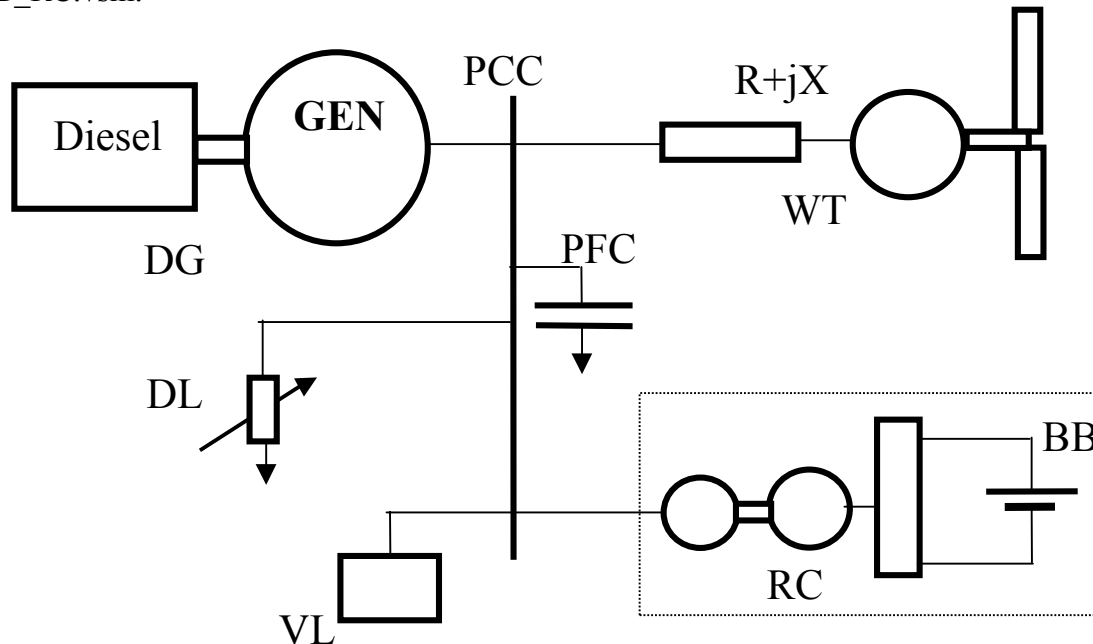


Figure 5.1 A single-line diagram of a hybrid power system with the RC part dot-framed

Figure 5.2(a) presents the top-view block diagram representing the RC. The rotary converter module has two outputs labeled RC_{kW} and RC_{kVAR} that make the real and the reactive power, respectively, available for monitoring. Figure 5.2(b), obtained by clicking the mouse on the battery module, shows the fully expanded simulation diagram of the battery, including parameters to be declared by the user. By clicking the mouse, the user also obtains the second-level block diagram of the rotary converter, shown in the Figure 5.2(c). This represents its principal functional blocks with their interconnections and all inputs and outputs clearly shown and labeled. As shown in Figure 5.2(c), the rotary converter simulation diagram consists of the following principal blocks:

- DC motor/generator,
- Synchronous generator/motor,
- DC machine field controller,
- Voltage regulator.

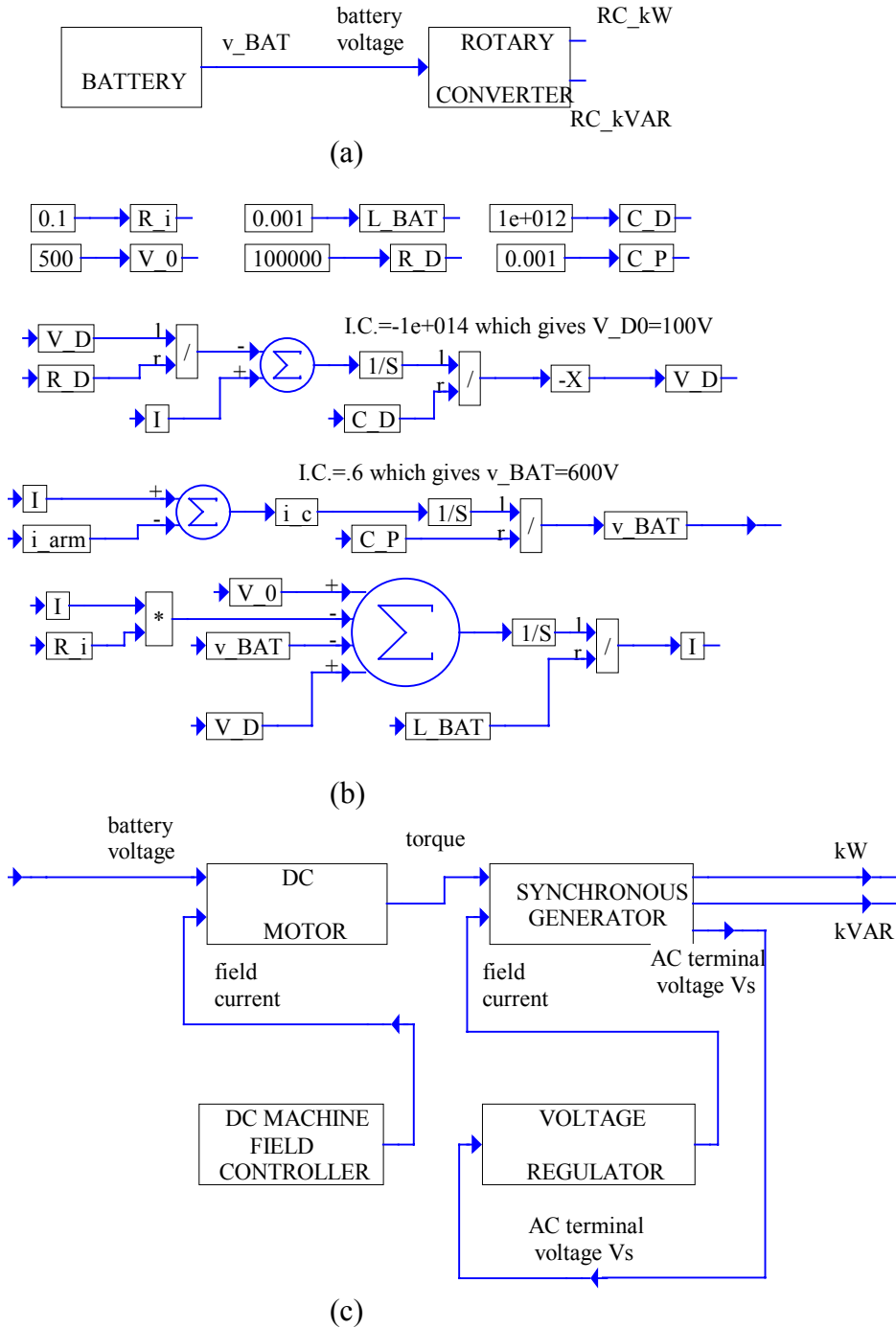


Figure 5.2 Block diagrams of the rotary converter/battery bank assembly: (a) top-view block diagram, (b) expansion of the battery module and (c) second-level diagram showing principle functional blocks of the rotary converter

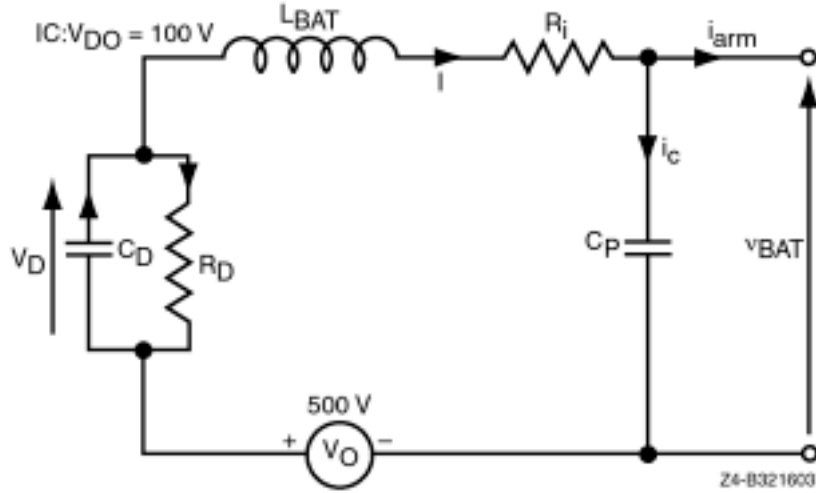


Figure 5.3 Circuit diagram of the battery

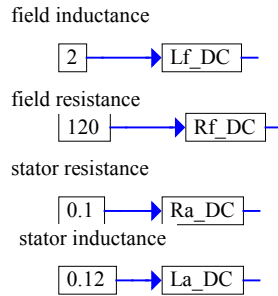
Note that this simulation diagram of the rotary converter module is very similar to that of the diesel generator module shown in Figure 3.2(b). We will take advantage of this when describing its operation. Let us first concentrate on the description of the simulation diagram of the battery module shown in Figure 5.2(b). Its circuit diagram is shown in Figure 5.3. In this diagram, the voltage source $V_0 = 500\text{V}$ represents the minimum battery voltage to which the battery can be discharged without damage. The other part of the voltage of the fully charged battery is represented by the initial value V_{D0} of the voltage V_D across the capacitor C_D which together with the parallel resistor R_D models the battery leakage. It is assumed for this particular simulation, that the fully charged and unloaded battery has the voltage of 600V . To make sure that this voltage is kept practically constant, as the power flow in/out of the battery fluctuates, a large capacitor $C_P = 1000\mu\text{F}$ is connected as is shown in this circuit diagram. With such a capacitor, the voltage drops on the inner resistance R_i and the inner inductance L_{BAT} , when the battery is loaded, can be practically neglected.

Following this explanation, we are ready to write the equations describing the assumed battery model represented by both the circuit diagram in Figure 5.3 and the simulation diagram in Figure 5.2(b). These equations are:

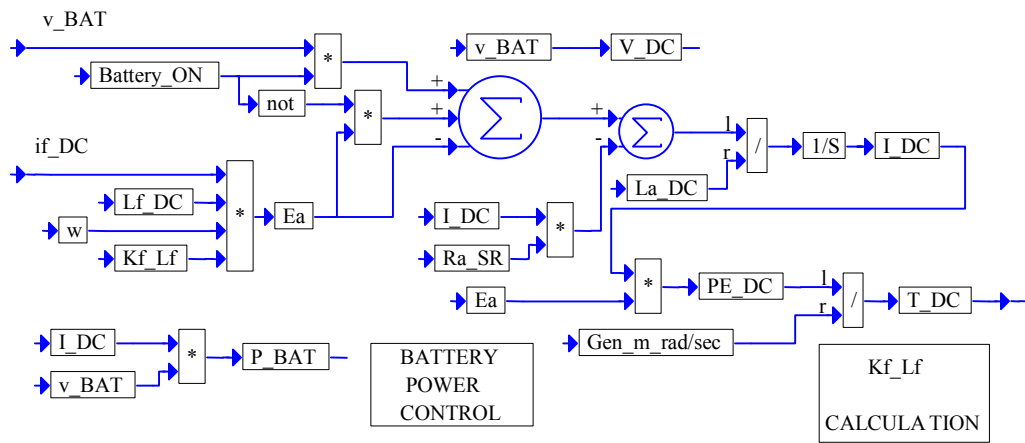
$$V_D = V_{D0} - \frac{1}{C_D} \left(I - \frac{V_D}{R_D} \right) dt ,$$

$$v_{BAT} = \frac{1}{C_P} \left(I - i_{arm} \right) dt ,$$

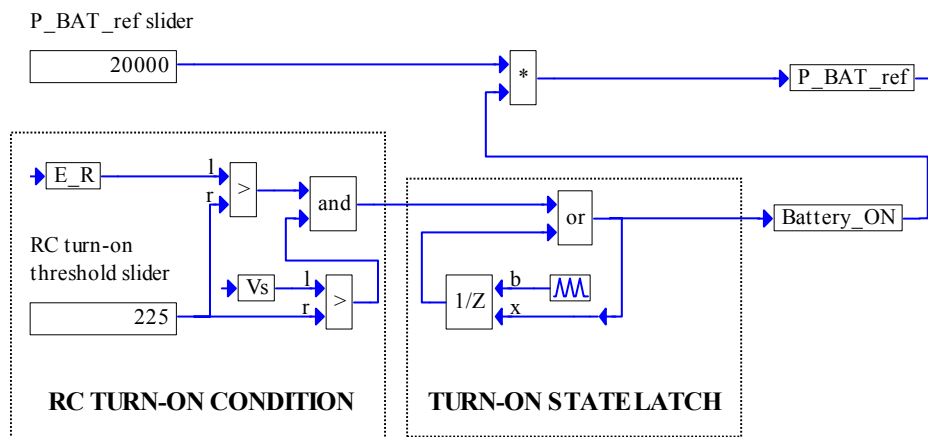
$$I = \frac{1}{L_{BAT}} \left(V_0 - IR_i + V_D - v_{BAT} \right) dt .$$



(a)



(b)



(c)

Figure 5.4 First-level expansion of the DC motor block: (a) parameter module, (b) simulation diagram and (c) expansion of the battery power control block

Now, we are ready to describe the rotary converter module. Clicking on any of the blocks shown in Figure 5.2(c), the user obtains its lower-level expansion. Such expansion of the DC motor block consists of two blocks: (1) the parameter module and (2) the simulation diagram. These blocks in an expanded form, again obtained by clicking the mouse, are shown in Figure 5.4(a) and (b), respectively. The parameter module specifies the following parameters to be declared by the user:

L_{f_DC} - field inductance,

R_{f_DC} - field resistance,

R_{a_DC} - stator resistance,

L_{a_DC} - stator inductance.

In the simulation diagram in Figure 5.4(b), the back emf E_a is proportional to the field current i_{f_DC} generated by the DC machine field controller. It is given by the following equation:

$$E_a = K_{f_Lf} \Phi_f \omega = K_{f_Lf} i_{f_DC} L_{f_DC} \omega.$$

The conversion constant K_{f_Lf} is calculated for every i_{f_DC} value (in the compound block shown in this figure) according to the following equation:

$$K_{f_Lf} = \frac{E_{ant}}{i_{f_DC} L_{f_DC} \omega_{DC_rated}}.$$

It is assumed that the nonlinear characteristic of the no load voltage E_{ant} versus i_f at a constant speed ω_{DC_rated} , resulting from the saturation of the magnetic path in the DC machine, is given. We represent this relation as a table. For each value of i_{f_DC} (in the first column of the table) we read E_{ant} , which we put in the second column of this table. Then, we represent this table as an ASCII file with the extension .map. This file is then used to define the VisSim map block used in the simulation. If this nonlinear characteristic is not given, then we have to use the name plate parameters of the DC machine to calculate the elements of the second column of this table. Using the rated parameters $I_a=350A$, $V_t=600V$ and $R_a=0.1\Omega$, we calculate the rated value of $E_a=565V$ from the equation

$$V_t = E_a + I_a R_a.$$

From the rated RPM value of 1800, we obtain $\omega_{DC_rated}=188.495\text{rad/s}$. Then, assuming the linear relation $E_{ant}=k i_{f_DC}$ and substituting the rated $E_a=565V$ for E_{ant} and the rated value of $i_f=1.49A$ for i_{f_DC} , we find the $k=379.2$. Now we can calculate the entries of the second column of our table. This approach is used in the standard simulation block of the batter/rotary converter. An example, which considers the field saturation curve for the real system is presented as the Case Study 8 in Chapter 8.

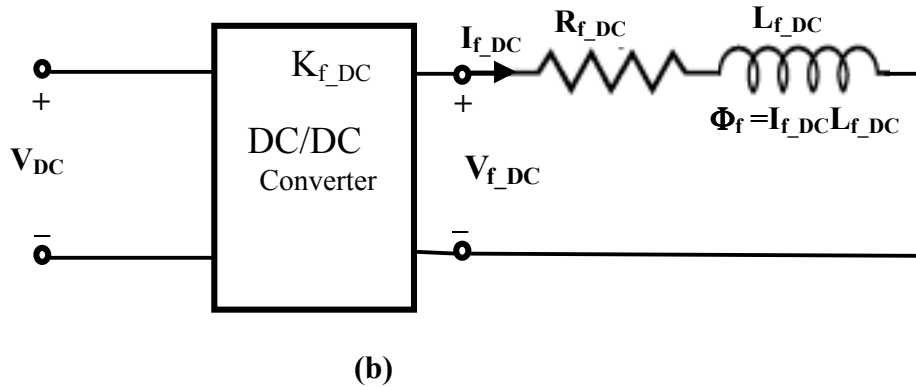
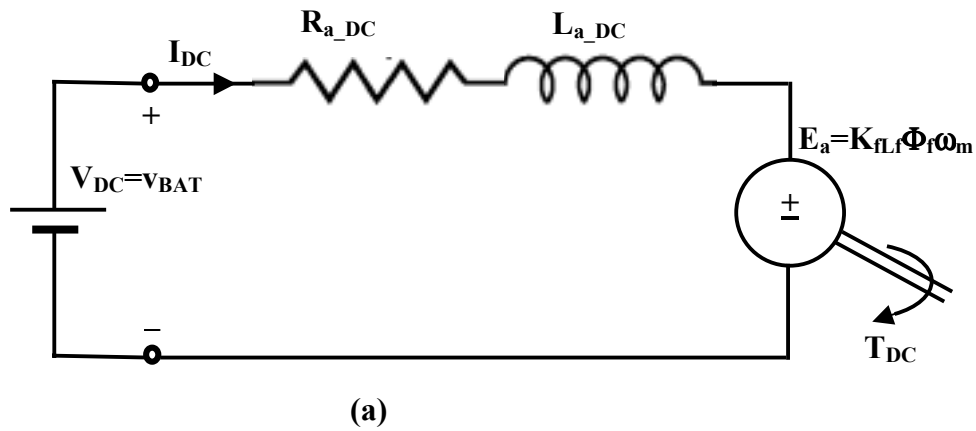


Figure 5.5 Circuit diagrams of the DC motor: (a) armature winding circuit diagram, (b) field winding circuit diagram

The field current i_{f_DC} is calculated so that the battery power

$$P_{BAT} = v_{BAT} I_{DC}$$

follows the battery reference power P_{BAT_ref} , that can be changed with a slider as shown in Figure 5.4(c). The variable P_{BAT_ref} can also be preprogrammed using the VisSim blocks or can be declared as a file. It may be chosen negative, which means that it is desired to charge the battery. In this case, the DC machine works as a generator. It may be chosen positive, which means that it is desired to discharge the battery. However, as can be seen from Figure 5.4(c), the battery reference power will be set to zero (irrespective of its adjusted value), during the start-up phase of the simulation, as long as the binary variable

$Battery_{ON}$ remains equal to zero. As seen in Figure 5.4(c) the binary variable $Battery_{ON}$ switches to 1 when both the per phase voltage V_s and the emf E_R (generated in the synchronous generator block of the rotary converter module) are close enough to the reference per phase voltage V_{s_ref} . This RC turn-on threshold condition can be changed with a slider. The RC turn-on condition implementation diagram, dot-framed in Figure 5.4(c), is introduced for performance stability of the power system in the start-up phase and, once fulfilled, is removed by the turn-on state latch circuit (dot-framed in Figure 5.4(c)). In other words, the binary variable $Battery_{ON}$ remains equal to one.

Going back to Figure 5.4(b), we can see that as long as $Battery_{ON} = 0$, the DC motor remains still. As soon as the condition $Battery_{ON} = 1$ is fulfilled, the DC motor starts its operation. It works as a generator for negative P_{BAT_ref} , i.e., it generates negative torque T_{DC} or is driven by the synchronous machine that, because of this condition, is forced to operate as a synchronous motor. On the other hand, with positive P_{BAT_ref} , the battery is being discharged, and the DC motor produces a positive torque T_{DC} , that in turn drives the synchronous generator. The DC power from the battery is being converted into AC power supplied to the grid. The equations describing the simulation diagram in Figure 5.4(b), under the condition $Battery_{ON} = 1$, are the following:

$$I_{DC} = \frac{1}{L_{a_DC}} (v_{BAT} - E_a - R_{a_DC} I_{DC}) dt ,$$

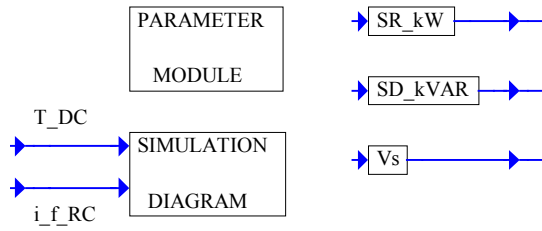
$$P_{E_DC} = E_a I_{DC} , \quad T_{DC} = \frac{P_{E_DC}}{Gen_m_rad/sec} = K_{\mu f} L_{f_DC} i_{f_DC} I_{DC} ,$$

where E_a has already been defined.

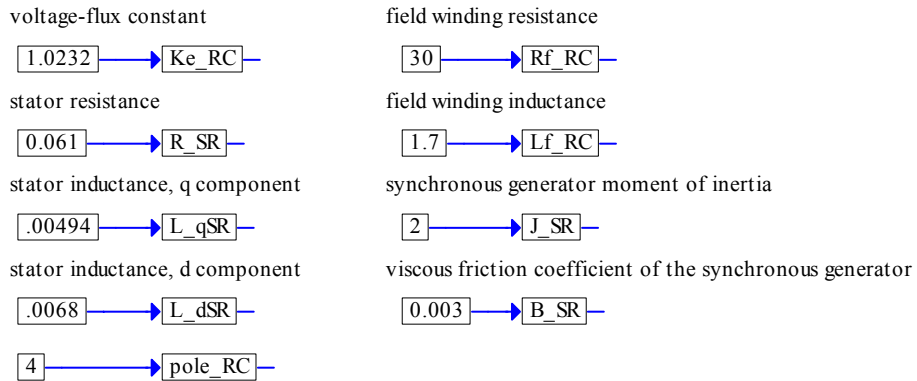
For better understanding of the interaction between the armature winding and the field winding of the DC machine, the relevant circuit diagrams are presented in Figure 5.5. This interaction is realized through the field winding flux Φ_f , that is proportional to the field current i_{f_DC} . We can use the DC/DC converter or AC/DC phase-controlled rectifier to control this current. In particular, as shown in Figure 5.8, the DC/DC conversion constant is controlled by the PID controller.

Figure 5.6 represents the first- and the second-level expansion of the synchronous generator compound block. This figure has the same structure as Figure 3.4 because they both represent the synchronous generator. The essential difference is between parts (c) of these figures. The generation of the voltage E_{qD} in Figure 3.4(c) and the generation of the voltage E_R in Figure 5.6(c) are both governed by the same equation. However, we chose E_{qD} to be a reference, i.e., we assumed that its phase is zero (so we have the input to the d-generator $E_{dD}=0$). Consequently, we cannot make the same assumption for the voltage E_R . This is accounted for in Figure 5.6(c) by calculating the angle

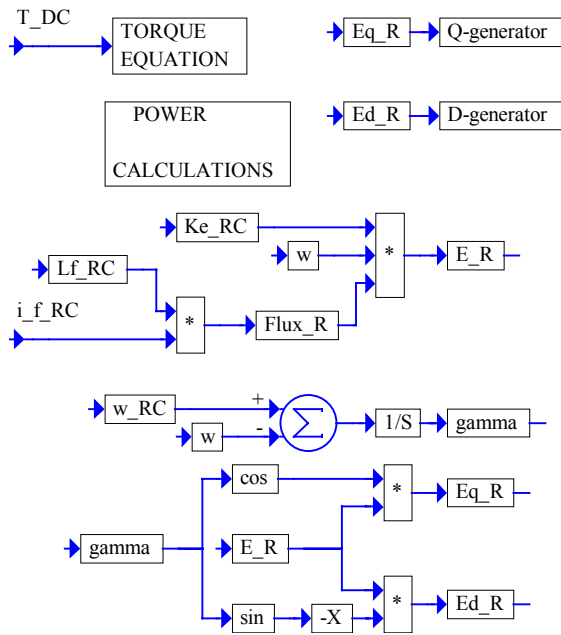
$$\gamma = (\omega_{RC} - \omega) dt$$



(a)

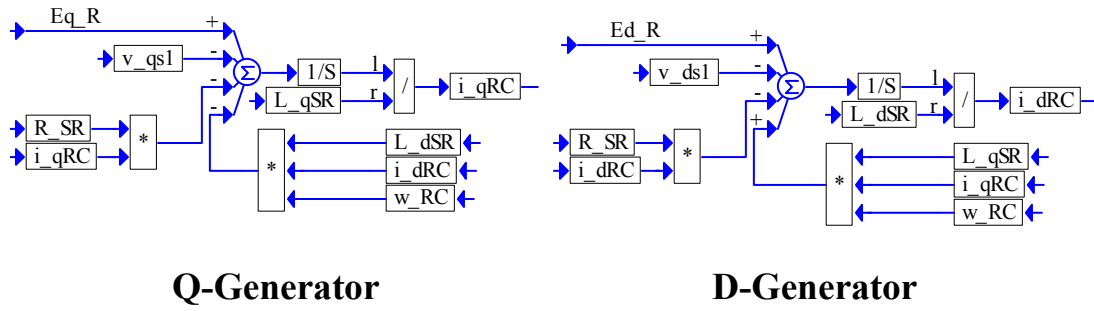


(b)



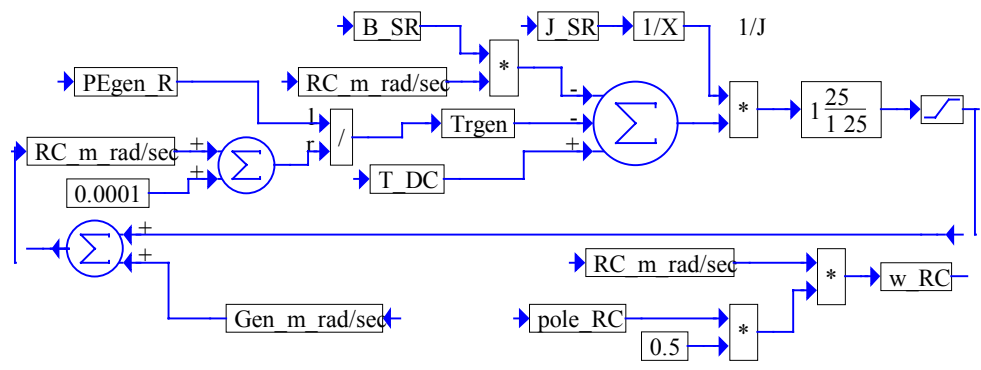
(c)

Figure 5.6 First- and second-level expansion of the synchronous generator block used as a part of rotary converter module: (a) first level expansion, (b) parameter module expansion and (c) simulation diagram expansion

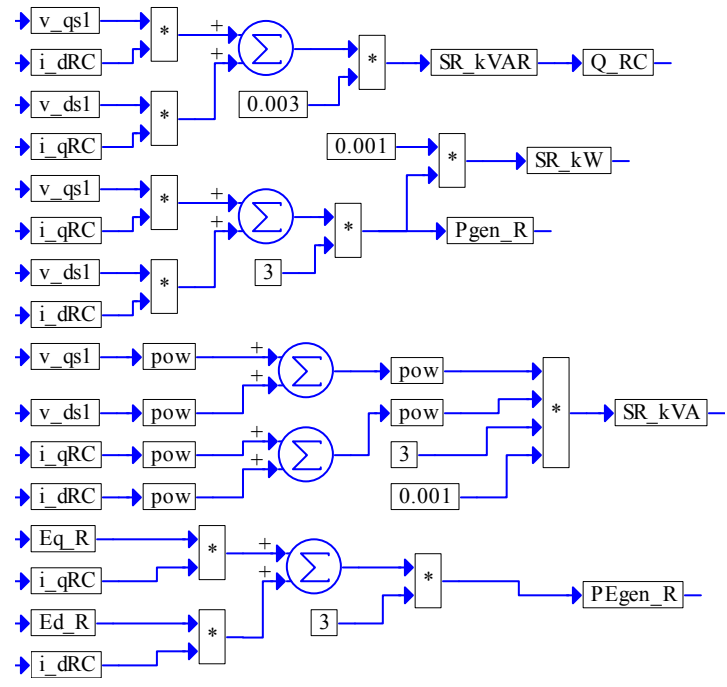


Q-Generator **D-Generator**

(a)



(b)



(c)

Figure 5.7 Simulation diagram of the synchronous generator (rotary converter module):
 (a)Q-generator and D-generator, (b) torque equation and (c) power calculations

and generating q and d components of E_R according to the following equations:

$$\begin{aligned} E_{q_R} &= E_R \cos \gamma, \\ E_{d_R} &= -E_R \sin \gamma, \end{aligned}$$

where ω_{RC} is the angular frequency calculated in Figure 5.7(b) based on the angular velocity of the rotary converter $RC_{m_rad/sec}$ which, in turn, is obtained from the simulation of the torque equation in Figure 5.7(b). Note that the difference $\omega_{RC} - \omega$ is non-zero only in the transient and is used here to establish the angle γ , which in steady-state remains constant or $\omega_{RC} = \omega$. The equation simulated in Figure 5.7(b) reads

$$RC_{m_rad/sec} - Gen_{m_rad/sec} = \frac{1}{J_{SR}} (T_{DC} - T_{rgen} - B_{SR} RC_{m_rad/sec}),$$

where

$$T_{rgen} = \frac{P_{Egen_R}}{RC_{m_rad/sec}}$$

and P_{EgenR} is the electrical power generated and calculated in Figure 5.7(c). In the simulation of this equation, a low-pass filter with the transfer function $25/(s+25)$ is added to filter out the higher harmonics. Power calculations in Figure 5.7(c) are self-explanatory. The Q-generator and the D-generator, shown in Figure 5.7(a), are the same as those in Figure 3.5(b).

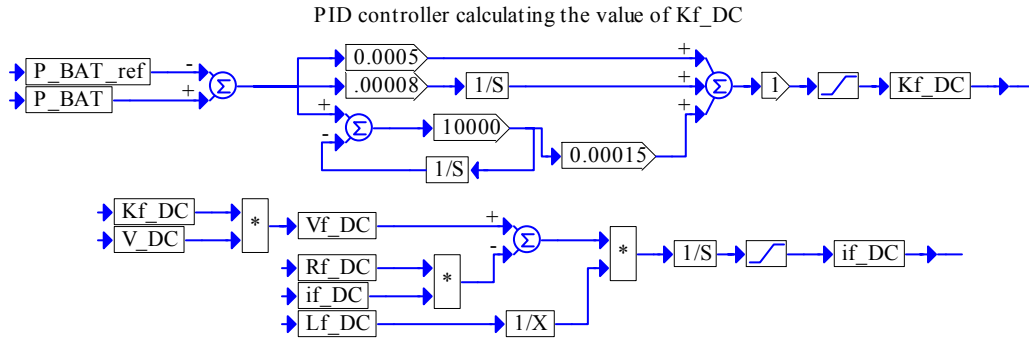


Figure 5.8 Simulation diagram of the DC machine field controller

In Figure 5.8, the simulation diagram of the DC machine field controller is presented. The field current i_{f_DC} is generated to drive the error $P_{BAT_ref} - P_{BAT}$ to zero. First of all, recall that in Figure 5.4(b) we renamed the variable v_{BAT} as follows:

$$V_{DC} \equiv v_{BAT}.$$

In the simulation diagram of Figure 5.8, the name V_{DC} is used for the battery voltage. The simulation diagram in the lower part of this figure is described by the following equations:

$$i_{f_DC} = \frac{1}{L_{f_DC}} (V_{f_DC} - R_{f_DC}i_{f_DC})dt,$$

$$V_{f_DC} = K_{f_DC}V_{DC},$$

and i_{f_DC} is controlled by the DC/DC conversion coefficient K_{f_DC} .

Figure 5.9 presents the simulation diagram of the voltage regulator, that in fact was designed as a voltage/reactive power controller. The purpose of control action **during the start-up period of the simulation** (of the duration to be chosen by the user and set up to be 2 seconds in the simulation diagram in Figure 5.9), generated in this regulator, is to drive the difference

$$err = V_{s_ref} - E_R$$

to zero.

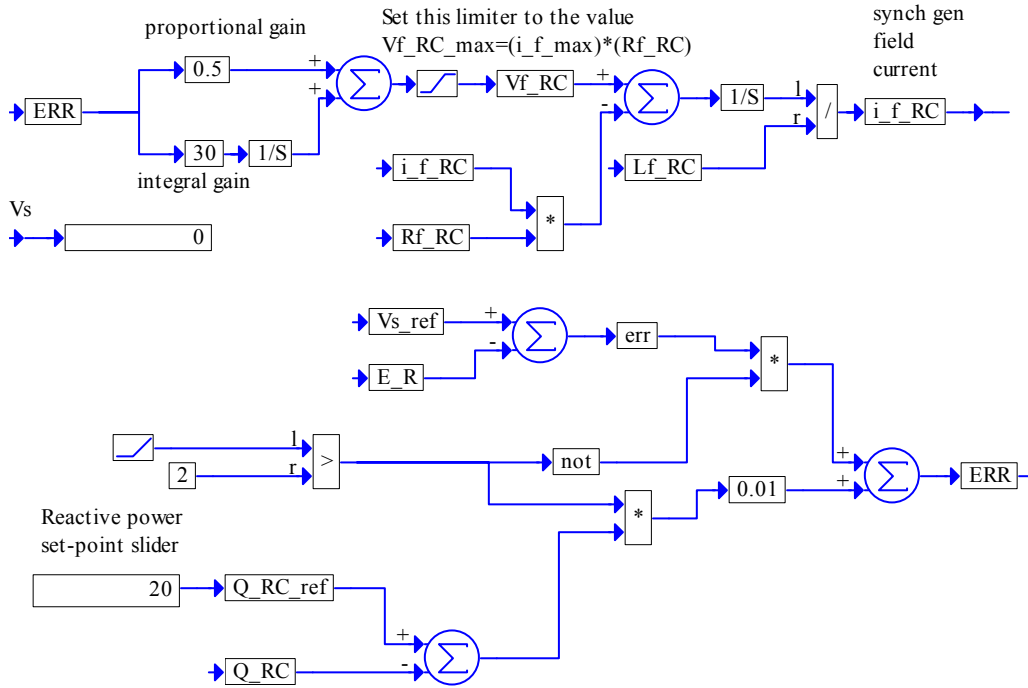


Figure 5.9 Simulation diagram of the voltage regulator

The emf E_R is, according to simulation diagram in Figure 5.6(c), given by the following equation:

$$E_R = K_{e_RC} Flux_R \omega,$$

where

$$Flux_R = L_{f_RC} i_{f_RC},$$

and i_{f_RC} is the field current (DC) of the synchronous generator, and K_{e_RC} is the voltage-flux constant. Therefore, the field current i_{f_RC} is used to control E_R . Consequently, as a result of PI action, the field voltage V_{f_RC} is generated. Then, as shown in Figure 5.9, the simulation of the following equation results in the field current i_{f_RC} :

$$i_{f_RC} = \frac{1}{L_{f_RC}} \int (V_{f_RC} - R_{f_RC} i_{f_RC}) dt .$$

After the start-up period of the simulation, the signal *err* is replaced by the difference

$$Q_{RC_ref} - Q_{RC},$$

where Q_{RC} is the reactive power generated (if positive) or absorbed (if negative) by the rotary converter and Q_{RC_ref} is its reference value, that can be varied with a slider.

Therefore, the user can control the reactive power Q_{RC} . In other words, with P_BAT_ref set to 0, the rotary converter becomes a reactive power source or the reactive power sink. The rotary converter operating in this mode is called a synchronous condenser.

Note that the limiter for V_{f_RC} should be properly set before running the program. The relevant instruction is given in the simulation diagram of Figure 5.9.

Village Load

In Figure 6.1, we present a single-line diagram (as in Fig.1.1) of a hybrid power system where we dot-framed the part of the diagram representing the village load (VL). The user brings the village load to the simulation screen using the **Add** command and selecting the file VL.vsm.

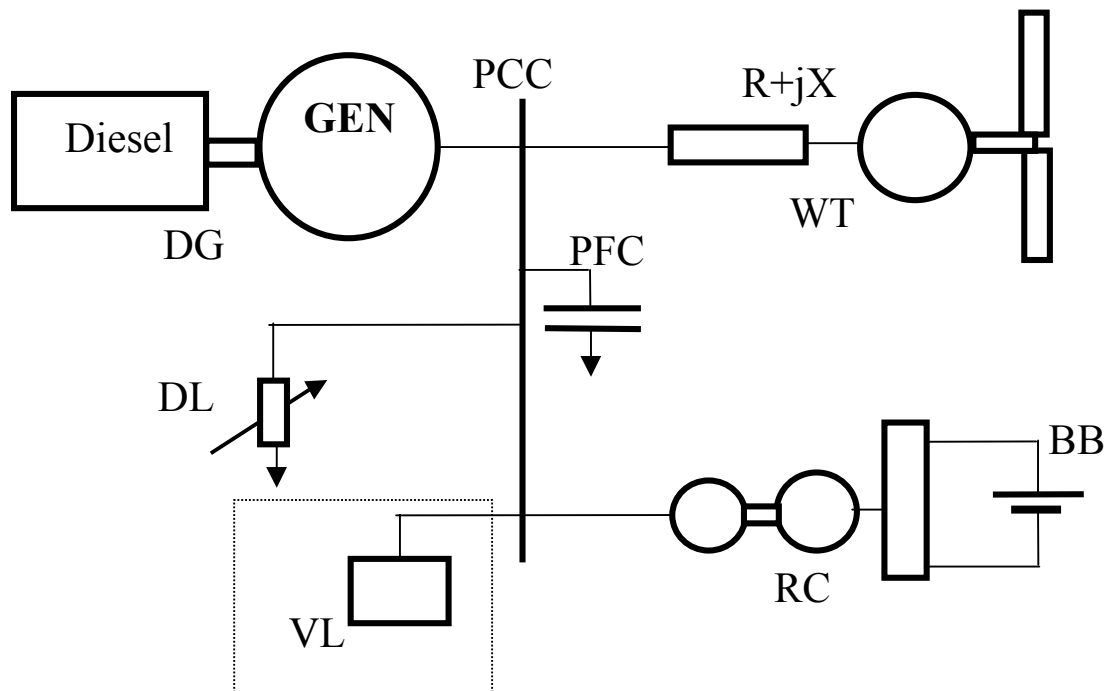


Figure 6.1 A single line diagram of a hybrid power system with the village load module (VL) dot-framed

Figure 6.2(a) represents the block diagram of the VL module as it appears in simulation diagrams. Its first-level expansion, shown in Figure 6.2(b), has two output variables, available for direct monitoring, i.e., the real power load P_V in [kW] and the reactive power load Q_V in [kVAR]. The expansion of its simulation diagram block is shown in Figure 6.2(c) and consists of three compound blocks: (1) power calculations, (2) q-axis and (3) d-axis representations of the load. The output variables of the last two blocks are the component i_{qV} and i_{dV} of the load current. These current components enter the PCC node if the user activates village load by clicking the mouse on the button in the top-view diagram of the PCC module. The parameter module in the first-level expansion is further expanded in Figure 6.2(d). The parameters declared by the user, specific to the application considered, are the rated real power consumption P_V and the power factor pf . The user has a choice between fixed load, declaring the values of variables P_{v1} and pf_1

and the load profile, declaring P_{v2} and pf_2 in a form of time series. The user makes his/her choice by clicking on the button in the parameter module of the VL. Button on (red) corresponds to fixed VL and button off corresponds to VL profile. In Figure 6.3, we show an example of a village load profile represented by the two time series

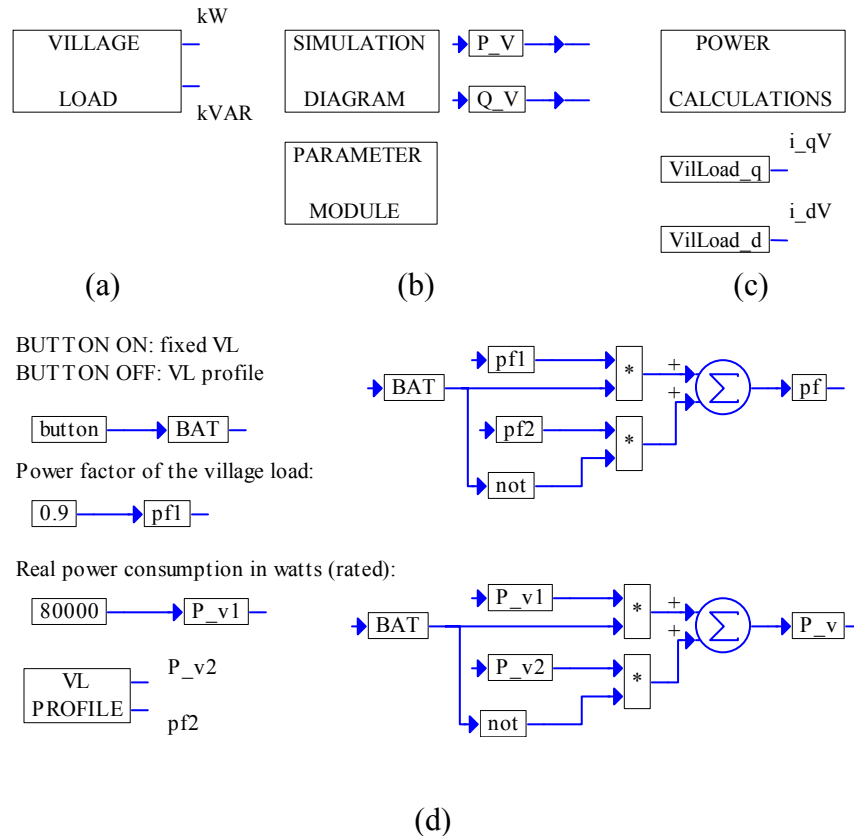


Figure 6.2 Block diagrams of the VL module: (a) representation of village load module in simulation diagrams, (b) first-level expansion, (c) second-level expansion of the simulation diagram and (d) second-level expansion of the parameter module

contained in the ASCII data files power.dat and pf.dat. The user can modify these data files according to the load profile to be represented or setup his own import block in Vissim. To open these files the user has to click on VL Profile (Figure 6.2(d)) and then on the blocks shown in Figure 6.3. The dialog box Import Setup comes up with a button Browse Data. The click on this button opens the data files in Notepad. The data files involved must have the format shown in Figure 6.3, where the first column is the time and the second column is the value of the variable.

In Figure 6.4, the compound blocks, which appear in Figure 6.2(c), are expanded. Figure 6.4(a) shows how both components of the load current are calculated. These calculations are realized by implementation of the equations describing the circuit diagram presented in Figure 6.5. First, however, it is necessary to determine the equivalent rated village load parameters: the resistance R_v and the inductance L_v . These (as shown in the upper part of Figure 6.4(a)) are found by simulation of the following equations:

$$\frac{P_v}{3} = \frac{V_{s_ref}^2}{R_v}, \quad \frac{Q_v}{3} = \frac{V_{s_ref}^2}{X_v}, \quad L_v = \frac{X_v}{\omega_b},$$

where the rated reactive power Q_v is defined as

$$Q_v = \sqrt{S_v^2 - P_v^2} = \sqrt{\left| \frac{P_v}{pf} \right|^2 - P_v^2}$$

with $S_v = P_v / pf$ being the apparent power. The equations mentioned above, describing the circuit diagram in Figure 6.5, are implemented here generate the components of the load current, and are listed below separately for each component. For the q-axis component, the equations read

$$i_{qv} = i_{qv1} + i_{qv2},$$

$$i_{qv1} = \frac{v_{qs1}}{R_v},$$

$$i_{qv2} = \frac{1}{L_v} (v_{qs1} - \omega i_{dv} L_v) dt .$$

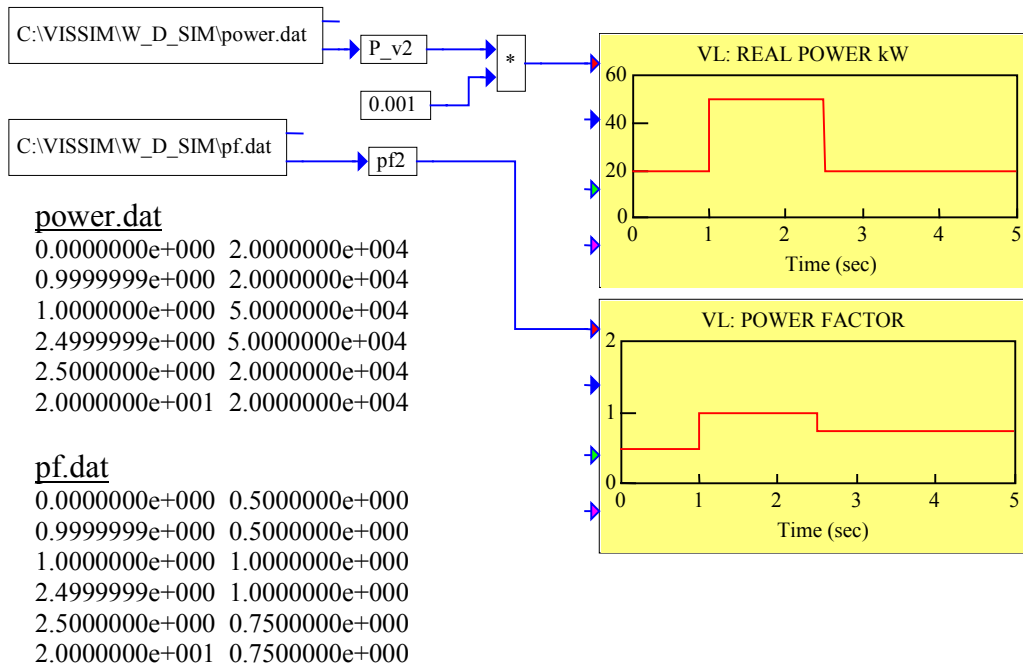
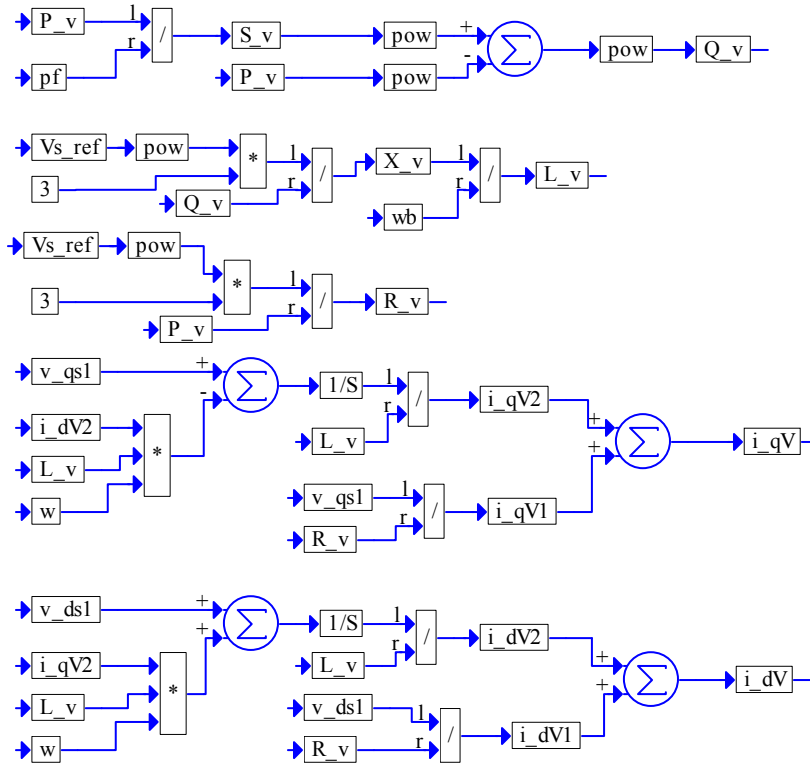
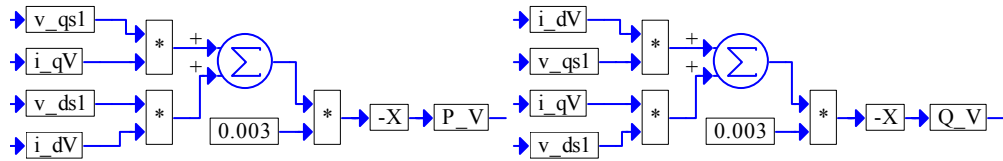


Figure 6.3 An example of a village load profile represented graphically and by ASCII data files power.dat and pf.dat



(a)



(b)

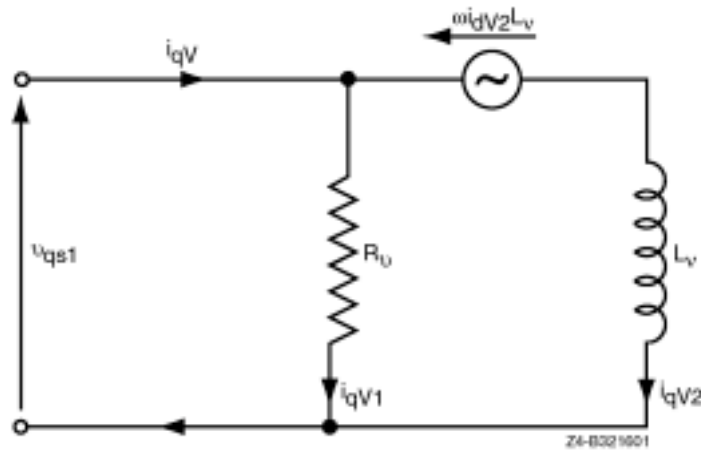
Figure 6.4 Expansions of the compound blocks shown in Figure 6.2(c): (a) calculations of the q and d components of the village load currents and (b) Power calculations

Similarly, for the d-axis component the equations read

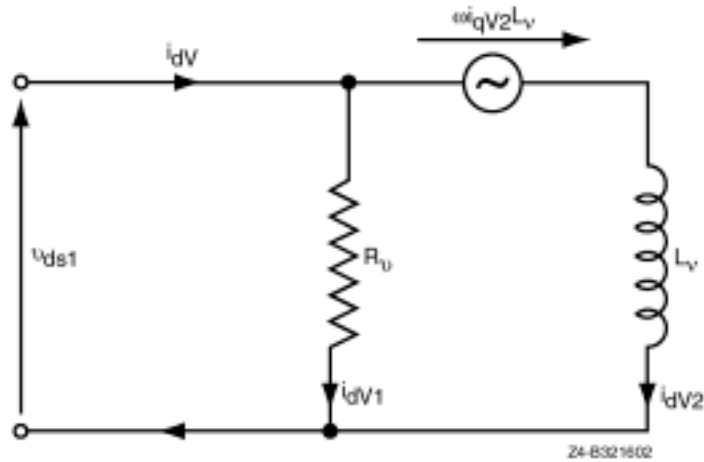
$$i_{dv} = i_{dV1} + i_{dV2},$$

$$i_{dV1} = \frac{v_{ds1}}{R_v},$$

$$i_{dV2} = \frac{1}{L_v} (v_{ds1} + \omega i_{qv} L_v) dt .$$



(a)



(b)

Figure 6.5 Circuit diagram explaining calculations of the VL currents:
(a) q-axis diagram and (b) d-axis diagram

Finally, the calculations of the real power P_V and the reactive power Q_V are implemented in Figure 6.4(b), according to the following equations:

$$P_V = -3 \times 10^{-3} (v_{qs1} i_{qV} + v_{ds1} i_{dV}) \quad [\text{kW}],$$

$$Q_V = -3 \times 10^{-3} (v_{qs1} i_{dV} + v_{ds1} i_{qV}) \quad [\text{kVAR}].$$

P_V and Q_V are computed based on general convention in this program package, i.e., both P_V and Q_V are negative because village always absorbs the real power and the reactive power (inductive load).

Dump Load

In Figure 7.1, we present a single-line diagram (as in Figure 1.1) of a hybrid power system where we dot-framed the part of the diagram representing the dump load (DL). The user brings the DL to the simulation screen using the **Add** command and selecting the file DL.vsm.

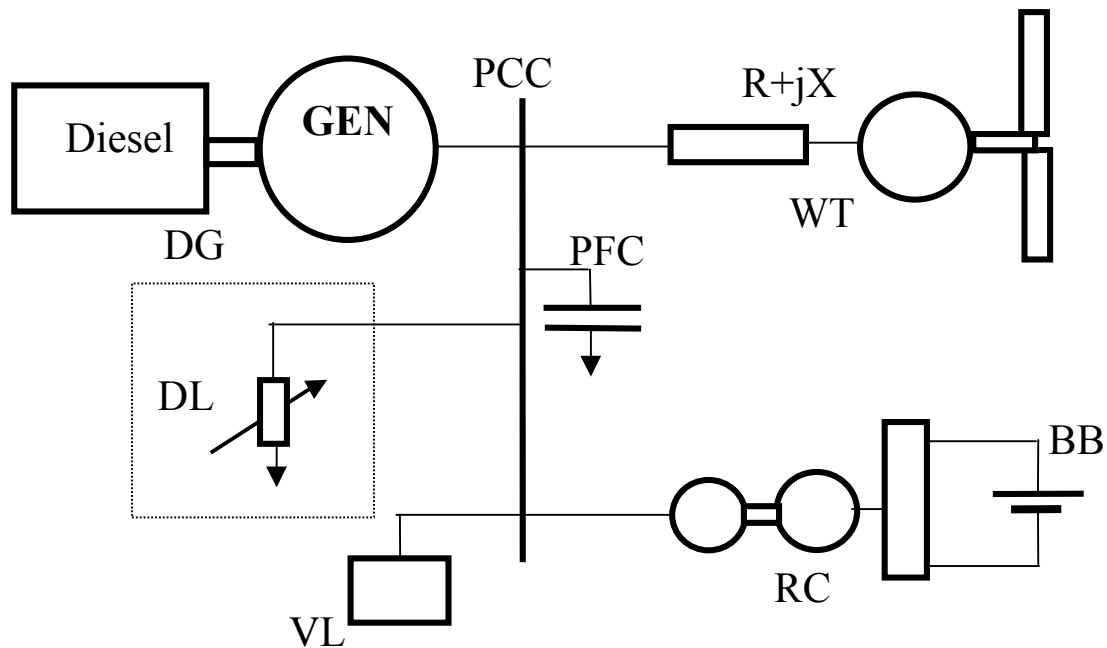


Figure 7.1 A single-line diagram of a hybrid power system with the DL module dot-framed

The DL is used either to keep the diesel generated power above a user-prescribed fraction of its rated power or to control the line frequency $f = \omega / 2\pi$. The choice of the control strategy is defined by the user through turning on and off the button by clicking the mouse in the first-level expansion diagram shown in Figure 7.2(b). In this figure, the principle blocks of the DL module along with their connections are presented. The top-view level representation of the DL module is in Figure 7.2(a). Each of the control strategies defines the number of load elements connected in parallel. The control strategy switch passes to its output the number of elements active, generated by the control strategy selected by the user. As seen in Figure 7.2, when the button is ON (red) or 1, this output is generated by the minimum diesel power controller and when it is OFF (white) or 0, the output is generated by the frequency-based DL controller. The control strategy switching is implemented as shown in Figure 7.3. The simulation diagram of the

frequency controller is shown in Figure 7.4(a). Its parameter module is expanded in Figure 7.4(b).

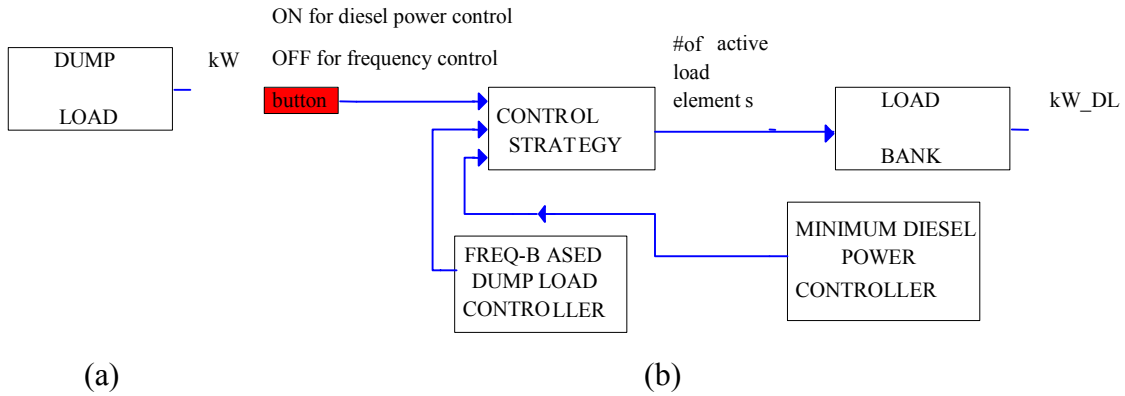


Figure 7.2 Block diagrams of the dump load module: (a) representation of the DL module in simulation diagrams and (b) first-level expansion

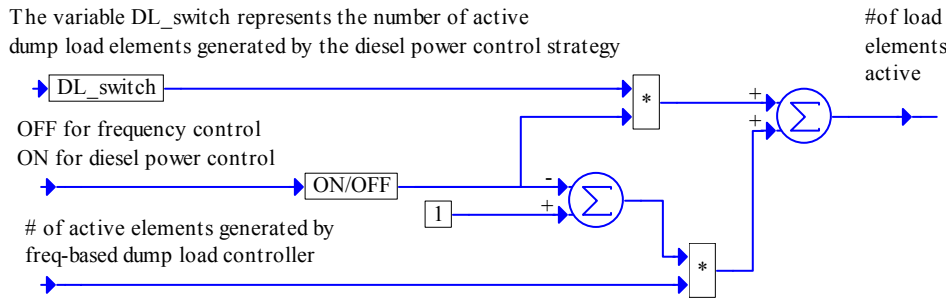


Figure 7.3 Control strategy switch of the DL module

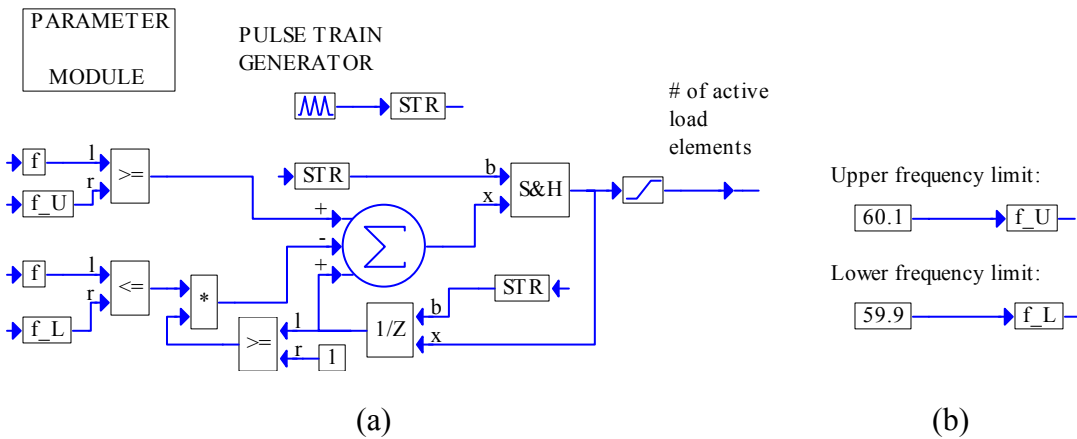


Figure 7.4 Frequency-based DL controller: (a) simulation diagram and (b) expansion of the parameter module

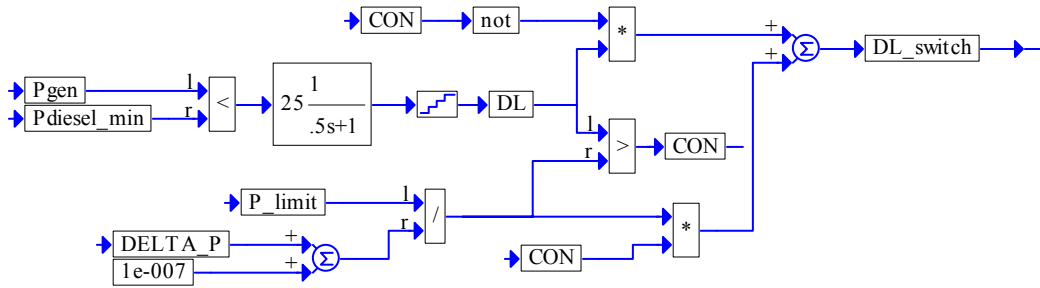


Figure 7.5 Minimum diesel power controller

It contains the upper frequency limit f_U and the lower frequency limit f_L , both are chosen by the user. The output of the frequency-based DL controller is updated every sampling period, established by the pulse-train generator. Its value is set to 0.1 s, but can be easily changed by the user. Because of the limiter connected at the output, the number of active load elements, generated by this controller is never less than one. So, the minimum load is represented by one active load element. Because of the unit delay element, activated every sampling period, the unconstrained (or taken before the limiter) number of active load elements, at the previous sampling instant, is obtained. If this number is greater than or equal to 1 and the current line frequency is less than or equal to f_L , then the controller decreases the number of active load elements by 1, which results in a decreased load. On the other hand, as long as the current line frequency remains greater than f_U , the number of active load elements will increase by 1 every sampling instant.

The simulation diagram of the minimum diesel power controller is shown in Figure 7.5. The system load, represented by the power P_{gen} , is compared with the minimum diesel load $P_{diesel_minimum}$. The goal is to implement diesel power control strategy by generating a number of active dump load elements (connected in parallel) needed to keep the generated power P_{gen} above a fraction $P_{diesel_minimum}$ of the diesel rated power prescribed by the user in the simulation diagram of the DG. In the simulation diagram in Figure 7.5, the variable DL_{switch} represents the number of active load elements. To determine the value of the variable DL_{switch} , we introduce an auxiliary variable DL, which assumes positive integer values whenever the diesel load P_{gen} drops below the minimum diesel load value. The increments of DL correspond to dump load power increments $DELTA_P$ as can be seen in Figure 7.6. The maximum number of these increments is calculated as

$$n = \frac{P_limit}{DELTA_P}.$$

Then, as shown in the simulation diagram in Figure 7.5, we have

$$DL_{switch} = \begin{cases} DL & \text{if } DL \leq n \\ n & \text{otherwise} \end{cases}.$$

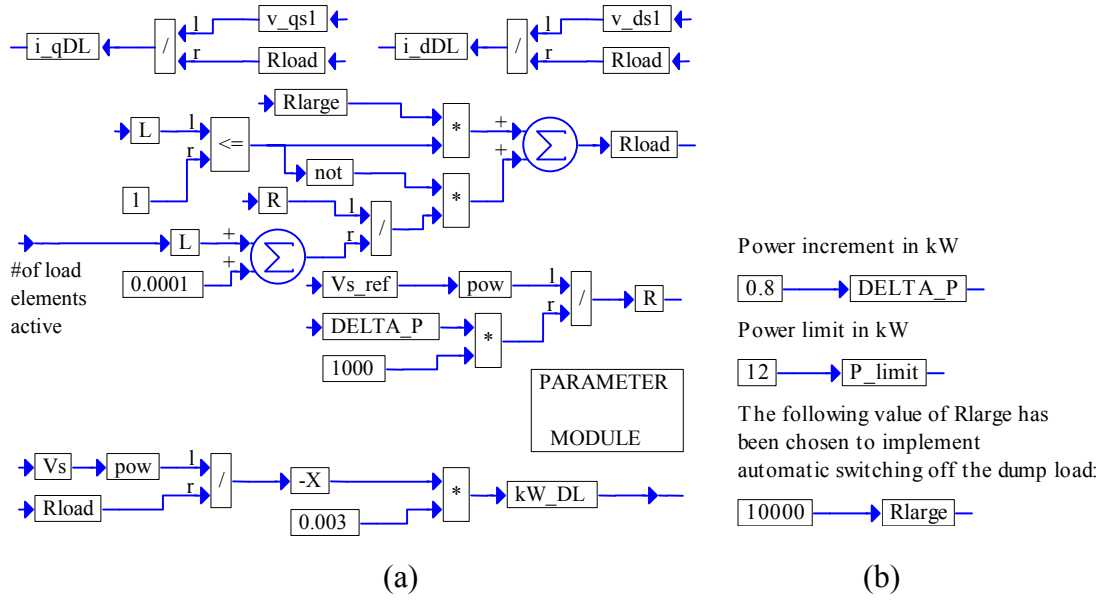


Figure 7.6 Load bank block: (a) simulation diagram with power calculation and (b) expansion of the parameter module

The implementation of the load bank block is shown in Figure 7.6(a) and its parameters in Figure 7.6(b). The user declares a value of the variable P_limit that is the power limit of the DL or total DL power that can be consumed in the system. In addition, the user must also declare the power increment $DELTA_P$ (per phase).

We now explain how the values of these two variables are related to the DL structure of the simulated power system. Consider the values shown in Fig.7.6(b) as an example. We determine that we need 15 increments of 0.8 kW to generate the load of 12 kW. Such load, can be implemented with 15 equal load sections or only 4 load sections if the load structure is binary, i.e., the load sections are 0.8 kW, 1.6 kW, 3.2 kW, and 6.4 kW. In general, if we have binary load with n sections and we want to have power increment of $DELTA_P$, then we may have

$$P_limit = (2^n - 1) DELTA_P.$$

The resistance of the dump load R_{load} is calculated and if the number of load elements active equals one (which corresponds to the smallest load), the dump load is practically disconnected by making R_{load} equal R_{large} . In the same simulation diagram, the components of the current contributed to the PCC module are determined, i.e.,

$$i_{qDL} = \frac{v_{qs1}}{R_{load}}, \quad i_{dDL} = \frac{v_{ds1}}{R_{load}}.$$

In addition, the real power consumed is found as $kW_{DL} = -10^{-3} \frac{V_s^2}{R_{load}}$ [kW].

PART II

CASE STUDIES

AND

VALIDATION TESTS

Case Studies

The modular simulation system RPM-SIM has been developed to

- Facilitate an application-specific and low-cost performance study of wind-diesel hybrid power systems (both mechanical and electrical components are simulated)
- Analyze both static and dynamic performance
- Help in the development of control strategies
- Simulate different wind speed profiles and different village load profiles.

The system has the following capabilities/characteristics:

- Modular and multilevel structure provided by the VisSim visual environment
- Clear and easy to understand system presentation
- Customized configuration setup is within a click of the mouse
- Modifications are easy to make
- Effects of system modifications can be immediately examined.

What Can this Simulation Tool be Used for?

- **Control strategy simulation**
A proper control strategy must be developed to take full advantage of the wind energy when it is available and to minimize diesel fuel consumption, while maintaining desired system performance.
- **Inclusion of constraints**
To implement this control strategy, a control system must be designed subject to the constraints specific for a particular application. These include the power generation limitations of the diesel generator, wind turbine generator, and battery bank/rotary converter assembly; excitation time constants; and dump load parameters.

- **Checking stability of the power system under time-varying conditions**

To properly control the system's voltage and frequency, the time-varying power generation/consumption conditions of the system must be considered. The levels of changes which drive the system into instability should be determined. The factors to be considered are

- Wind speed: high winds may try to drive the diesel engine resulting in the loss of frequency control and instability
- Village load (represented by the real power and the power factor) including events such as start-up of induction motor load, start-up of large heating load, loss of load and sudden change of power factor.

To maintain the system stability by keeping the diesel generation at a required minimum level, a proper dump load control strategy must be developed.

Using case studies of a hybrid system, we demonstrate some of the benefits that result from the ease of understanding the effects of the modifications introduced in these complex dynamic systems by the designer. In all case studies, we assumed the following power sign convention:

- Power generated is positive
- Power consumed is negative.

Using Case Study 3 as an example, Appendix 1 has a step-by-step procedure on how to set up the simulation diagram and how to run the simulation.

CASE STUDY 1: PCC+DG+VL

Principal modules in this case study include the following:

- Diesel generator with a rated power of 200 kW
- Village load of 50 kW at the power factor $pf = 0.75$, switched to 150 kW at $t = 6$ s and switched again to 75 kW at $t = 12$ s.

A power system with this configuration is presented in Figure 8.1, where we show both the single-line diagram and the top-view RPM-SIM simulation diagram. This simulation diagram is obtained by adding the following files to the simulation screen: PCC.vsm, DG.vsm and VL.vsm. For this system, we obtained traces of power, voltage, and frequency shown in Figure 8.2. Here, we explain the sequence of simulation events documented in Figure 8.2.

TIME/EVENT SEQUENCE

$t = 0$	Diesel generator starts up.
$t = 4$ s	Line voltage V_s reaches the reference value of 266 V and the relative frequency is close to 1. Power generated by the diesel generator is at the level of 50 kW and the same power is consumed by the village load.
$t = 6$ s	Village load is increased to 150 kW. This increment is followed by the sharp increase to the value of 150 kW of the power provided to the system by the diesel generator. Transient small dips of frequency and line voltage can be seen.
$t = 12$ s	Village load is reduced to 75 kW. Power generated by the diesel generator decreases sharply to this value. Transient small jumps of frequency and line voltage can be seen.
$t > 16$ s	Steady-state with all variables constant is reached.

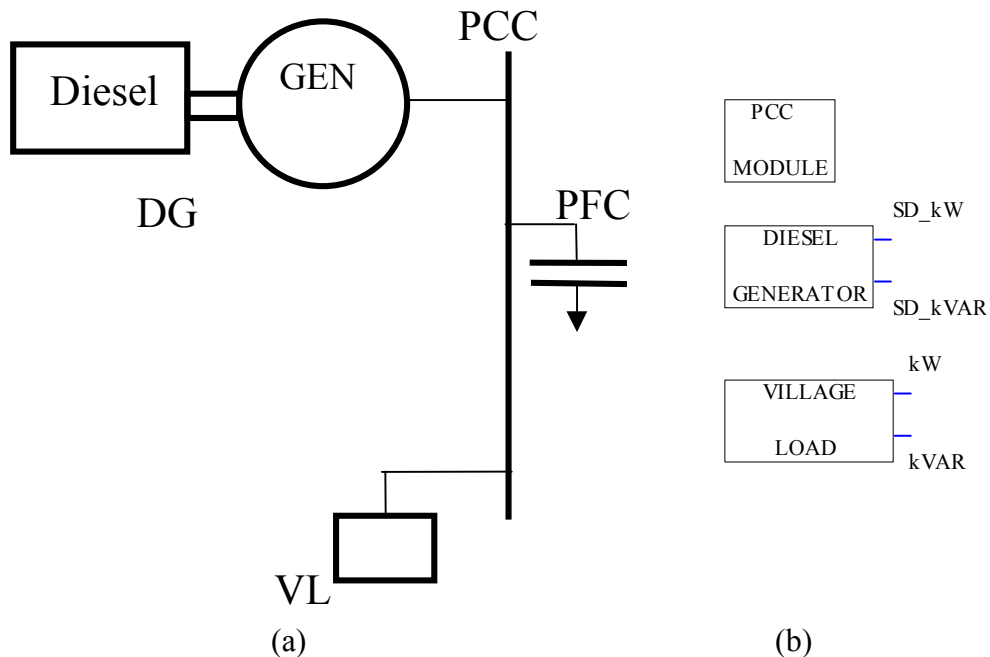


Figure 8.1 Power system composed of a diesel generator (DG) and village load (VL):
(a) single-line diagram and (b) top view of the RPM-SIM simulation

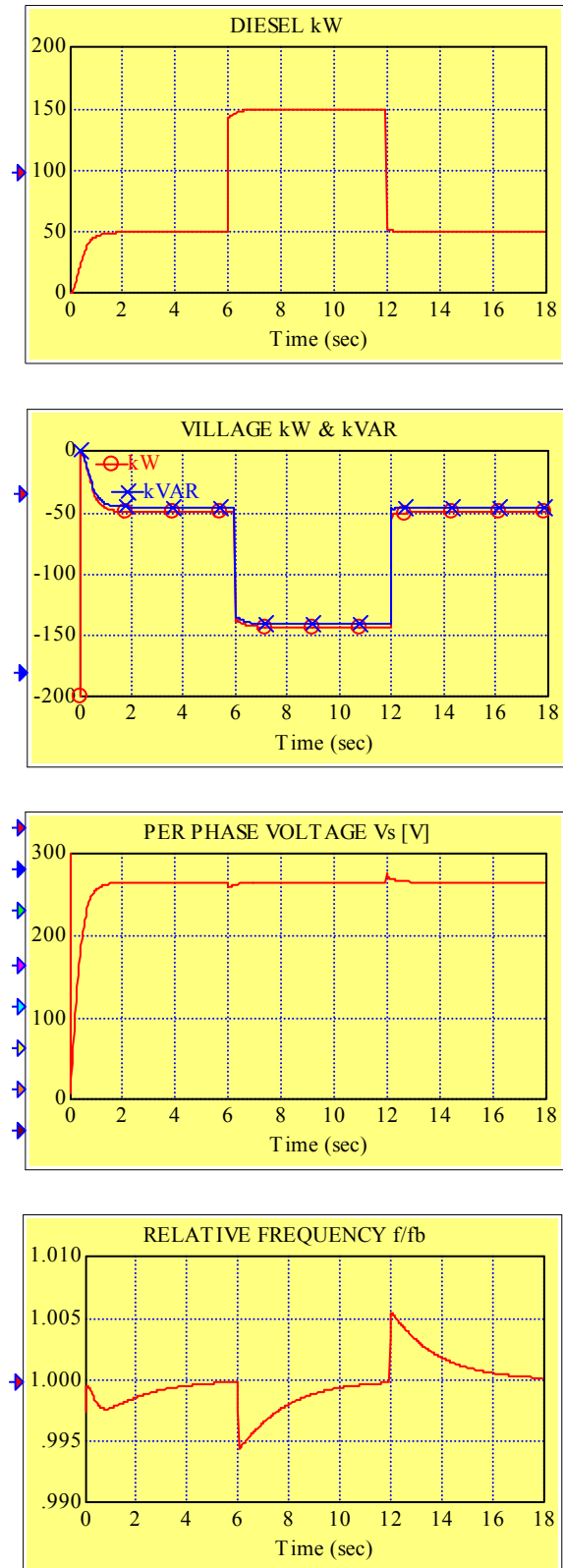


Figure 8.2 Traces of power, voltage, and frequency for the system composed of a diesel generator and a variable village load

CASE STUDY 2: PCC+DG+WT+VL

Principal modules in this case study include the following:

- Diesel generator with rated power of 200 kW
- AC wind turbine driven by the wind given by a file of the wind speed time series
- Village load of 30 kW at the power factor $pf = 0.75$.

A power system with this configuration is presented in Figure 8.3 where we show both the single-line diagram and the top-view RPM-SIM simulation diagram. The simulation diagram is obtained by adding the following files to the simulation screen: PCC.vsm, DG.vsm, VL.vsm and wtg_base.vsm. For this system, we obtained traces of power, voltage and frequency shown in Figure 8.4. Here, we explain the sequence of simulation events documented in Figure 8.4.

TIME/EVENT SEQUENCE

$t = 0$	Diesel generator starts up.
$t = 4$ s	Line voltage V_s reaches the reference value of 266 V and the relative frequency is close to 1. Power generated by the diesel generator is at the value of 30 kW (without the dump load no minimum value can be imposed) and the same power is consumed by the village load.
$t = 6$ s	Induction machine starts to motor the wind turbine and creates a large load. Power generated by the diesel generator increases sharply. transient small frequency and line voltage dips are observed.
$t = 8.5$ s	Power consumption of the induction machine, reaching the synchronism, rapidly drops.
$t = 10$ s	Wind turbine generator starts to generate. Power generated by the diesel generator decreases below 30 kW, the consumption level of the village.
$t > 12.5$ s	Diesel generator is overpowered by the wind turbine generator and the frequency control is lost.

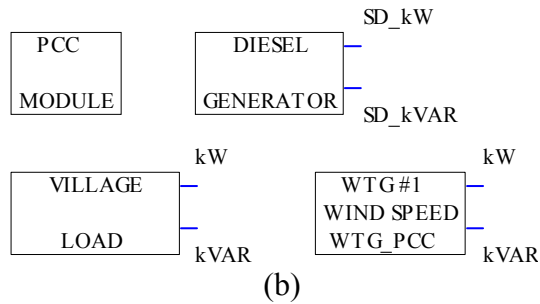
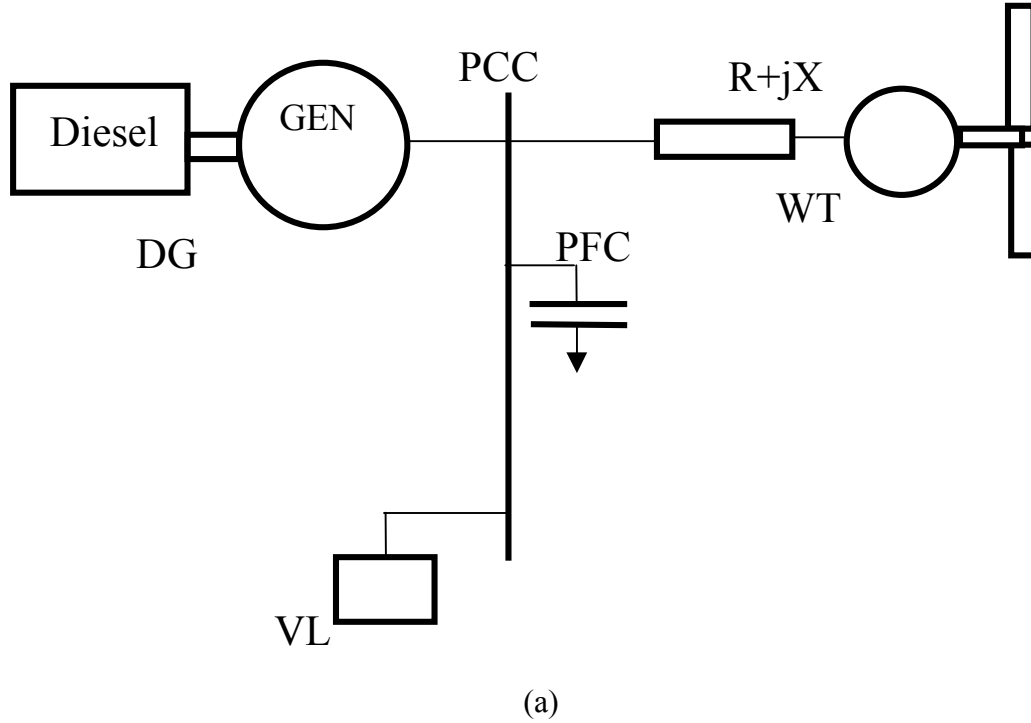


Figure 8.3 Power system composed of a diesel generator (DG), an AC wind turbine (WT), and village load (VL): (a) single line diagram and (b) top view of the RPM-SIM simulation.

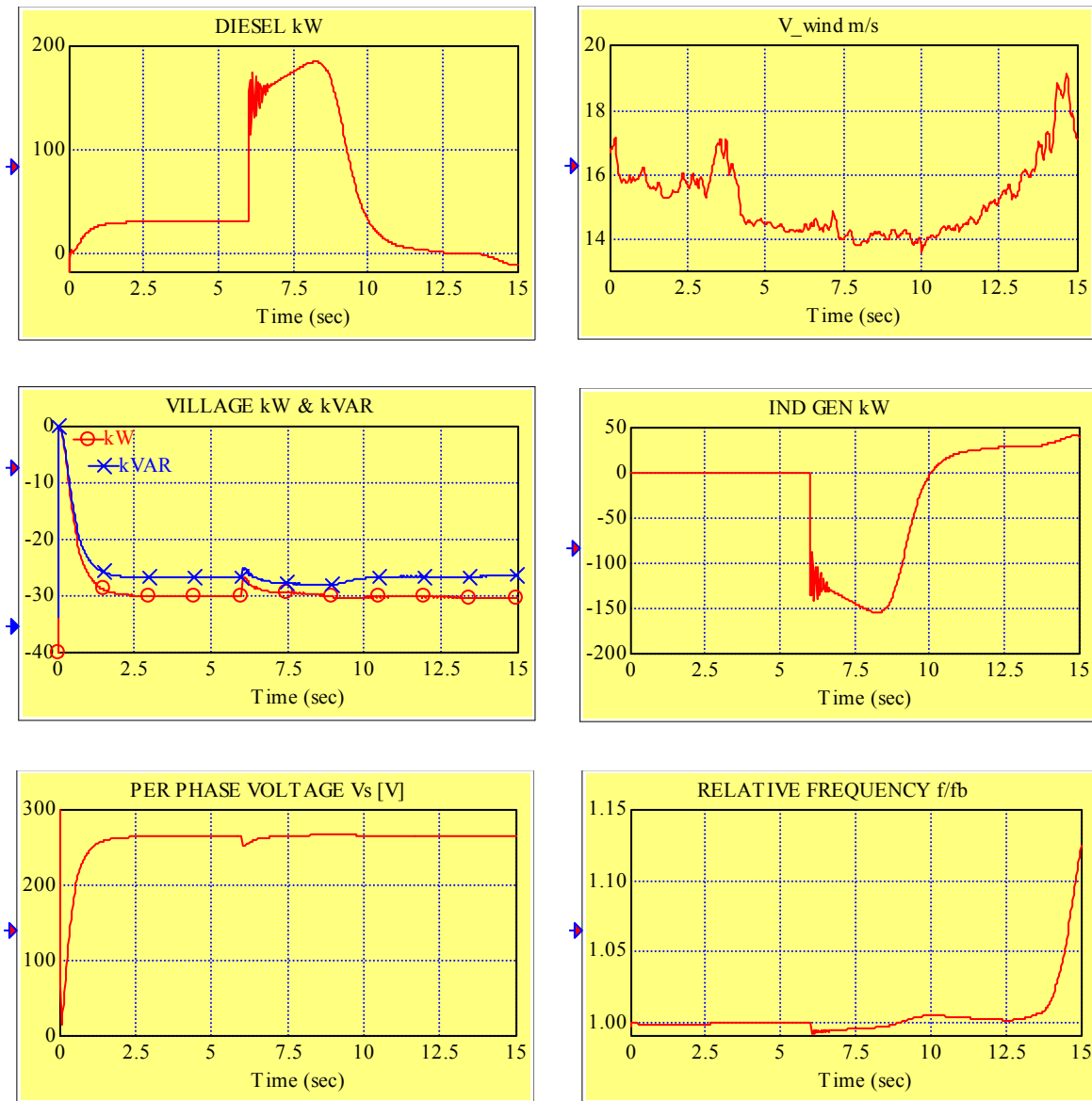


Figure 8.4 Traces of power, voltage, and frequency for the system composed of a diesel generator, an AC wind turbine, and the constant village load

CASE STUDY 3: PCC+DG+WT+VL+DL

Principal modules in this case study include the following:

- Diesel generator with a rated power of 200 kW and minimum load of 50 kW
- AC wind turbine driven by the wind determined by a file of the wind speed time series
- Village load of 30 kW at the power factor $pf = 0.75$
- Dump load incremented by the diesel power control strategy.

A power system with this configuration is presented in Figure 8.5 where we show both the single-line diagram and the top-view RPM-SIM simulation diagram. The simulation diagram is obtained by adding the following files to the simulation screen: PCC.vsm, DG.vsm, VL.vsm, DL.vsm and wtg_base.vsm. For this system, we obtained traces of power, voltage, and frequency shown in Figure 8.6. Here, we explain the sequence of simulation events documented in Figure 8.6.

TIME/EVENT SEQUENCE

$t = 0$	Diesel generator starts up. Power generated by the diesel generator increases to its specified minimum value of 50 kW, and the power consumed by the village load increases to its specified required value of 30 kW; the steady-state power difference of 20 kW is consumed by the dump load controlled by the diesel power control strategy.
$t = 4$ s	Line voltage V_s reaches the reference value of 266 V and the relative frequency is close to 1. Power generated by the diesel generator is at its specified minimum value of 50 kW. The induction machine starts to motor the wind turbine and creates a large load. Power generated by the diesel generator increases sharply. Dump load is immediately reduced to zero. Transient small dips of frequency and line voltage are observed.
$t = 7$ s	Power consumption of the induction machine, reaching the synchronism, rapidly drops.
$t = 7.5$ s	Power generated by the diesel drops to its minimum level of 50 kW. Diesel power control strategy compensates for the power surplus by incrementing the dump load.

$t > 10$ s

Steady state is reached and all system variables remain constant.

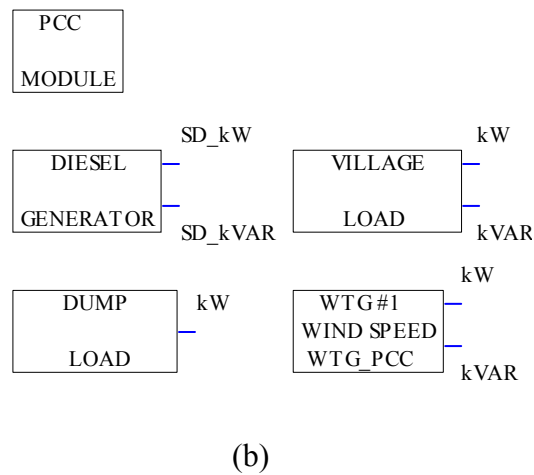
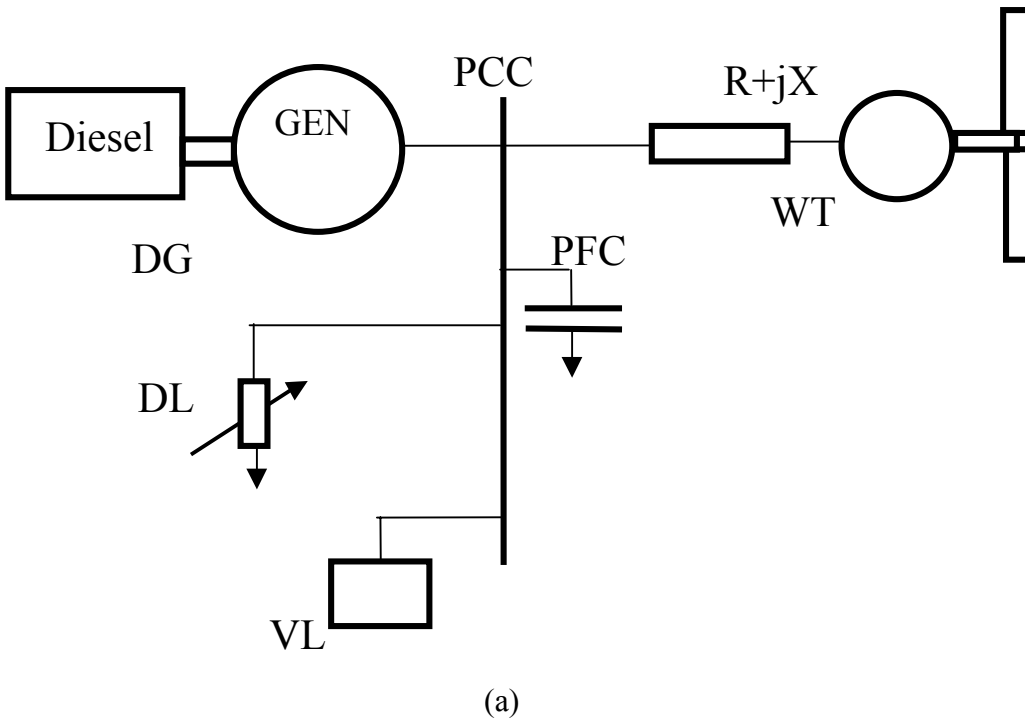


Figure 8.5 Power system composed of a diesel generator (DG), an AC wind turbine (WT), a dump load (DL) and a village load (VL): (a) single-line diagram and (b) top view of the RPM-SIM simulation.

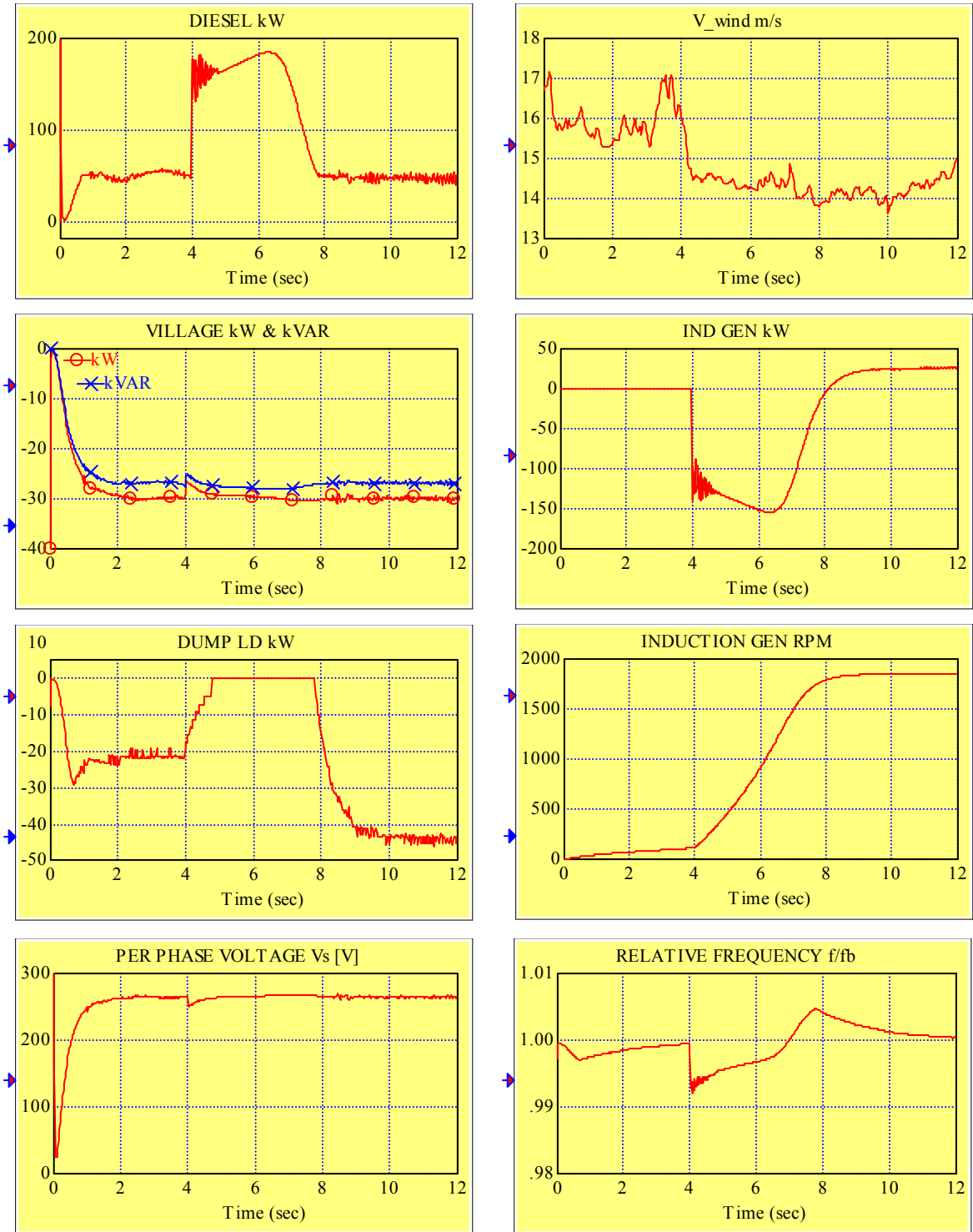


Figure 8.6 Traces of power, rpm, voltage, and frequency for the system composed of a diesel generator, an AC wind turbine, the constant village load and a dump load

CASE STUDY 4: PCC+DG+RC+VL

Principal modules in this case study include the following:

- Diesel generator with rated power of 200 kW and minimum load of 50 kW
- Village load of 100 kW at the power factor $pf = 0.75$
- Rotary converter with a preprogrammed battery reference power

A power system with this configuration is presented in Figure 8.7 where we show both the single line diagram and the top-view RPM-S_{IM} simulation diagram. The simulation diagram is obtained by adding the following files to the simulation screen: PCC.vsm, DG.vsm, VL.vsm and RC.vsm. For this system, we obtained traces of power, voltage, and frequency shown in Figure 8.8. Here we explain the sequence of simulation events documented in Figure 8.8.

TIME/EVENT SEQUENCE

$t = 0$	Diesel generator starts up.
$t = 5$ s	Line voltage V_s reaches the reference value of 266 V and the relative frequency is close to 1. The power generated by the diesel generator is at 100 kW and the same power is consumed by the village load. The battery reference power $P_{BAT_ref} = 0$.
$t = 6$ s	The battery reference power is switched to -20 kW (which according to our convention is a request for charging the battery). This increment is followed by the power consumed and transmitted to the battery by the rotary converter (slow response because of a large time constant of the field-controlled DC motor of the rotary converter). The power generated by the diesel generator reaches approximately the level of 120 kW to cover the demand of 100 kW from the village and 20 kW from the battery. The line voltage remains constant. The frequency after a slight dip recovers to its reference value.
$t = 21.5$ s	The battery reference power is switched to 20 kW (which according to our convention is a request for discharging the battery). This increment is followed by the power generated by the rotary converter, i.e., this corresponds to the increment of 40 kW.

The power generated by the diesel generator decreases from the level of 120 kW with the same time constant and at the new steady-state reaches the value of 80 kW.

The transient power changes result in a small transient increase of the frequency.

Line voltage remains constant.

The power consumed by the village remains constant and is partially provided by the diesel generator and partially provided by the battery.

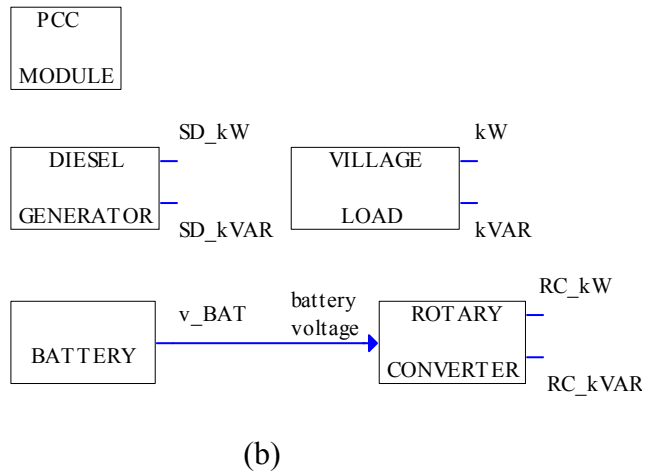
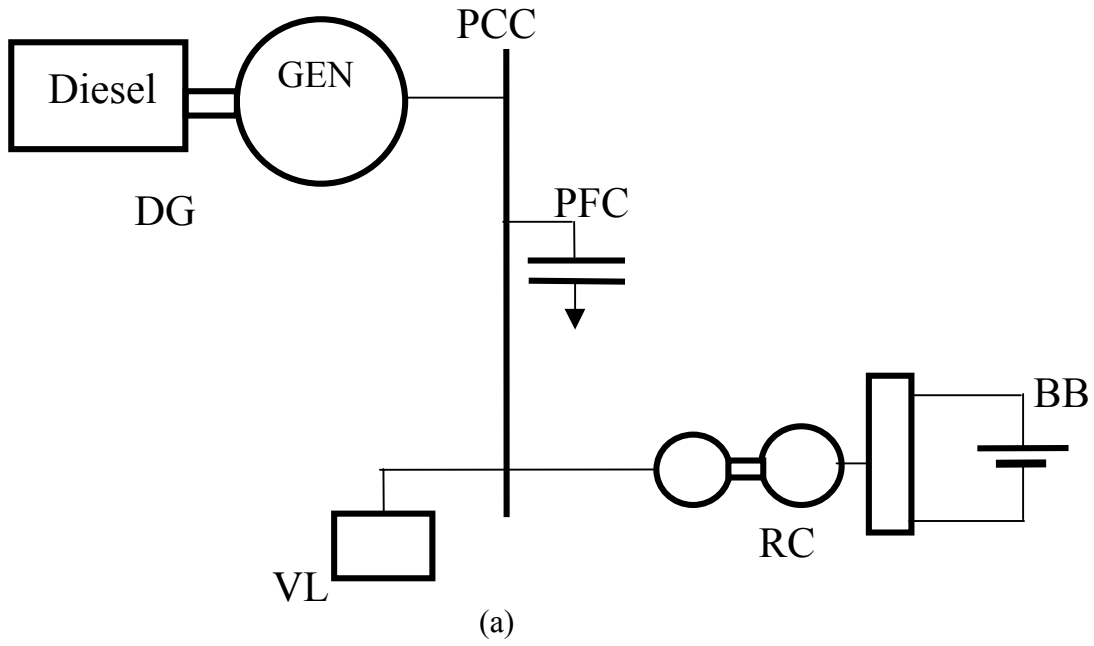


Figure 8.7 A power system composed of a diesel generator (DG), a village load (VL), and a rotary converter/battery bank assembly (RC):
 (a) single-line diagram and (b) top view of the RPM-SIM simulation

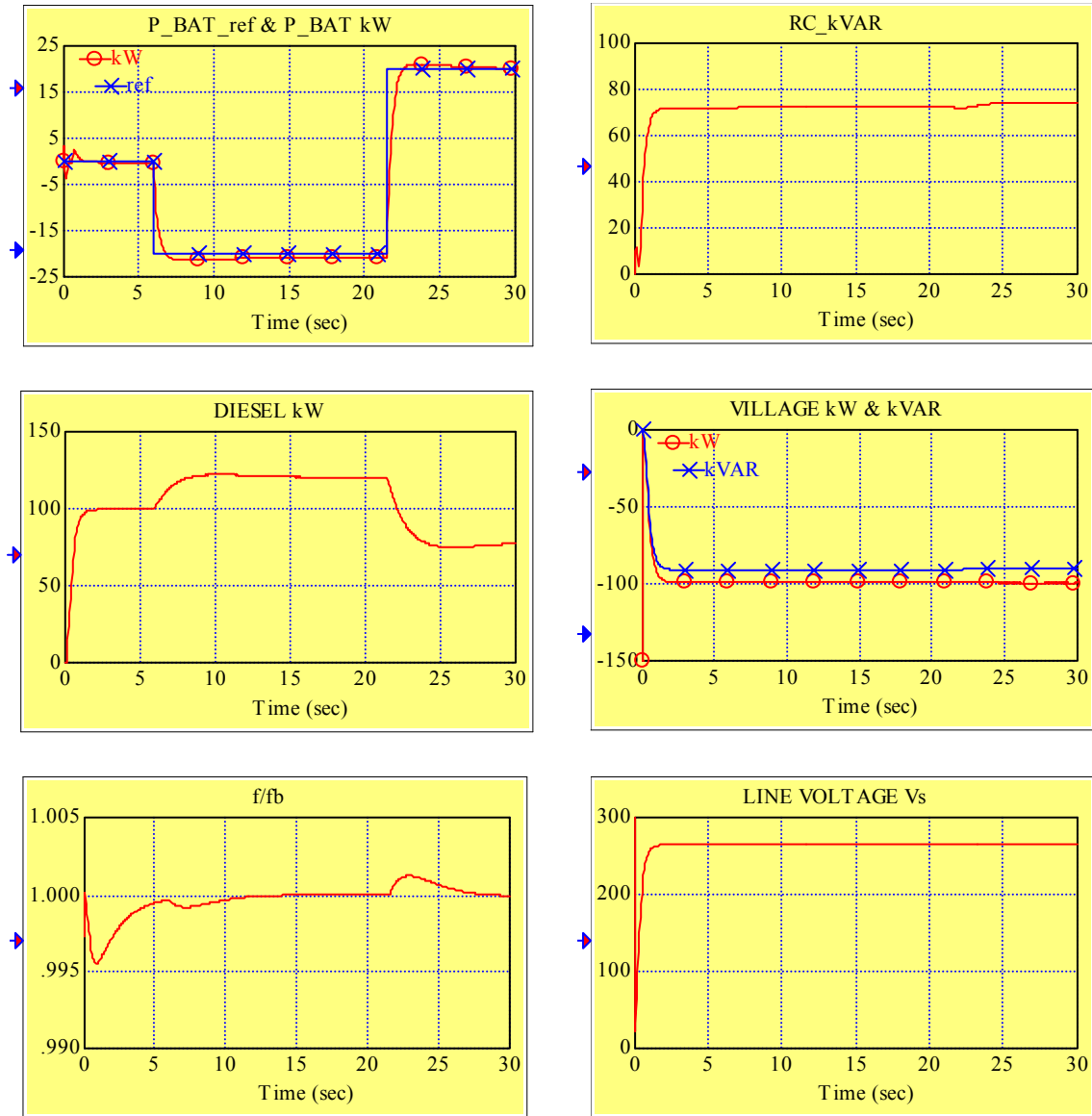


Fig.8.8 Traces of power, voltage, and frequency for the system composed of a diesel generator, a rotary converter, and the constant village load

CASE STUDY 5: PCC+DG+WT+RC+VL+DL

Principal modules in this case study include the following:

- Diesel generator with rated power of 200 kW and minimum load of 50 kW.
- AC wind turbine driven by the wind given by a file of the wind speed time series.
- Village load of 50 kW at the power factor $pf=0.75$, switched to 80 kW at $t= 10.5$ s.
- Rotary converter with a preprogrammed battery reference power.
- Dump load incremented by the diesel power control strategy.

A power system with this configuration is presented in Figure 8.9 where we show both the single-line diagram and the top-view RPM-S_{IM} simulation diagram. The simulation diagram is obtained by adding the following files to the simulation screen: PCC.vsm, DG.vsm, VL.vsm, DL.vsm, wtg_base.vsm and RC.vsm. For this system, we obtained traces of power, voltage, and frequency shown in Figure 8.10. We explain below the sequence of simulation events documented in this figure.

TIME/EVENT SEQUENCE

- | | |
|-------------|--|
| $t = 0$ | The diesel generator starts up. |
| $t = 4$ s | The line voltage V_s reaches the reference value of 266 V and the relative frequency is close to 1.
The power generated by the diesel generator is at its specified minimum value of 50 kW and the same power is consumed by the village load
The battery reference power $P_{BAT_ref} = 0$. |
| $t = 4.5$ s | The battery reference power is switched to 20 kW.
This increment is followed by the power provided to the system by the rotary converter (slow response because of a large time constant of the field-controlled DC motor of the rotary converter).
The dump load is gradually incremented by the diesel power control strategy in order to keep the diesel generator load at its minimum of 50 kW.
The line voltage and frequency remain constant. |
| $t = 7.5$ s | The induction machine starts to motor the wind turbine and creates a large load.
The power generated by the diesel generator increases sharply. |

- The dump load is immediately reduced to 0.
The transient small dips of frequency and line voltage are observed.
- $t = 10$ s The power consumption of the induction machine, reaching the synchronism, rapidly drops.
- $t = 10.5$ s The village load is increased to 80 kW.
- $t = 11$ s The wind turbine generator starts to generate.
- $t = 11.5$ s The diesel power control strategy tries to compensate for the transient power surplus by incrementing the dump load.
- $t = 12$ s The reference battery power is set at -10 kW, i.e., the battery is being charged (consumes the power surplus).
The dump load is now set at 0.
The diesel generated power remains at the minimum level of 50 kW.
The line voltage and frequency remain constant.
- $t > 14$ s The wind gusts occur.
The power generated by the wind turbine increases.
The dump load increments can be seen in order to keep the diesel generated power at its required minimum.
The line voltage and frequency remain constant.

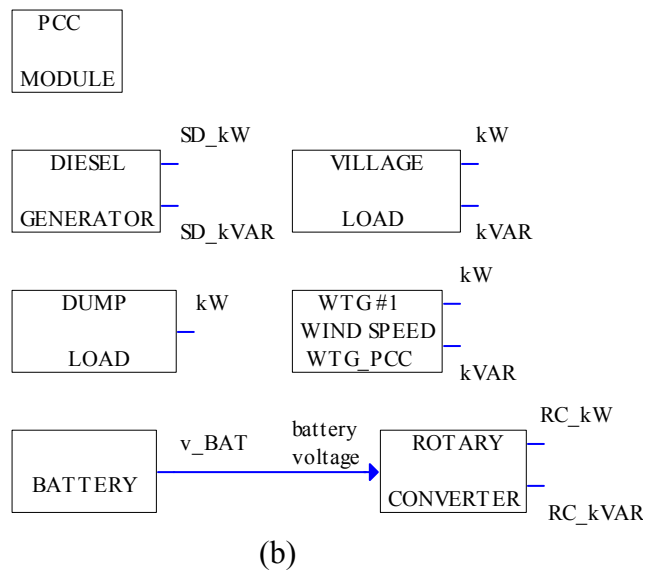
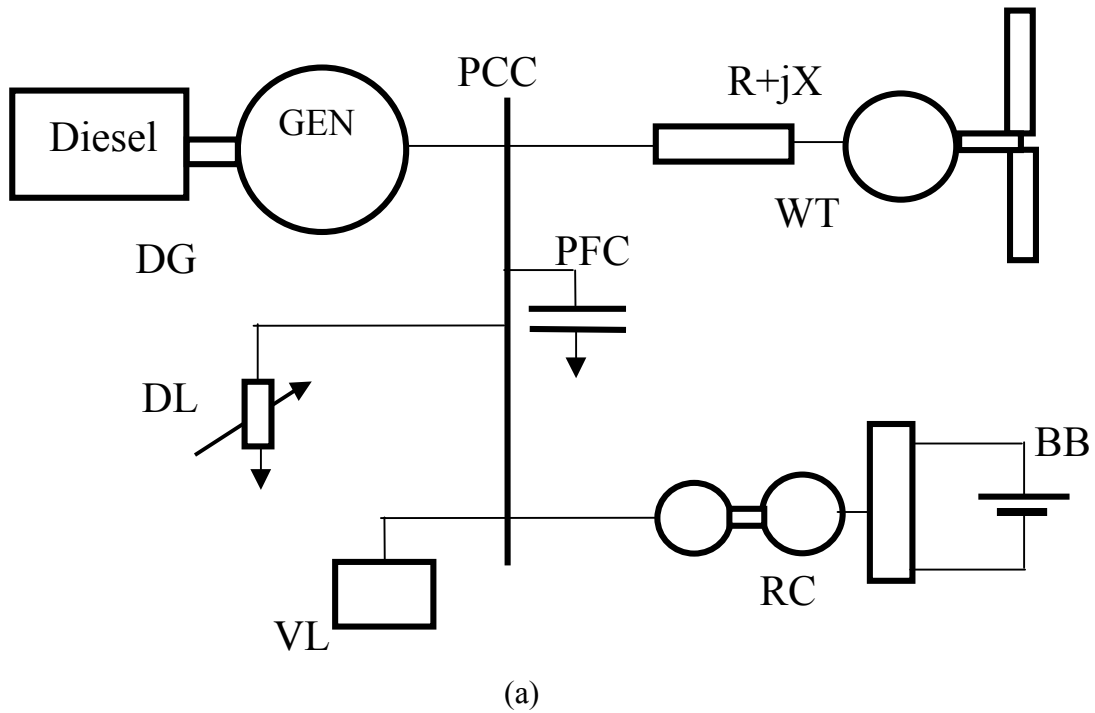


Figure 8.9 A power system composed of a diesel generator (DG), an AC wind turbine (WT), a rotary converter/battery bank assembly (RC), a village load (VL), and a dump load (DL):

(a) single-line diagram and (b) top view of the RPM-SIM simulation

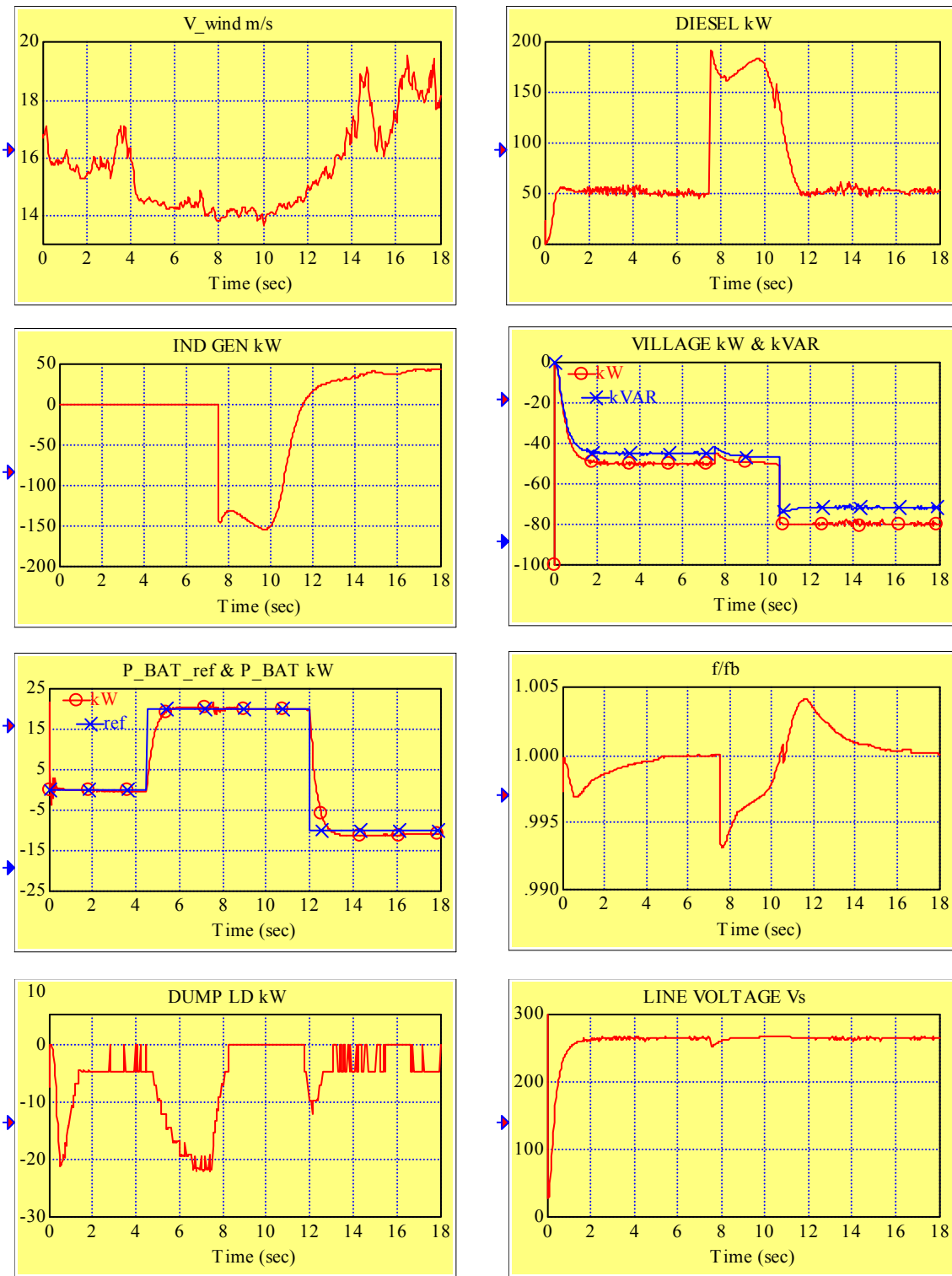


Figure 8.10 Traces of power, voltage, and frequency for the system composed of a diesel generator, a rotary converter, an AC wind turbine, a variable village load, and a dump load

CASE STUDY 6: PCC+DG+WT+RC+VL+DL WITH RC IN SYNCHRONOUS CONDENSER MODE

Principal modules in this case study include the following:

- Diesel generator with rated power of 200 kW and minimum load of 50 kW
- AC wind turbine driven by the wind given by a file of the wind speed time series with induction machine motoring preprogrammed to start at $t = 4$ s
- Village load of 30 kW at the power factor $pf = 0.98$, switched to $pf = 0.75$ at $t = 1.5$ s, switched to 100 kW at $t = 9$ s, switched to $pf = 0.98$ at $t = 13$ s, switched to 20 kW at $t = 15.5$ s
- Rotary converter in synchronous condenser mode ($P_{BAT_ref} = 0$) started at $t = 2$ s with a preprogrammed reference value of the reactive power of 20 kVAR, switched to 50 kVAR at $t = 5$ s, switched to -10 kVAR at $t = 10.5$ s, and to 20 kVAR at $t = 14$ s
- Dump load incremented by the diesel power control strategy.

The power system configuration remains the same as the one presented in Figure 8.9 where we show both the single-line diagram and the top-view RPM-SIM simulation diagram. The simulation diagram is obtained by adding the following files to the simulation screen: PCC.vsm, DG.vsm, VL.vsm, DL.vsm, wtg_base.vsm and RC.vsm. For this system, we obtained traces of power, voltage and frequency shown in Figure 8.11. Here, we explain the sequence of simulation events documented in Figure 8.11.

TIME/EVENT SEQUENCE

$t = 0$	The diesel generator starts up.
$t = 1.5$ s	The power factor of the village load switched from $pf = 0.98$ to $pf = 0.75$.
$t = 2$ s	The rotary converter started in synchronous condenser mode ($P_{BAT_ref}=0$) with a preprogrammed reference value of the reactive power equal 20 kVAR.
$t = 4$ s	The line voltage V_s reaches the reference value of 266 V and the relative frequency is close to 1. The power generated by the diesel generator is at its specified minimum value of 50 kW and is consumed by the village load and the dump load.

The reactive power generated by the rotary converter reaches the value of $Q_{SR} = 20$ kVAR equal to the current reference value and is absorbed by the village load and by the diesel generator.

The induction machine starts to motor the wind turbine and creates a large load in both the real power and the reactive power.

The real and reactive power generated by the diesel generator increases sharply.

The dump load is immediately reduced to 0.

The transient small dips of frequency and line voltage are observed.

- $t = 5$ s The preprogrammed reference value of the reactive power generated by the synchronous condenser of 20 kVAR is switched to 50 kVAR.
- This increment is followed by the gradual increase of Q_{SR} ; because, at the same time, the reactive power absorbed by the induction generator sharply decreases, the reactive power generated by the diesel generator must decrease and even reverses sign (becomes to be absorbed).
- The real power consumption of the induction machine, reaching the synchronism, rapidly drops.
- $t = 8$ s The wind turbine generator starts to generate power.
- The dump load is gradually incremented by the diesel power control strategy in order to keep the diesel generator load at its minimum of 50 kW.
- The reactive power generated by the rotary converter reaches the value of $Q_{SR} = 50$ kVAR equal to the current reference value and is absorbed by the village load and by the diesel generator.
- Small transient changes in the line voltage and frequency can be observed.
- $t = 9$ s The village load is increased to 100kW and its power factor remains unchanged, i.e., the demand for real power and reactive power in the system increases sharply.
- The diesel generator starts to generate the reactive power and sharply increases the level of generated real power.
- The dump load decreases to zero.
- $t = 10.5$ s The preprogrammed reference value of the reactive power generated by the synchronous condenser of 50 kVAR is switched to -10 kVAR; with the village load unchanged, this results in additional demand for reactive power of 60 kVAR.

- The diesel generator provides the required reactive power.
- $t = 13$ s The village load of 100 kW at the power factor $pf = 0.75$ is switched to $pf = 0.98$, i.e., the demand for reactive power drops sharply.
- The reactive power generated by the diesel generator decreases accordingly.
- $t = 14$ s The preprogrammed reference value of the reactive power absorbed by the synchronous condenser of -10 kVAR is switched to 20 kVAR; during steady-state this means an additional 30 kVAR of reactive power to be absorbed in the system.
- The diesel generator reduces the generated reactive power and finally starts to absorb the reactive power.
- $t = 15.5$ s The village load of 100 kW at the power factor $pf = 0.98$ is switched to 20 kW at the same power factor
- The wind turbine tries to overpower the diesel generator; for a short time the diesel real power drops below 0 causing a frequency glitch.
- The diesel power control strategy is fast enough to compensate for this power surplus by incrementing the dump load to save the synchronism.
- The real power provided to the system by the diesel generator returns to its minimum value of 50 kW.
- $t > 17$ s Wind gusts occur.
- The power generated by the wind turbine increases.
- The real power generated by the diesel generator and wind turbine generator is absorbed by the village load and the dump load.
- The reactive power provided by the synchronous condenser is absorbed by the village load, the diesel generator, and the induction generator.
- The dump load increments occur to keep the diesel generated power at its required minimum.
- The line voltage and frequency remain constant.

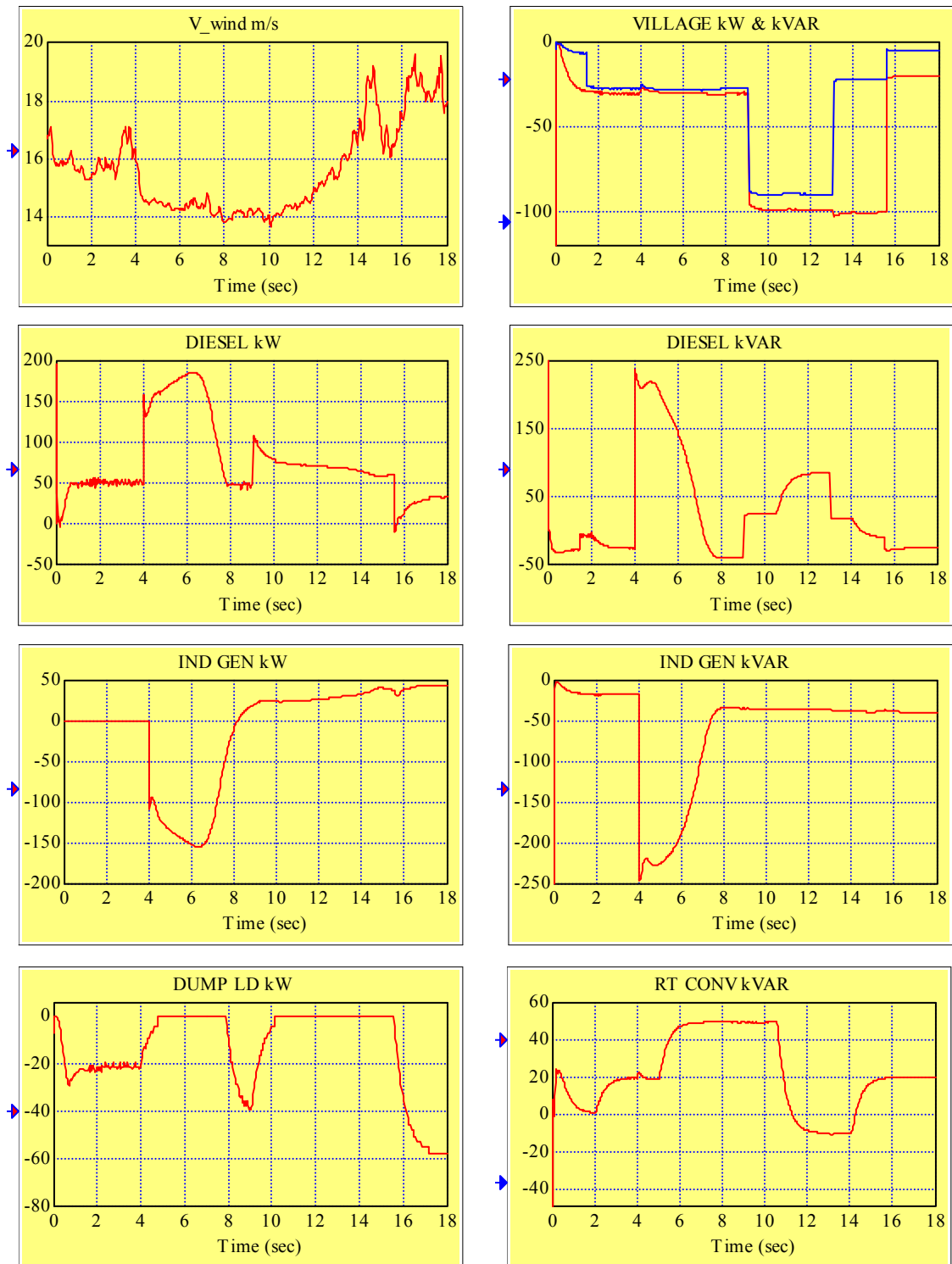


Figure 8.11 Traces of power, voltage, and frequency for the system composed of a diesel generator, a rotary converter, an AC wind turbine, a variable village load, and a dump load (continued on the next page)

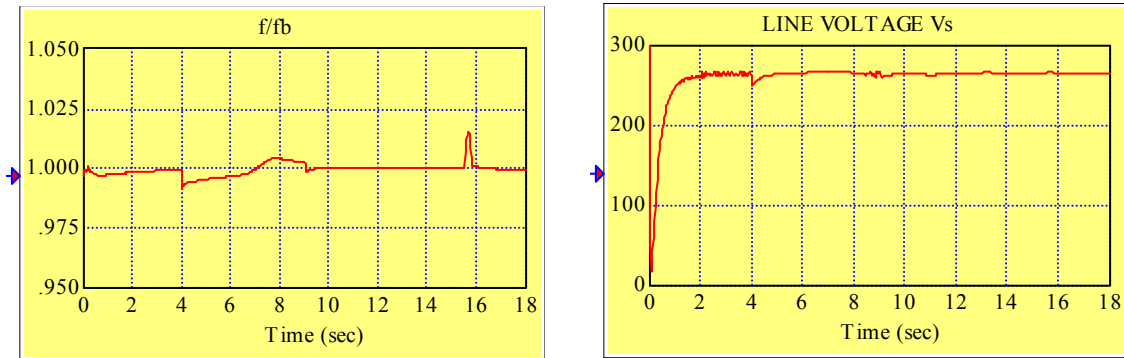


Figure 8.11 Traces of power, voltage, and frequency for the system composed of a diesel generator, a rotary converter, an AC wind turbine, a variable village load and a dump load (continued from the previous page)

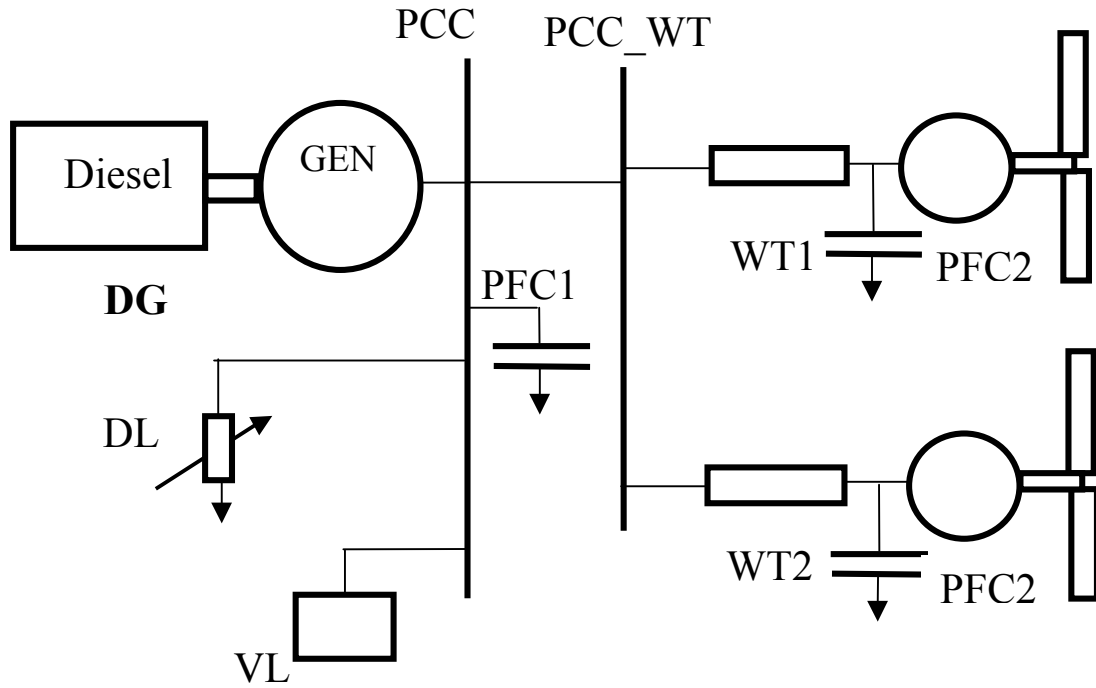
CASE STUDY 7: PCC+DG+WT1+WT2+VL+DL

Principal modules in this case study include the following:

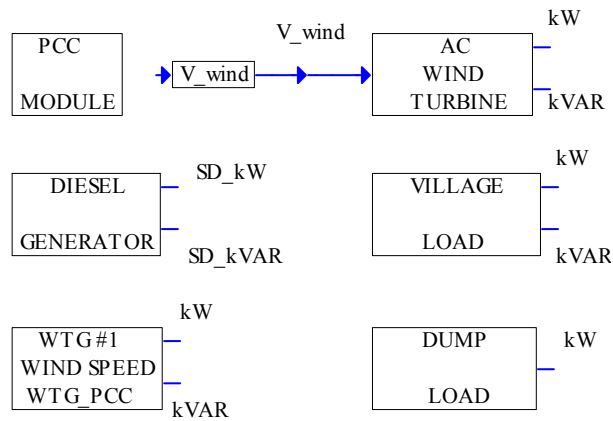
- Diesel generator with a rated power of 200 kW and minimum load of 50 kW
- AC wind turbine (WT1) driven by the wind determined by a file of the wind speed time series with induction machine motoring preprogrammed to start at $t = 4.5$ s
- AC wind turbine (WT2) driven by the wind given by a file of the wind speed time series with induction machine motoring preprogrammed to start at $t = 9$ s
- Village load of 30 kW at the power factor $pf = 0.75$, switched to 150 kW at $t = 12.5$ s to provide adequate load for both wind turbines
- Dump load incremented by the diesel power control strategy.

The power system configuration is presented in Figure 8.12 where we show both the single-line diagram and the top-view RPM-SIM simulation diagram. The simulation diagram is obtained by adding the following files to the simulation screen: PCC.vsm, DG.vsm, VL.vsm, DL.vsm, wtg_base.vsm (adds WT1) and WTG.vsm (adds WT2). Then the variable V_wind must be added and connected to the input of AC wind turbine block representing WT2. Moreover, the wind turbine WT2 must be connected to the system through PCC_WT by adding d- and q-components of its transmission line current. It is assumed that both turbines have the same wind profile as shown in Figure 1.3. For

more details on the simulation of a multiple wind turbine system refer to Chapter 1 and Chapter 4. For the system in this case study, we obtained traces of power, voltage, and frequency shown in Figure 8.13. Next, we explain the sequence of simulation events documented in this figure.



(a)



(b)

Figure 8.12 A power system composed of a diesel generator (DG), an AC wind turbine (WT1), an AC wind turbine (WT2), a village load (VL), and a dump load (DL): (a) single-line diagram, and (b) top view of the RPM-SIM simulation

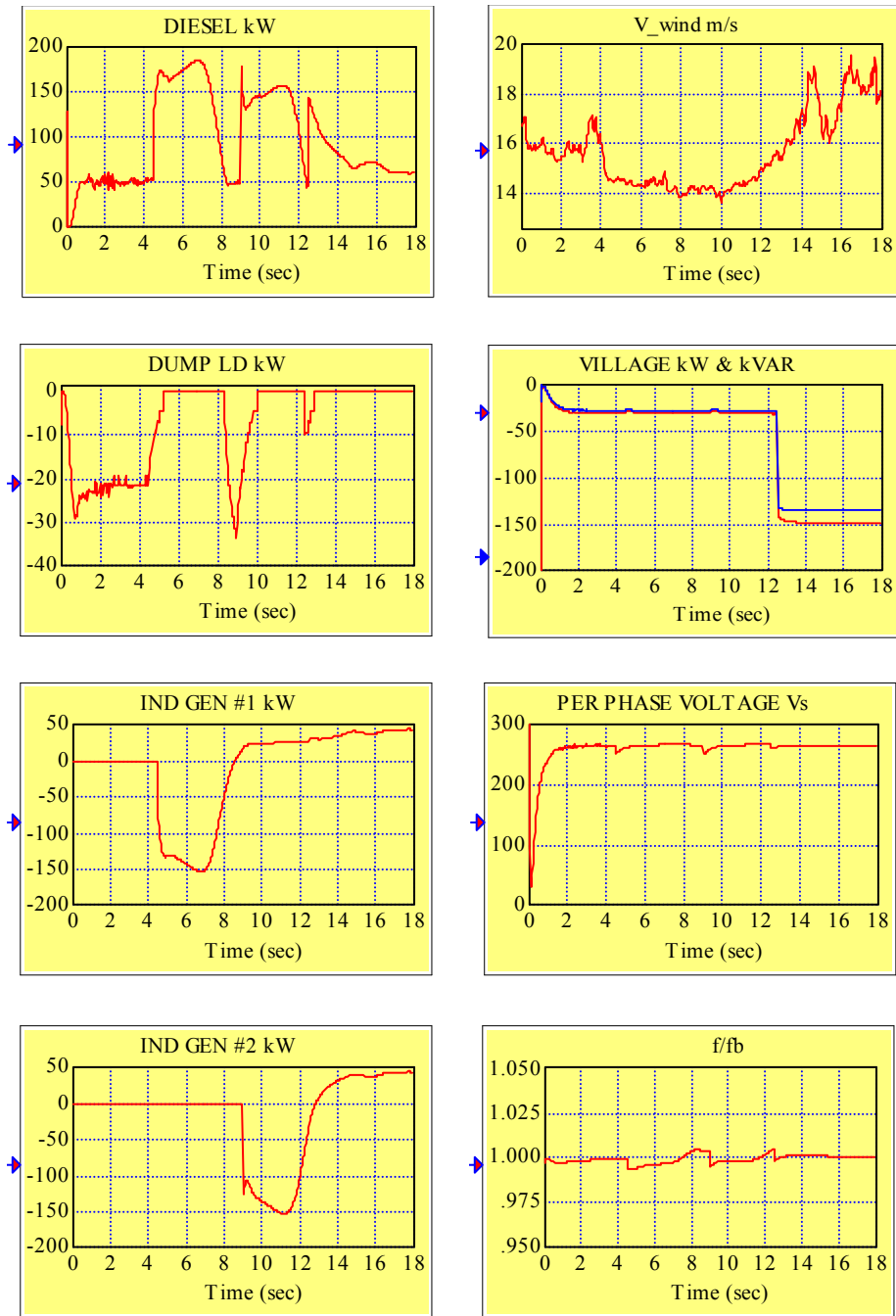


Figure 8.13 Traces of power, voltage, and frequency for the system composed of a diesel generator, an AC wind turbine WT1, an AC wind turbine WT2, a variable village load and a dump load

TIME/EVENT SEQUENCE

- $t = 0$ The diesel generator starts up.
The dump load is incremented to bring the power generated by the diesel generator to a minimum value of 50 kW.
- $t = 4$ s The line voltage V_s reaches the reference value of 266 V and the relative frequency is close to 1.
The power generated by the diesel generator is at its specified minimum value of 50 kW and is consumed by the village load and the dump load.
- $t = 4.5$ s The induction machine starts to motor the wind turbine WT1 and creates a large load.
The power generated by the diesel generator increases sharply.
The dump load is immediately reduced to 0.
Transient small frequency and line voltage dips are observed.
- $t = 7$ s Real power consumption of the induction machine #1, reaching the synchronism, rapidly drops and so does the power generated by the diesel generator.
- $t = 8.5$ s The dump load is incremented by the diesel power control strategy to keep the diesel generator load at its minimum of 50 kW.
The wind turbine generator WT1 starts to generate power.
Small transient changes in the line voltage and frequency are observed.
- $t = 9$ s The induction machine starts to motor the wind turbine WT2 and creates a large load.
The dump load is immediately reduced to 0.
The power generated by the diesel generator increases sharply.
- $t = 11.5$ s Real power consumption of the induction machine #2, reaching the synchronism, rapidly drops and so does the power generated by the diesel generator.
- $t = 12.5$ s The village load is increased to 100 kW.
The power generated by the diesel generator sharply increases.
Transient small frequency and line voltage changes are observed.

- $t = 13$ s The wind turbine generator WT2 starts to generate power.
The power generated by the diesel generator decreases.
- $t > 14$ s Both WT1 and WT2 are generating power.
Transient changes of the diesel power correlate well with the wind gusts influencing the power generated by wind turbine generators.
Both frequency and line voltage stabilize at their reference values.

CASE STUDY 8: PCC+RC (125 HP Reliance Electric DC Machine & 125 kW KATO AC Machine)+WT (AOC 15/50)+VL+DL

In this case study, we report the simulation study of the above listed configuration of the Hybrid Power Test Bed system at the National Renewable Energy Laboratory's National Wind Technology Center. Note that the DG is not included in this configuration. The simulation study was performed for the following modes of operation:

1. Mode 1 operation, frequency control by the DC machine

Wind turbine on line
RC AC machine on line
RC DC machine doing frequency control
No dump load

2. Mode 2 operation, frequency control by the DL, battery disconnected

Wind turbine on line
RC AC machine on line
RC DC machine off line

3. Mode 3 operation, frequency control by the DL, battery connected

Same as Mode 2 except DC machine is on line in zero current control mode.

All three modes were tested using the system configuration shown in Figure 8.14 with each of the components either on or off line as specified above for each mode of operation.

The RPM-S_{IM} models of the following machines are used in this study:

- AOC 15/50 wind turbine generator (WT)
- 125 kW KATO synchronous machine (RC AC machine)
- 125 HP Reliance Electric DC motor (RC DC machine). The field saturation effect is included in the DC machine model.

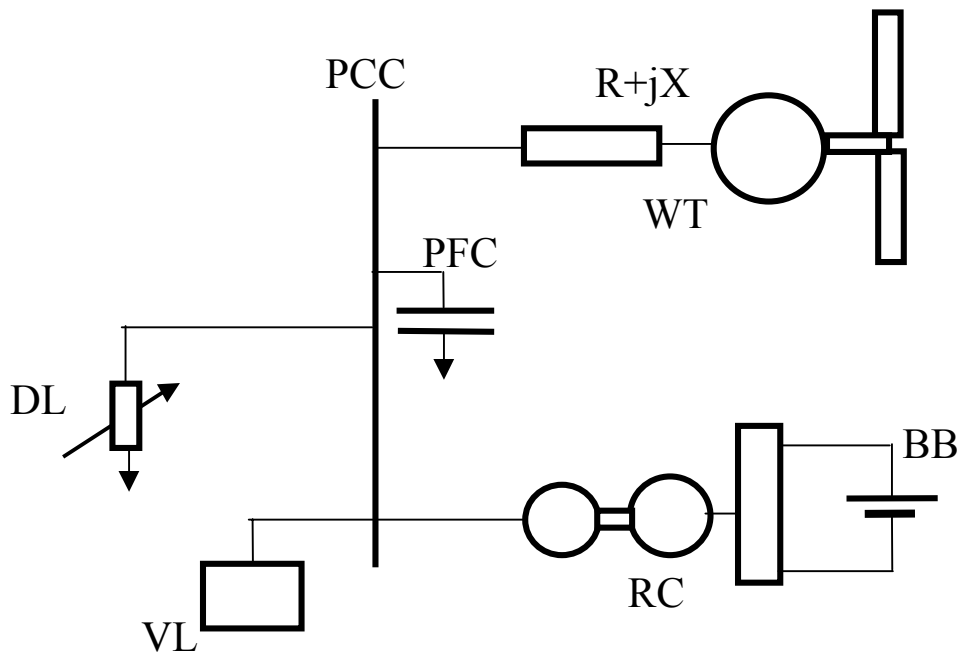


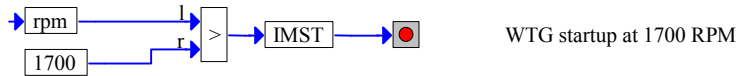
Figure 8.14 Single-line diagram of the system configuration used in the simulation study

In addition, to be able to start up the system, we included the RPM-SIM model of the village load (VL). Since the VL is not included in any of the operation modes to be investigated, it is then set to zero.

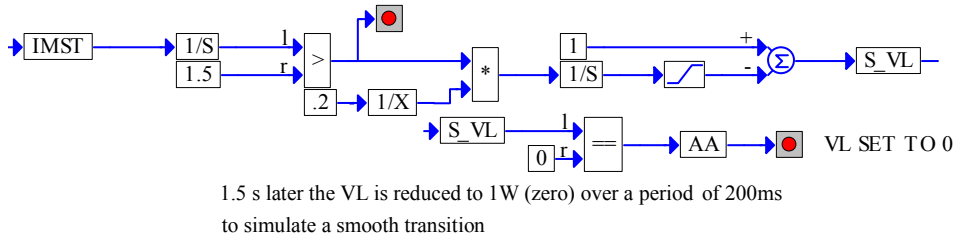
The compound block named Sequence of Events is added to the simulation screen. This block in an expanded form is shown in Figure 8.15 for the mode 1 operation and in Figure 8.17 for the mode 2 and mode 3 operation. Note that the light indicators connected at several locations in this simulation diagram turn red when an associated signal switches from 0 to 1, indicating that a particular event took place. Consequently, the user can easily identify the current state of the simulation. To reach mode 1 operation, we start with the configuration in which the RC discharges the battery and transfers the energy to the VL, controlling both the voltage and frequency. In the mean time, the wind drives the wind turbine generator (WTG). The WTG start up takes place at 1700 rpm and the wind energy is now being transferred to the battery and to the VL. Then, 1.5 s later the VL is reduced to zero over a period of 200 ms. The wind energy is now being entirely transferred to the battery, i.e., the system operates in mode 1. The traces of the system variables of interest are shown in Figure 8.16. Comparing the real power traces of the RC (negative, indicating energy consumption) and the WTG (positive, indicating energy generation), we can see that at any time instant $t > 6.5$ s, their absolute values are equal.

SEQUENCE OF EVENTS

The RC controls the voltage and frequency and transfers energy from the battery to the VL



WIND ENERGY TRANSFERRED TO THE BATTERY AND TO THE VILLAGE LOAD



ALL WIND ENERGY CAPTURED IS TRANSFERRED TO THE BATTERY

Figure 8.15 Sequence of events compound block for mode 1 operation (charging the battery):
the RC DC machine controls the system frequency and
the RC AC machine controls the system voltage

To reach mode 2 or mode 3 operation, we pass through mode 1 operation. This is documented by the sequence of events shown in Figure 8.17. To make the initial phase of the simulation shorter and to better model the real system we added the pony motor driving the RC. This motor is disconnected when the angular frequency reaches 355 rad/s. Two seconds after reaching mode 1 operation, indicated by the binary variable AA switching from 0 to 1, the DL is connected and takes over the frequency control. Simultaneously, setting the frequency error (in the field current controller) to zero disables the frequency control by the DC machine. To reach

- mode 2 operation, the DC machine and the battery are disconnected by opening the armature circuit of the DC machine, which is simulated by the ramp increase of the armature impedance. As a consequence of setting the frequency error to zero, the field voltage $V_{f,DC}$ is frozen and the field current assumes some steady-state value, irrelevant for the system operation.
- mode 3 operation, the DC machine field current is so adjusted that its armature current assumes the value of 0 resulting in a 0 torque. This is accomplished by feeding the armature current I_{DC} (treated as the error to be driven to 0) as the input to the PI controller whose output is then fed to the PID controller formerly used to control frequency through the proper adjustment of the DC machine field current. The field current control for this mode is shown in Figure 8.18.

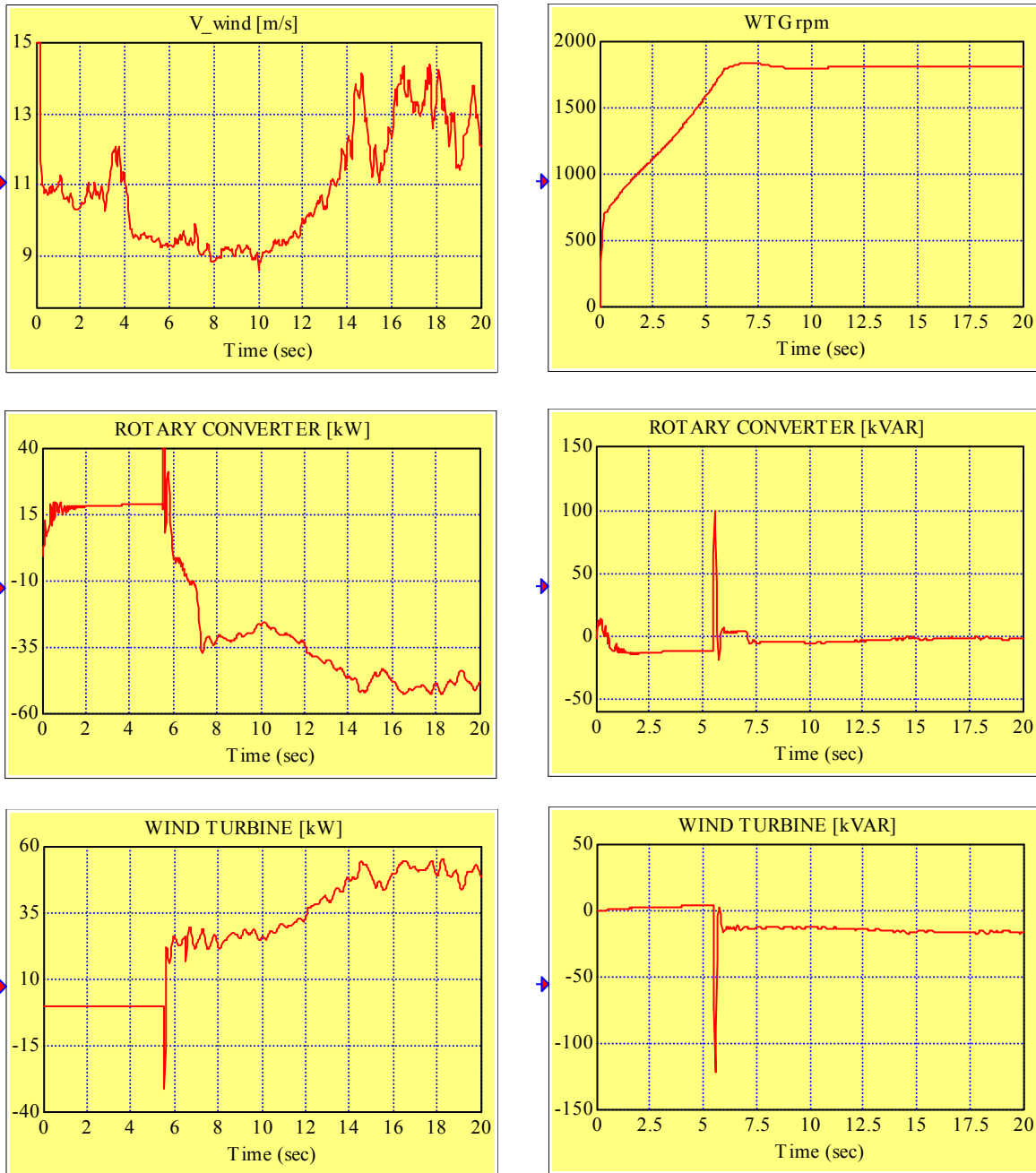


Figure 8.16 Traces of system variables for the mode 1 operation which starts approximately at $t = 6.5$ s when the VL is disconnected and the wind energy is transferred entirely to the battery (visible sudden increment of the real power consumed by the RC)
(continued on the next page).

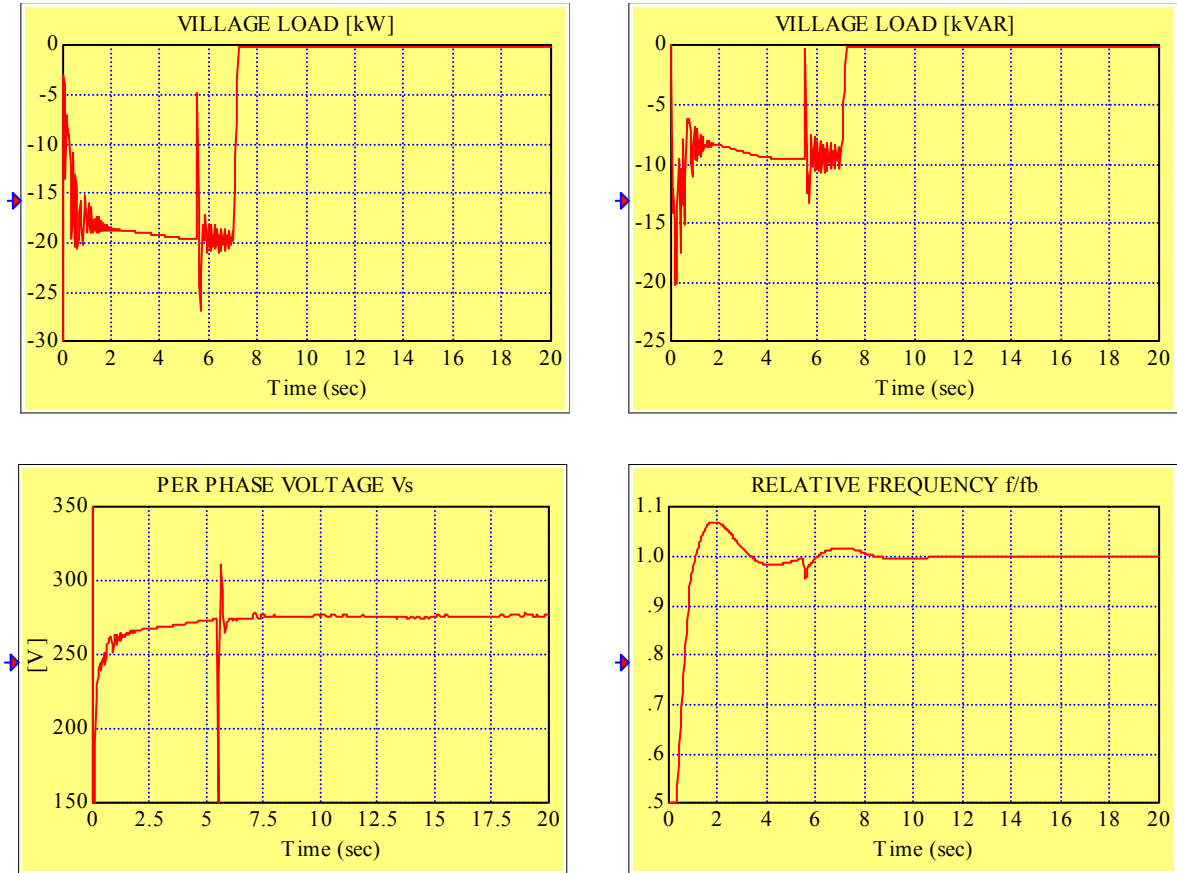


Figure 8.16 Traces of system variables for mode 1 operation which starts at approximately $t = 6.5$ s when the VL is disconnected and the wind energy is transferred entirely to the battery (visible sudden increment of the real power consumed by the RC) (continued from the previous page).

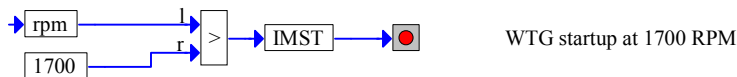
NOTE: It is important for all three modes to set properly the low limit $THETA_{Llimit}$ for the angle $THETA$ of the DC machine field power supply. To find this limit, we determine the approximate value of the field current, at which the no-load characteristic or field saturation curve $E_{a_nl}(i_{f_DC})$ enters the saturation region. For the DC machine involved in this simulation, this is (as shown in Figure 8.19) the approximate value of 2A. Then, we take 25% of this value, which is 0.5A and we request $THETA_{Llimit}$ to be the value, which results in the steady-state field current of 0.5A, i.e., for the field power supply shown in Figure 8.18, we have the following equation:

$$\frac{650(1 - \cos THETA_{Llimit})}{R_f} = 0.5, \quad R_f = 70,$$

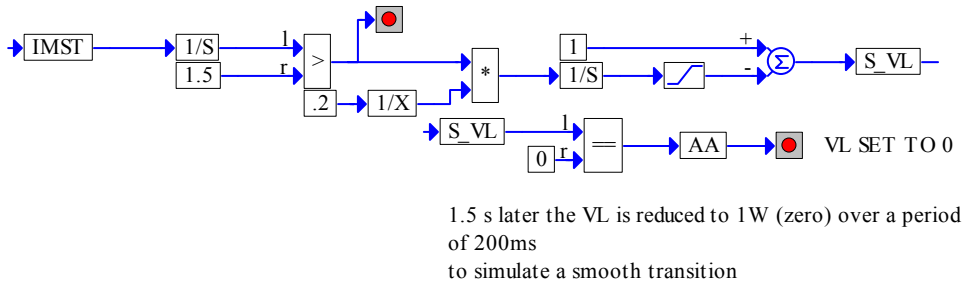
from which we find $THETA_{Llimit} = 0.33$ radians.

SEQUENCE OF EVENTS

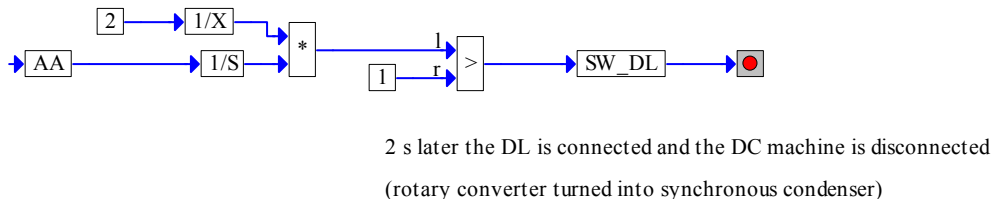
The RC controls the voltage and frequency and transfers energy from the battery to the VL



WIND ENERGY TRANSFERRED TO THE BATTERY AND TO THE VILLAGE LOAD



ALL WIND ENERGY CAPTURED IS TRANSFERRED TO THE BATTERY



FREQUENCY CONTROL IS TAKEN OVER BY THE DL.
THE SYNCHRONOUS CONDENSER CONTROLS THE VOLTAGE.

THE WIND ENERGY IS TRANSFERRED TO THE DL AND TO THE SYNCHRONOUS CONDENSER
(OPERATING AS THE SYNCHRONOUS MOTOR)

Figure 8.17 Sequence-of-events compound block for mode 2 and 3 operation (wind energy transferred to the DL and to the synchronous condenser): the system frequency control taken over by the dump load and the RC AC machine controls the system voltage

As a result of the sequence of events shown in Figure 8.17, for both mode 2 and mode 3 operation, the synchronous generator functions as a synchronous condenser. The field current of the synchronous condenser controls the system voltage. Ensuring that the rotor speed of the synchronous condenser is constant controls the system frequency.

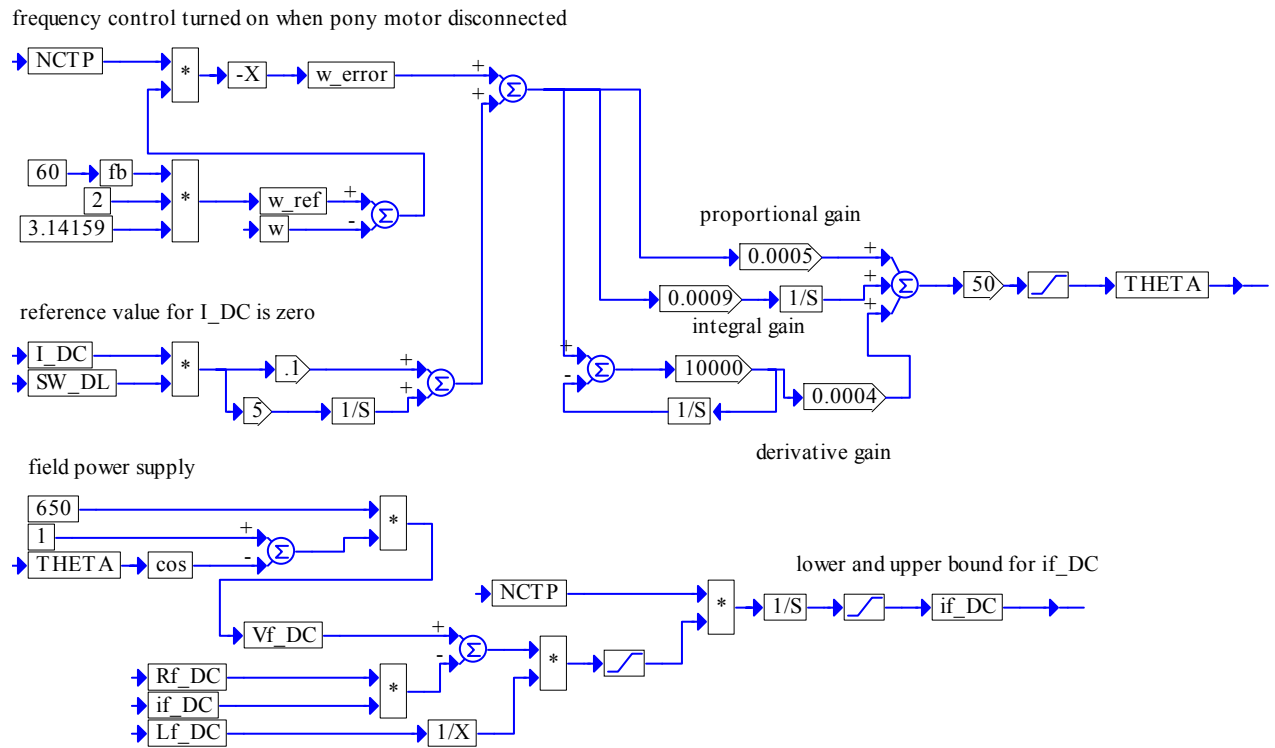


Figure 8.18 Field current controller and circuit

This is accomplished by controlling the DL so that the power generated by the WTG is almost totally consumed by the DL. The small amount of the real power enters the synchronous condenser to cover the losses. Consequently, for both modes of operation, the traces of the system variables, shown in Figure 8.20, are identical. The DL takes over the frequency control at $t = 8.5$ s.

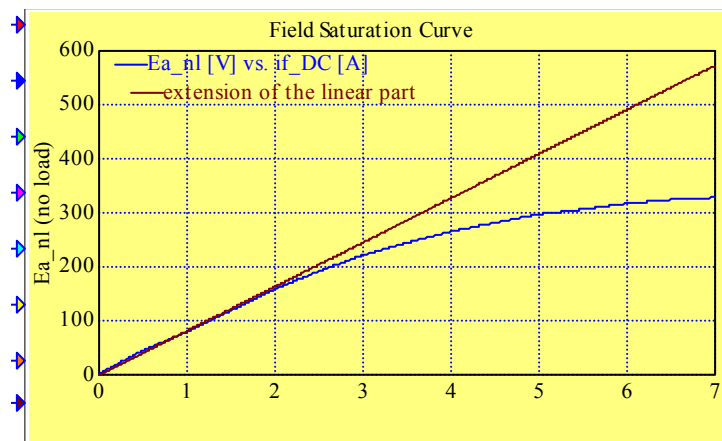


Figure 8.19 The field saturation effect: the characteristic remains linear for $i_{f_DC} < 2$ A

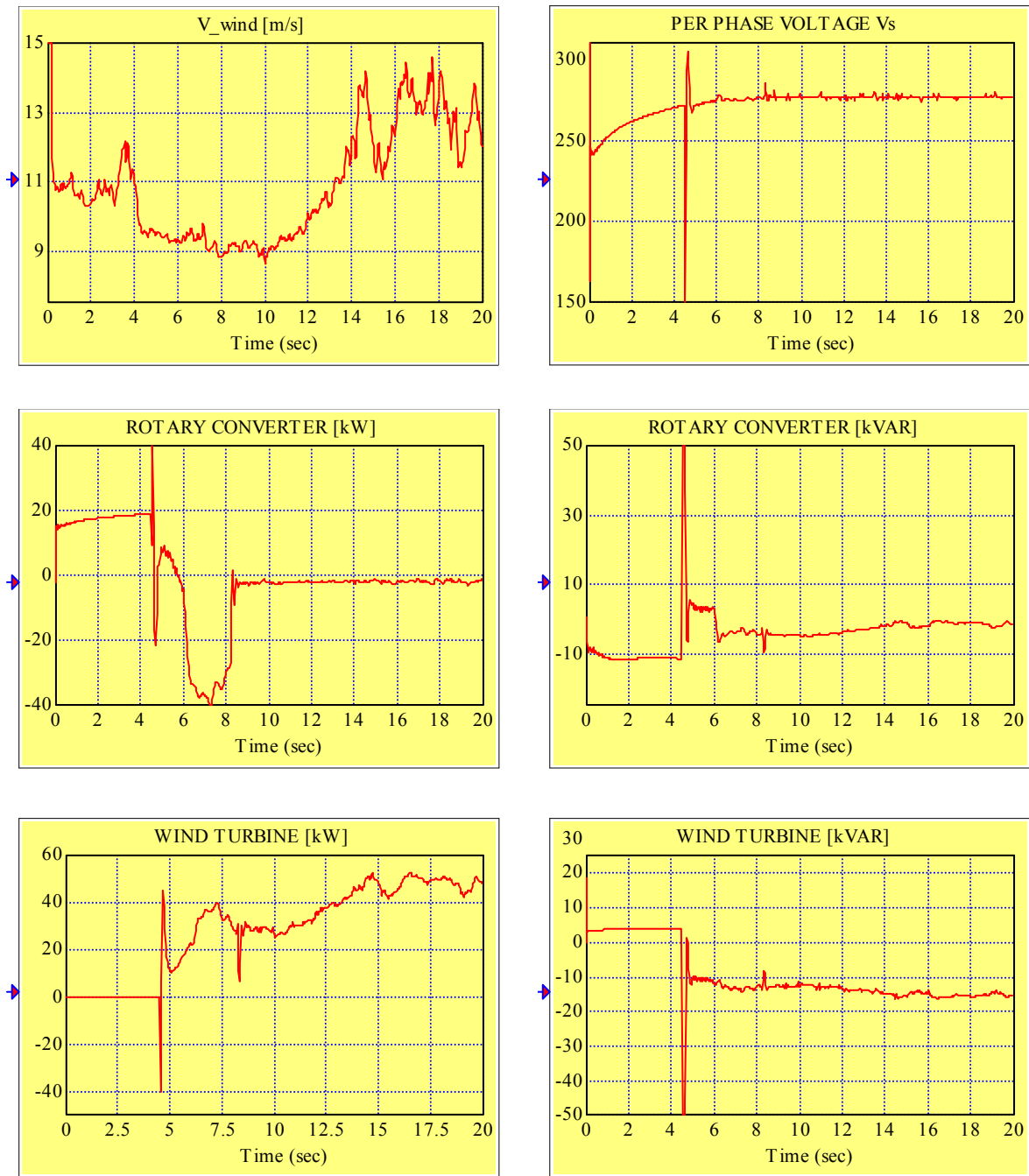


Figure 8.20 Traces of the system variables for mode 2 and mode 3 operation, which starts at approximately $t = 8.5$ s when the DL takes over the frequency control and consumes almost all of the wind energy with the exception of the RC AC machine losses (continued on the next page).

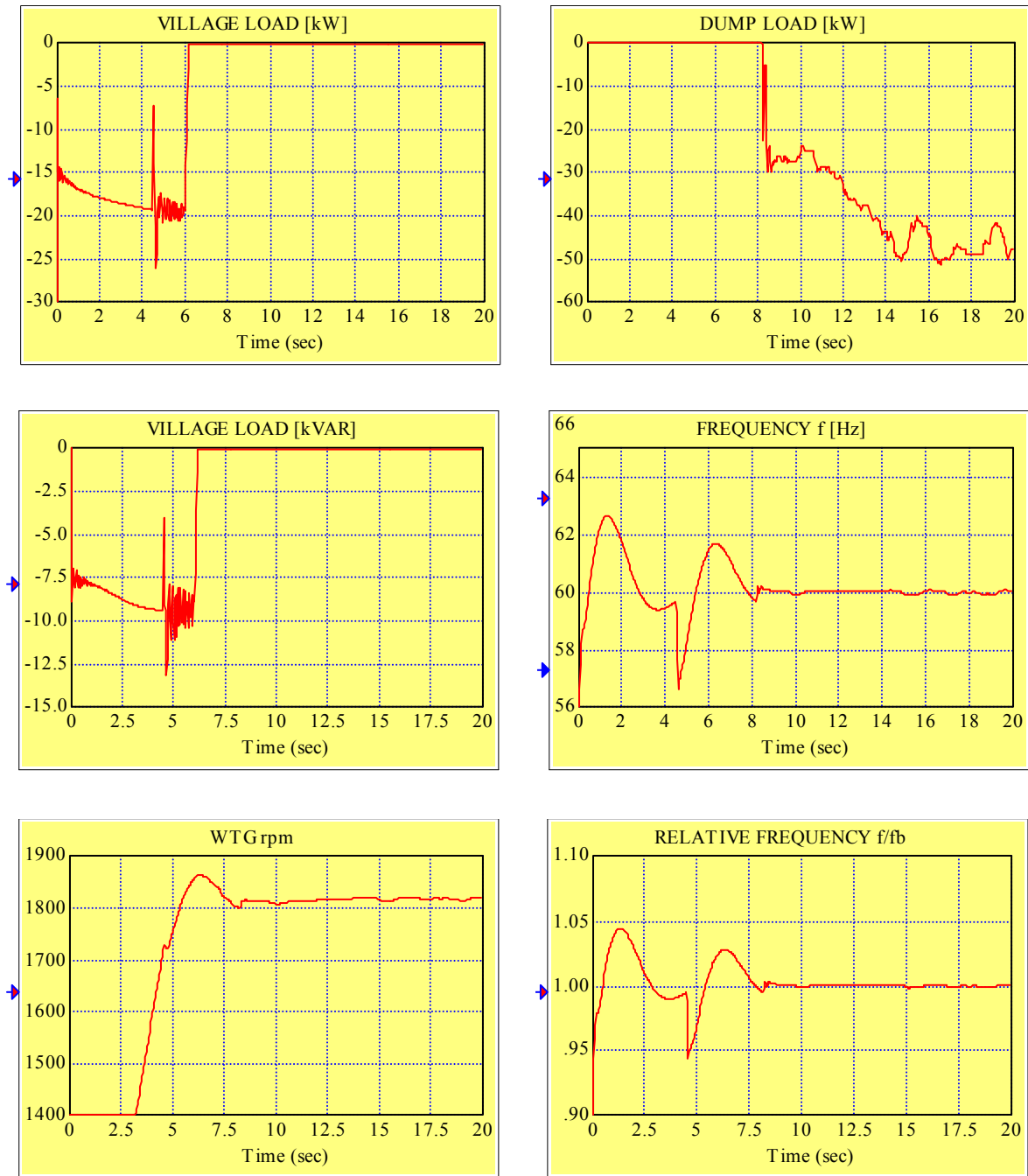


Figure 8.20 Traces of the system variables for mode 2 and mode 3 operation, which starts at approximately $t = 8.5$ s when the DL takes over the frequency control and consumes almost all of the wind energy with the exception of the RC AC machine losses (continued from the previous page).

The difference between mode 2 and mode 3 operation can be seen by comparing the traces of the RC DC machine field current and armature current shown in Figure 8.21 for mode 2 operation and in Figure 8.22 for mode 3 operation. In the former case and starting at $t = 8.5$ s (Figure 8.21), the RC DC machine is off line which is equivalent to zero shaft torque or zero armature current obtained by opening the armature circuit. At the same time, the field voltage remains frozen and the field current reaches certain (and irrelevant) steady-state value. In the latter case and starting at $t = 8.5$ s (Figure 8.22), the battery remains connected and the field current is so adjusted (approximately at 1.5 A) that the armature current assumes the value of 0, i.e., the RC DC machine remains on line in the zero current control mode. All the actions described, associated with switching from mode 1 to mode 2 or to mode 3, are initiated by the change of the value of the binary variable SW_DL from 0 to 1. However, the control mechanisms are of course different for each of the two cases.

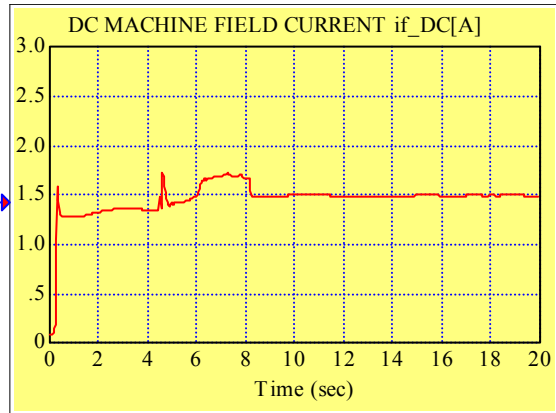
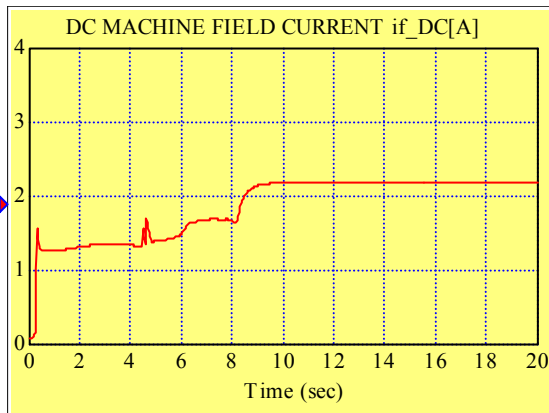
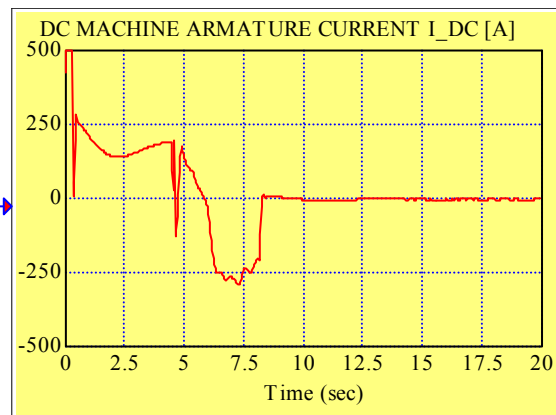
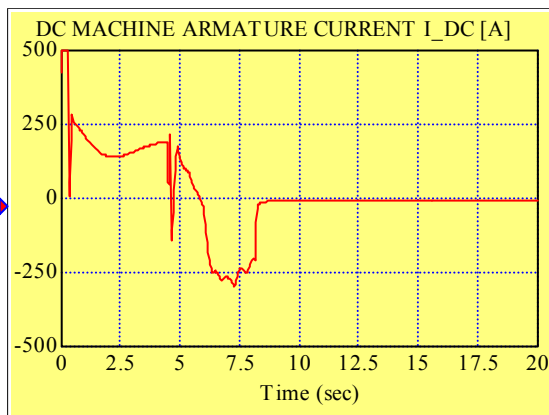
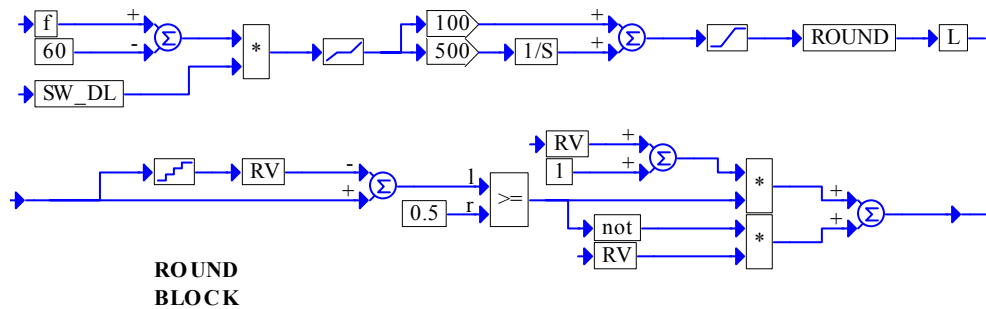


Figure 8.21 Switching from mode 1 to mode 2 operation at $t = 8.5$ s: battery disconnected and RC DC machine off line ($I_{DC} = 0$, I_{fDC} is no longer controlled and reaches a steady-state value)

Figure 8.22 Switching from mode 1 to mode 3 operation at $t = 8.5$ s: battery connected and RC DC machine on line in zero current control mode ($I_{DC} = 0$ due to $I_{fDC} \approx 1.5$ A)

FREQUENCY CONTROL BY THE DUMP LOAD

The DL frequency controller, used in mode 2 and mode 3 operation, is shown in Figure 8.23. It starts to operate when the value of the variable SW_DL, defined in Figure 8.17, switches from 0 to 1. The PI controller determines the number of active dump load elements. The round block converts this number to an integer. The power increment, declared by the user, relates this number to the DL power.



The following value of Rlarge has been chosen to implement automatic switching off the dump load:



Power increment in kW (per phase)

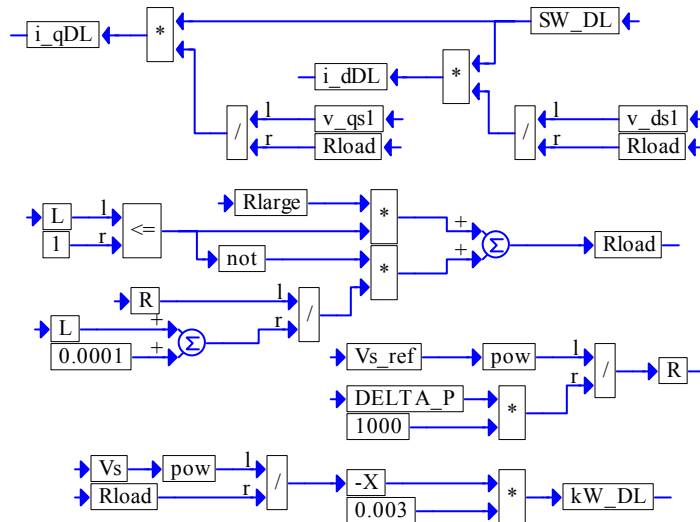


Figure 8.23 The DL frequency controller

Validation Tests at the Component Level

In this chapter, we report the results of the validation tests performed at the individual module or component level. We vary one independent variable very slowly and we observe the dependent variable. Thus, the quasi-steady-state behavior can be simulated. During the test, we hold certain quantities constant. Under the same conditions, and after reaching the steady-state operation, we obtain the response of the key dependent variable to a step change of the independent variable. The validation cases presented below are summarized in the following table:

Component	Hold constant	Independent variable	Dependent variables
Diesel generator	<ul style="list-style-type: none"> AC voltage & frequency 	Load	<ul style="list-style-type: none"> % fuel
AC wind turbine	<ul style="list-style-type: none"> AC voltage & frequency 	Wind speed	<ul style="list-style-type: none"> Real power output Reactive power output
Synchronous condenser	<ul style="list-style-type: none"> AC voltage & frequency Shaft torque = 0 	Field current	<ul style="list-style-type: none"> Real power output Reactive power output
DC motor	<ul style="list-style-type: none"> DC voltage Shaft rpm 	Field current	<ul style="list-style-type: none"> Armature current DC power output Shaft torque
DC motor	<ul style="list-style-type: none"> Shaft rpm Armature current = 0 	Field current	<ul style="list-style-type: none"> Open circuit armature voltage
Synchronous generator	<ul style="list-style-type: none"> AC voltage & frequency 	Shaft torque	<ul style="list-style-type: none"> AC power output Armature current
Induction generator	<ul style="list-style-type: none"> AC voltage & frequency 	Shaft rpm	<ul style="list-style-type: none"> Shaft torque Armature current
Rotary converter	<ul style="list-style-type: none"> AC voltage & frequency DC voltage 	DC motor field current	<ul style="list-style-type: none"> AC power output Rotary converter efficiency

DIESEL GENERATOR

In order to test the diesel generator, we setup the simulation diagram, which includes a variable load. Elements of this simulation diagram are shown in Figure 9.1. The village load was used as a variable load. The independent variable was the rated village power P_v and the dependent variable was $\%_FUEL$.

To examine the steady-state performance, we set the load power factor equal to 0.85 and the initial rated power $P_v = -100$ kW (as shown in Figure 9.2). Let us recall that the negative power convention is used for the power consumed. After the steady state was reached, the voltage V_s and the frequency f were kept constant by the voltage and frequency control systems and the commanded rated power was linearly varied between -50 kW and -150 kW. The results of the test are shown in Figure 9.2. It can be seen that $\%_FUEL$ varies linearly as a function of P_v , as expected.

The same test setup was used to obtain the $\%_FUEL$ response to step changes in the commanded rated power P_v . As before, the line voltage and the frequency were kept constant after the diesel generator reached the commanded power of 100 kW at $pf = 0.9$. At $t = 20$ s the power factor was changed to $pf = 0.75$. The load was varied stepwise between -50 kW and 150 kW. The results shown in Figure 9.3 are as expected.

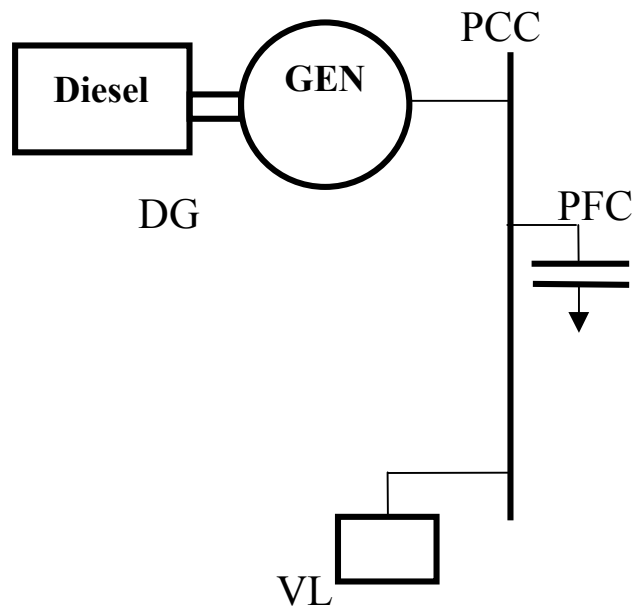


Figure 9.1 Elements of the simulation diagram for testing the diesel generator

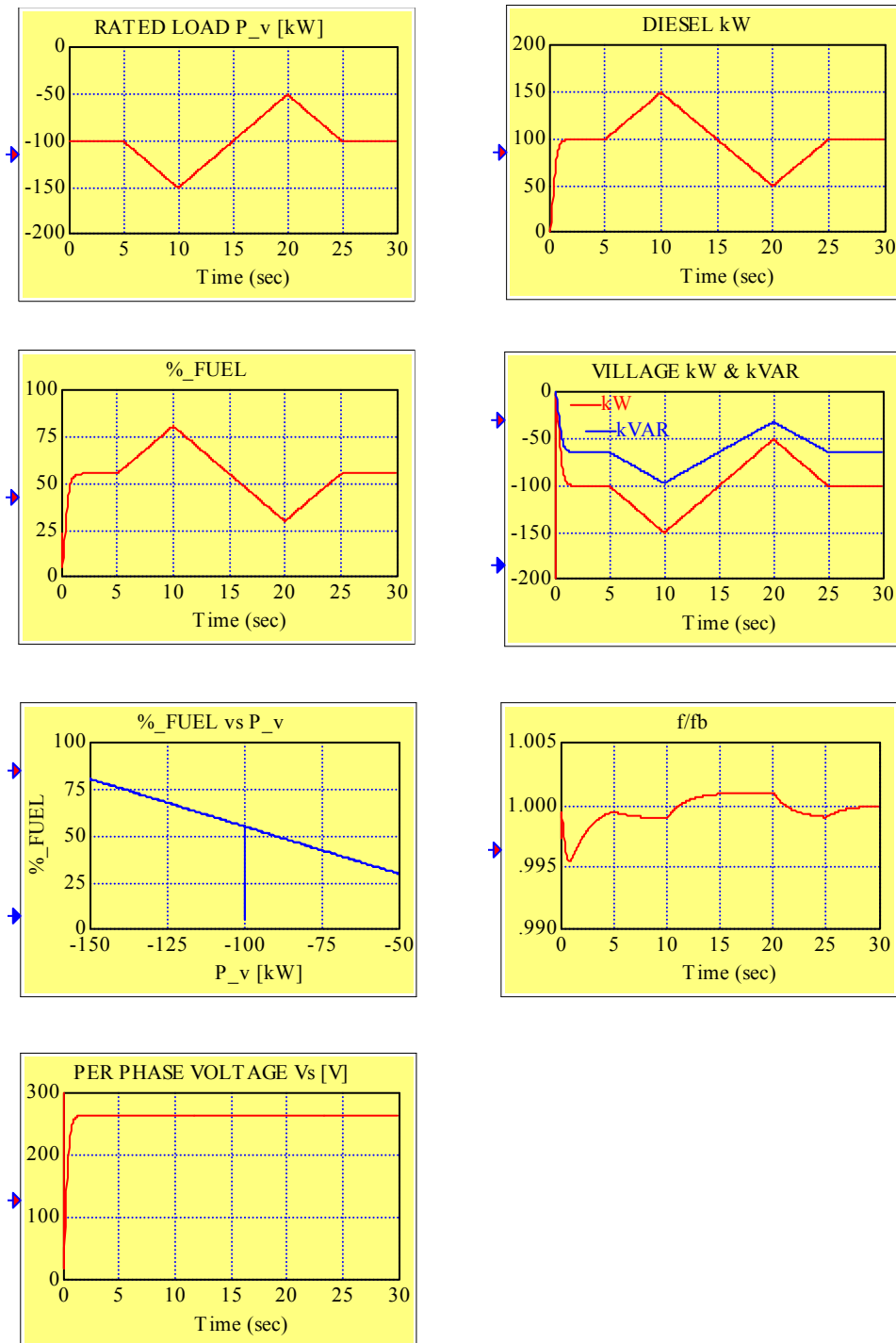


Figure 9.2 Results of the steady-state performance test of the diesel generator

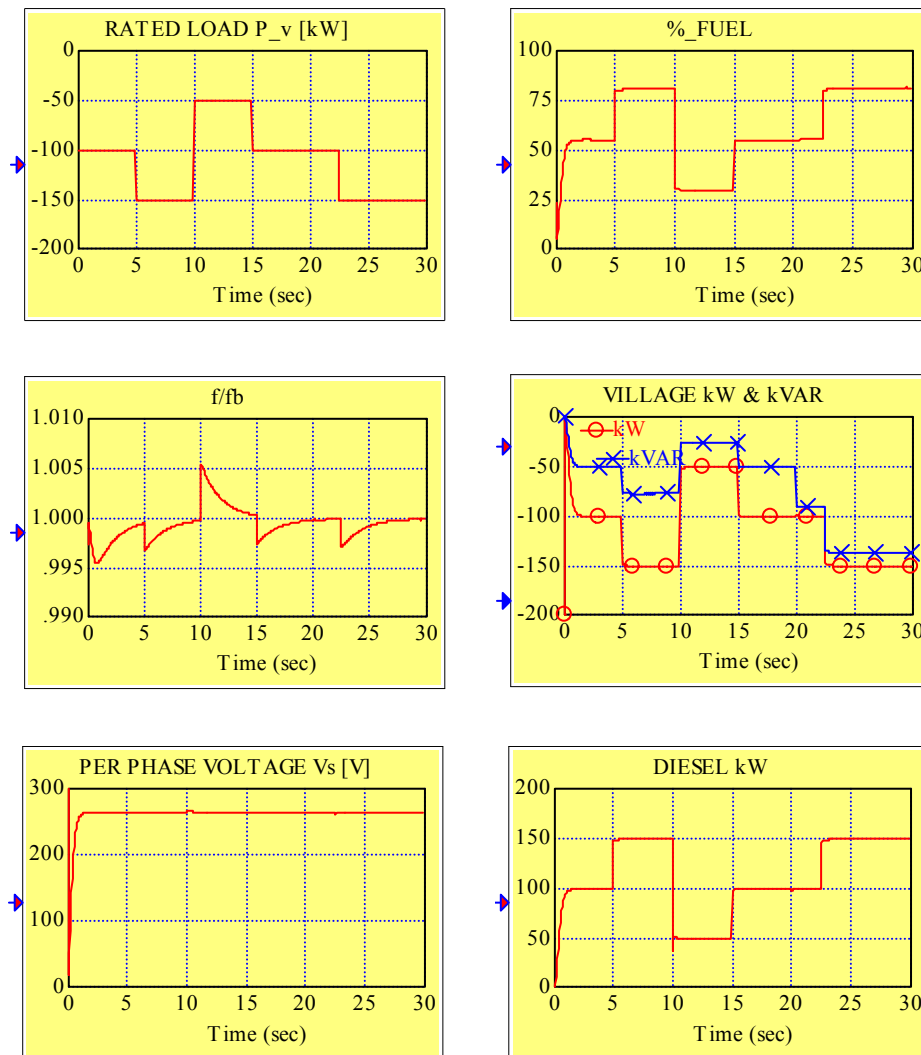


Figure 9.3 Diesel generator response to a step-wise change in the commanded load, represented by the village rated power.

AC WIND TURBINE

The simulation diagram, with elements shown in Figure 9.4, consists of the AC wind turbine generator module along with the wind speed source, the diesel generator used to startup the wind turbine generation and to maintain constant line voltage and frequency and the village load. The rated power of the village load is initially set to 30 kW at $pf = 0.9$ and then at $t = 8$ s it is switched to 100 kW to provide the necessary load for the wind turbine generator. The wind speed is initially set to the value of 15 m/s and is kept constant until the steady state is reached in the system. It can be seen from the traces shown in Figure 9.5 that at $t = 10$ s the line voltage V_s and the frequency f are constant, the wind turbine provides the real power of approximately 30 kW, the diesel generator provides approximately 70 kW and the village consumes 100 kW. This steady-state power balance can be better observed from the enlarged power traces in Figure 9.6. This state is used as the initial state for testing the steady-state and transient performance. The wind speed is used as an independent variable.

To test the steady-state performance of the wind turbine generator we developed the wind speed profile shown in Figure 9.7. It can be observed, that after reaching the steady state described above, we start to vary the wind speed linearly up to 25 m/s, then down to 5 m/s and then again up to 15 m/s. All traces of interest are shown in Figure 9.5 with the enlargements of the relevant power traces presented in Figure 9.6. We see that the power balance is preserved. We also notice that at the time instants, at which the slope of the wind speed changes, we do not have sharp changes in the power slope. This is the result of the inertia involved. This effect can be seen even better as an hysteresis in the plots of the real and reactive power of the wind turbine generator versus wind speed shown in Figure 9.8.

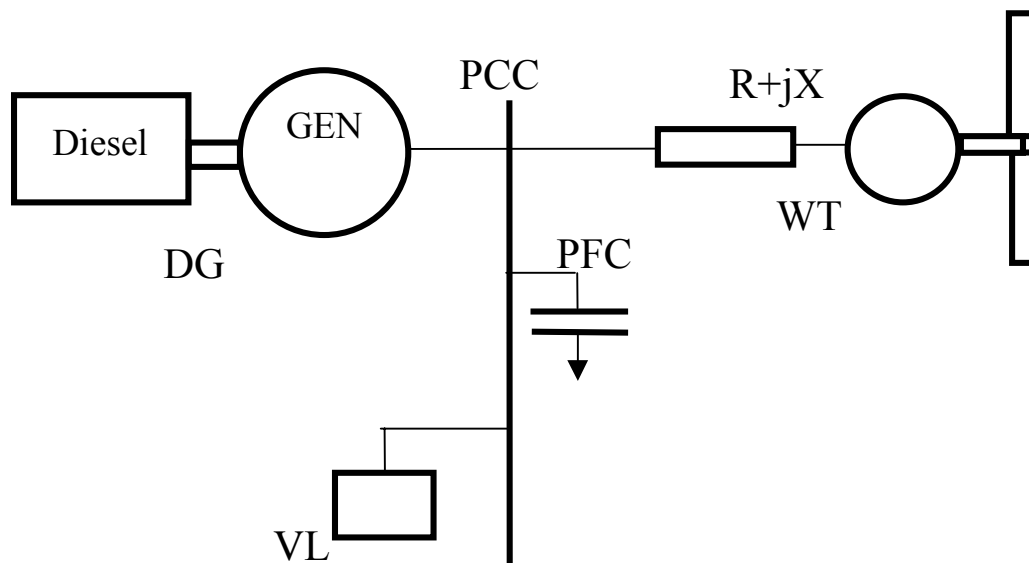


Figure 9.4 Elements of the simulation diagram for testing the AC wind turbine

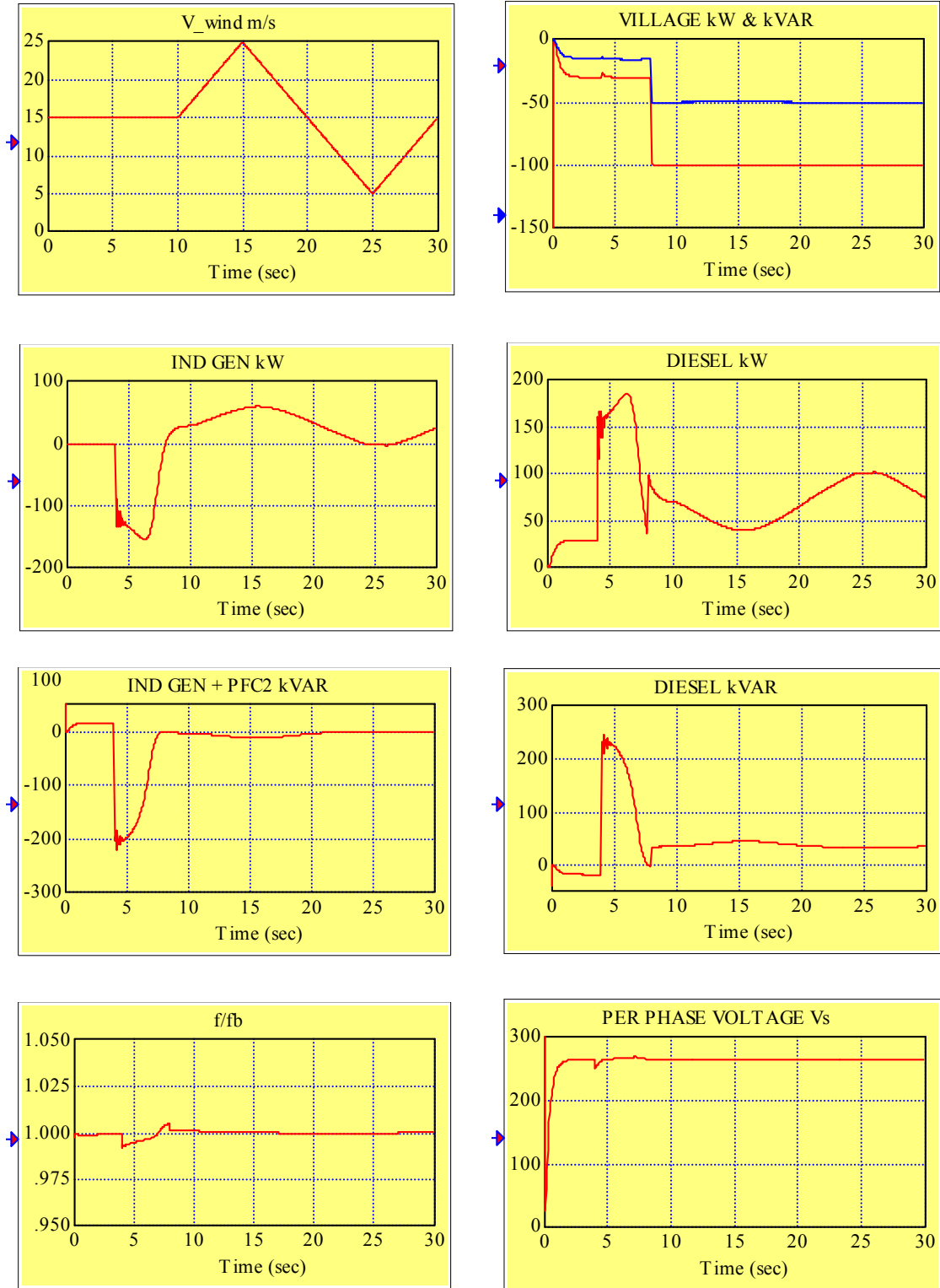


Figure 9.5 Results of the steady-state performance test of the AC wind turbine with the wind speed as an independent variable

The same initial steady state was used to obtain the induction generator real- and reactive-power response to the step changes in the wind speed. The results shown in Figure 9.9 are as expected.

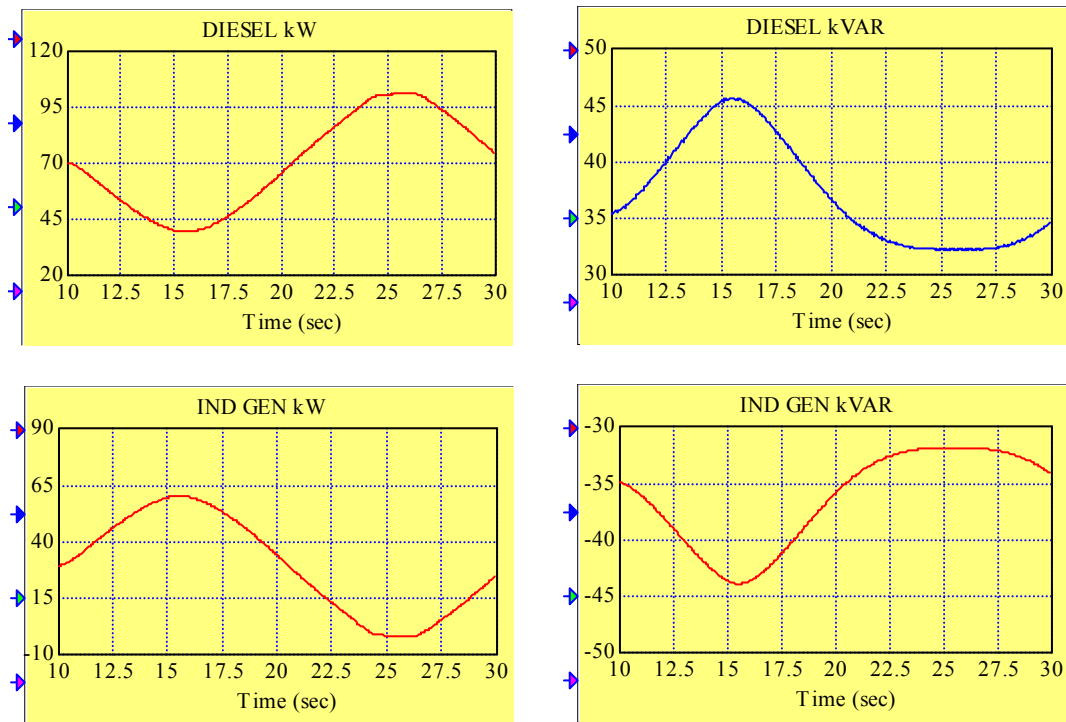


Figure 9.6 Enlarged (from Figure 9.5) real- and reactive-power traces of the diesel and induction generator

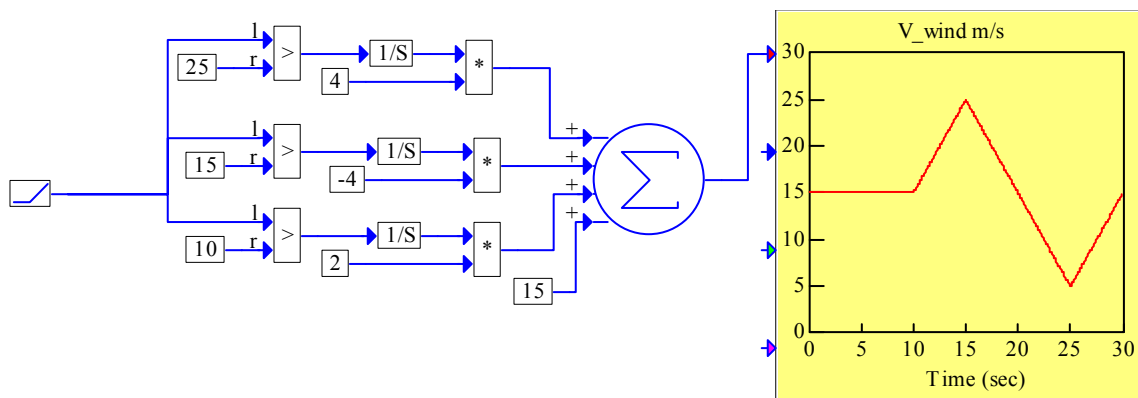


Figure 9.7 The wind speed profile used as an independent variable in the steady-state performance test of the AC wind turbine generator

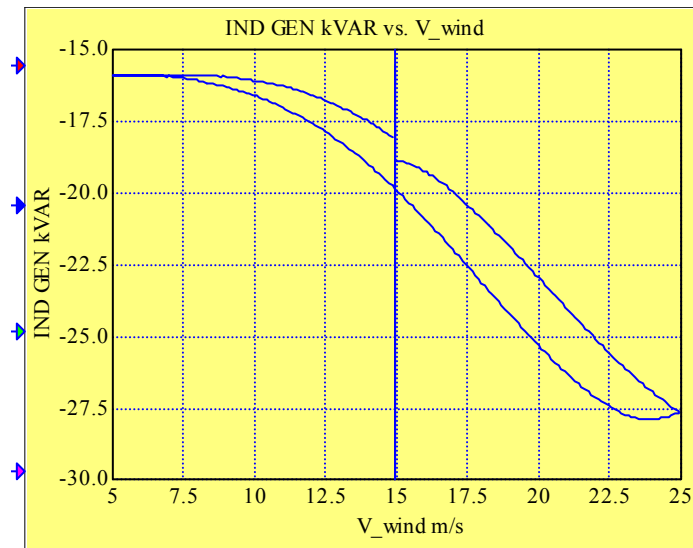
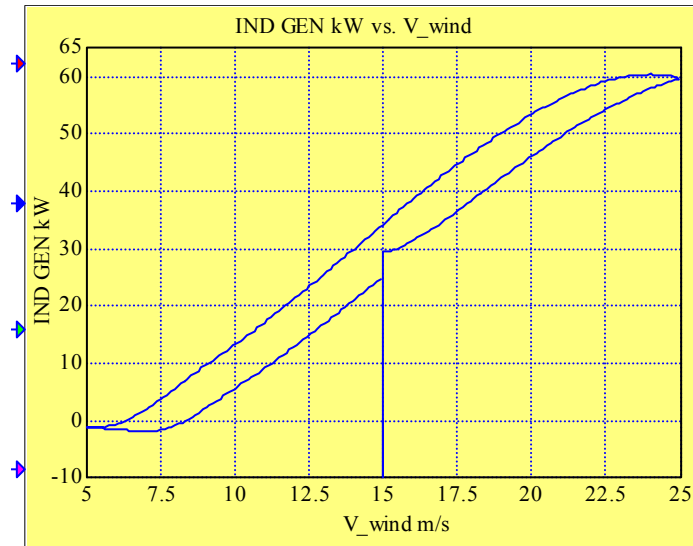


Figure 9.8 Real- and reactive-power output of the induction generator versus the wind speed varied linearly (as shown in Figure 8.3) around the value of 15 m/s

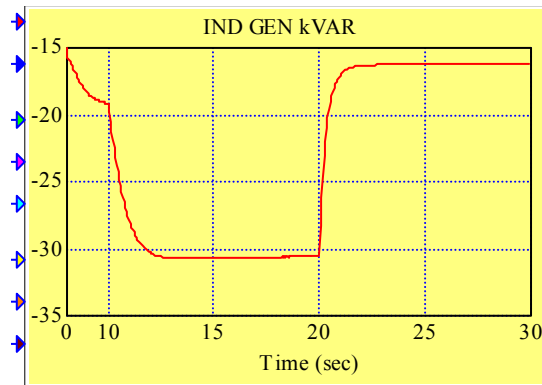
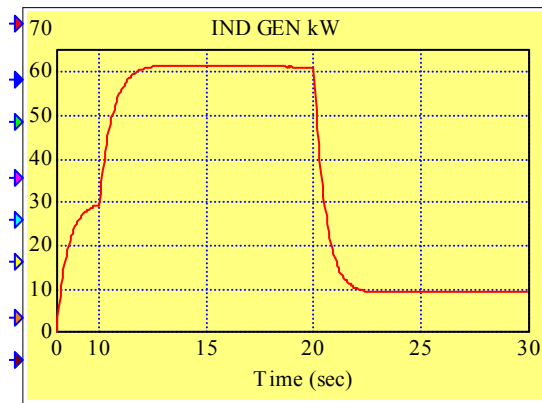
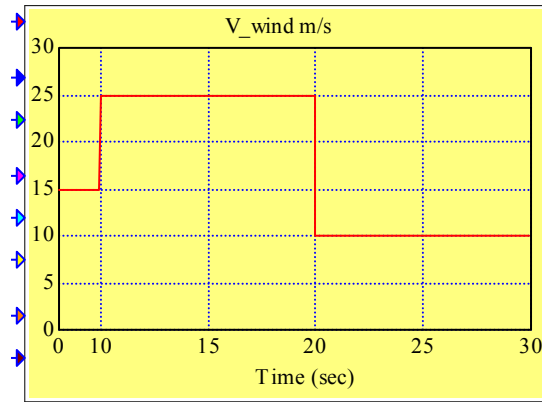


Figure 9.9 Responses of real and reactive power of the induction generator to step-wise changes (around the value of 15 m/s) in the wind speed

SYNCHRONOUS CONDENSER

The simulation diagram consists of the rotary converter/battery module, the constant village load, and the diesel generator to maintain constant line voltage V_s and frequency f and to provide the real power to the load and balance the reactive power. The simulated system is shown in Figure 9.10. The rotary converter is set up to operate in the synchronous condenser mode, i.e., to provide or to absorb reactive power with the real power generated set to 0. This is accomplished by setting to 0 the variable P_{BAT_ref} and consequently maintaining zero shaft torque, represented by the variable T_{rgen} , and zero real power output.

We see from the traces shown in Figure 9.11 that by $t = 8$ s all relevant variables stabilize, the real- and reactive-power outputs of the synchronous condenser are both zero and the reactive power of 75 kVAR is delivered to the load by the diesel generator. In other words, the steady state is reached. This state is used as the initial state for testing the steady state and transient performance. As an independent variable, we can consider either the commanded (reference) reactive power Q_{RC_ref} or the synchronous generator field current i_{f_RC} .

To test the steady-state performance of the synchronous condenser, we developed the reference reactive power profile shown in Figure 9.11. Observe that we start to vary Q_{RC_ref} linearly between 50 kVAR and -50 kVAR at $t = 8$ s. The reactive power output closely follows. The commanded changes of the reactive power are reflected by the proportional changes in the field current with zero reactive power corresponding to $i_{f_RC} = 0.4$ A. We see, that the balance of reactive power is preserved, i.e., when the condenser reactive power output is positive the reactive power provided by the diesel generator decreases by the same value and opposite. The reactive power output versus the field current and versus the reference reactive power is shown in Figure 9.9. The hysteresis or delay type of the latter relationship is caused by the field current time constant that is not involved in the former relationship.

The same initial steady state was used to obtain the traces of all relevant variables to the step changes in the reference reactive power. The results shown in Figure 9.13 are as expected.

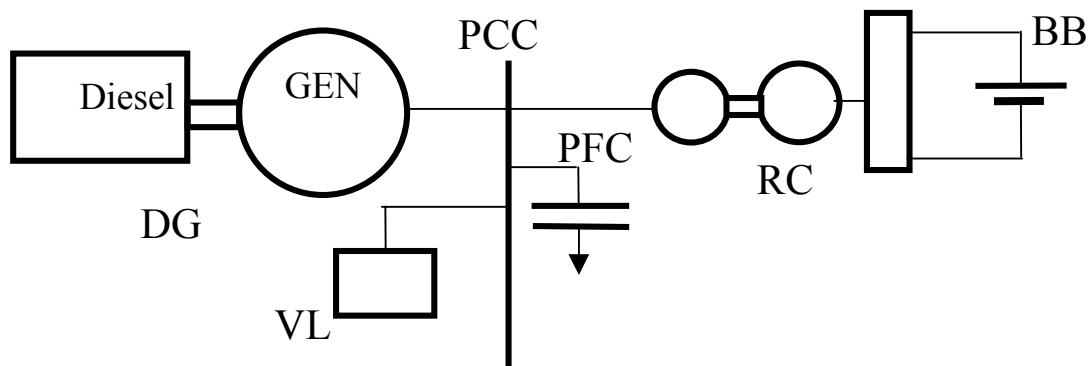


Figure 9.10 The system simulated for testing the synchronous condenser

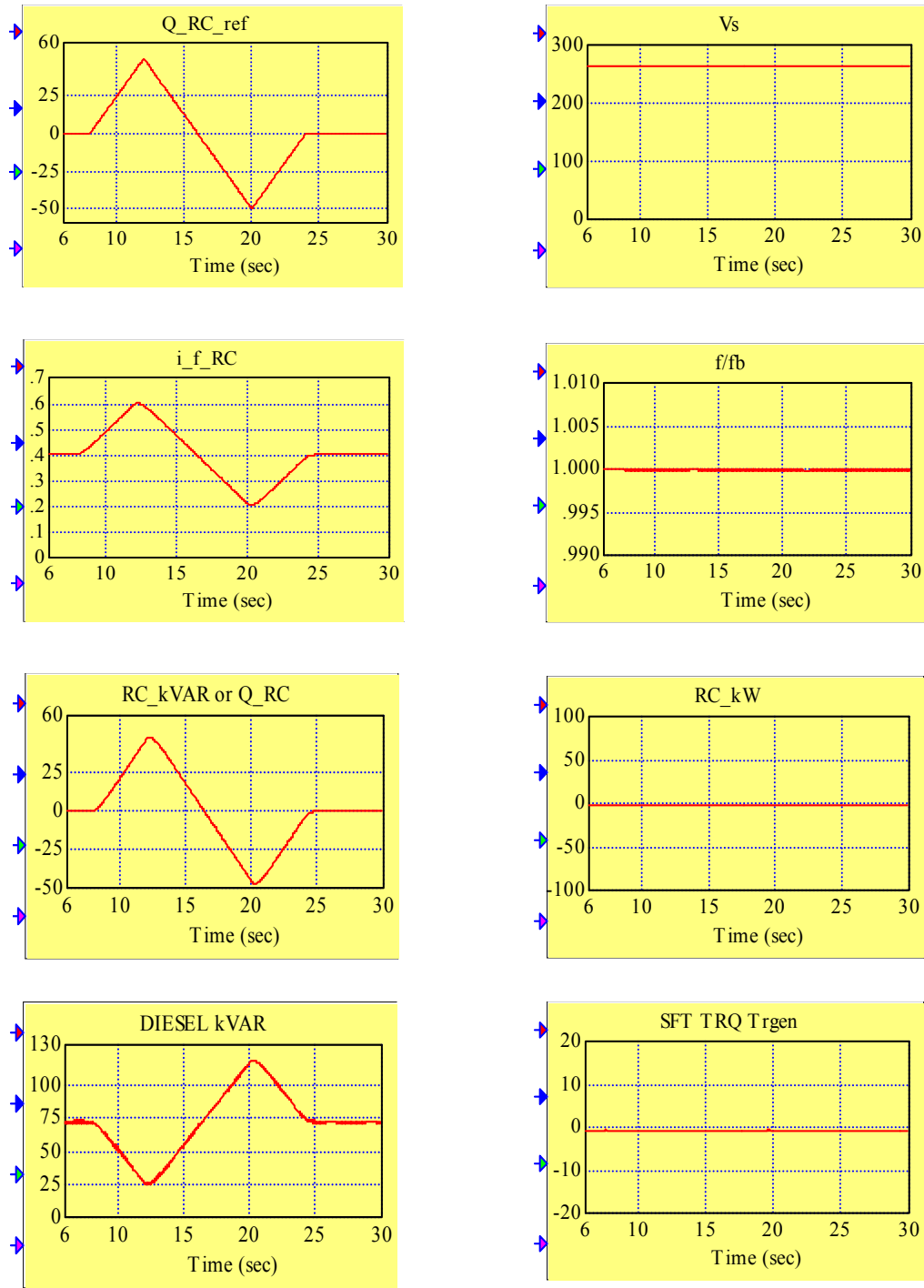


Figure 9.11 Results of the steady-state performance test of the synchronous condenser

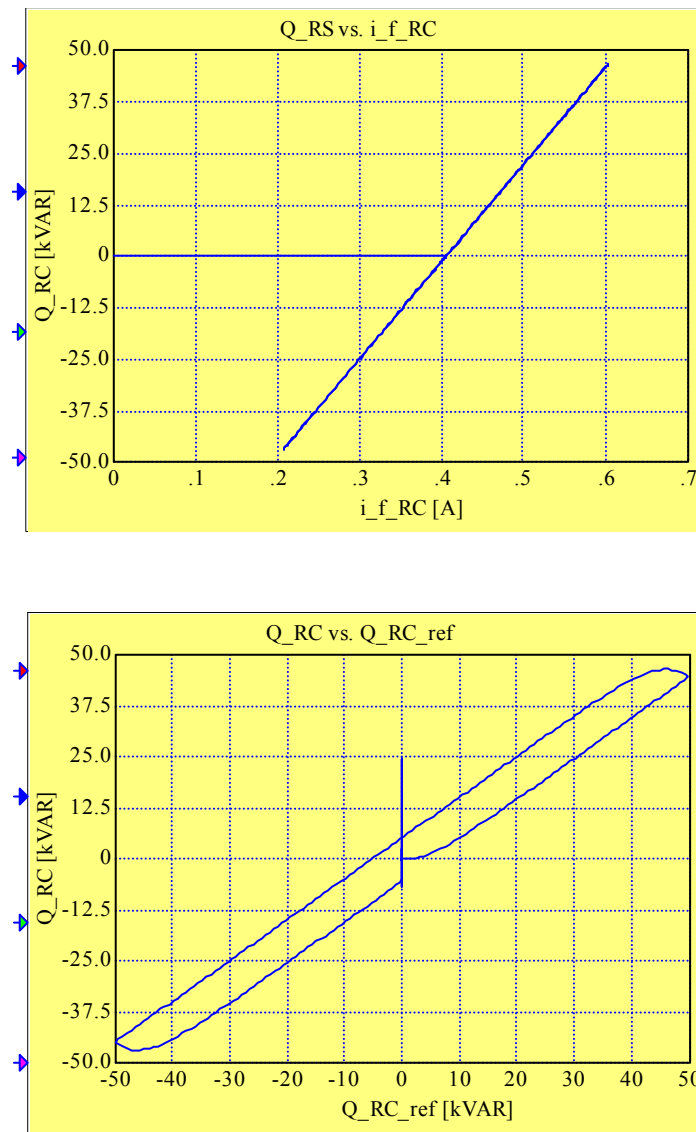


Figure 9.12 Reactive power output of the synchronous condenser versus the synchronous generator field current $i_{f_{RC}}$ and versus the commanded reactive power $Q_{RC_{ref}}$

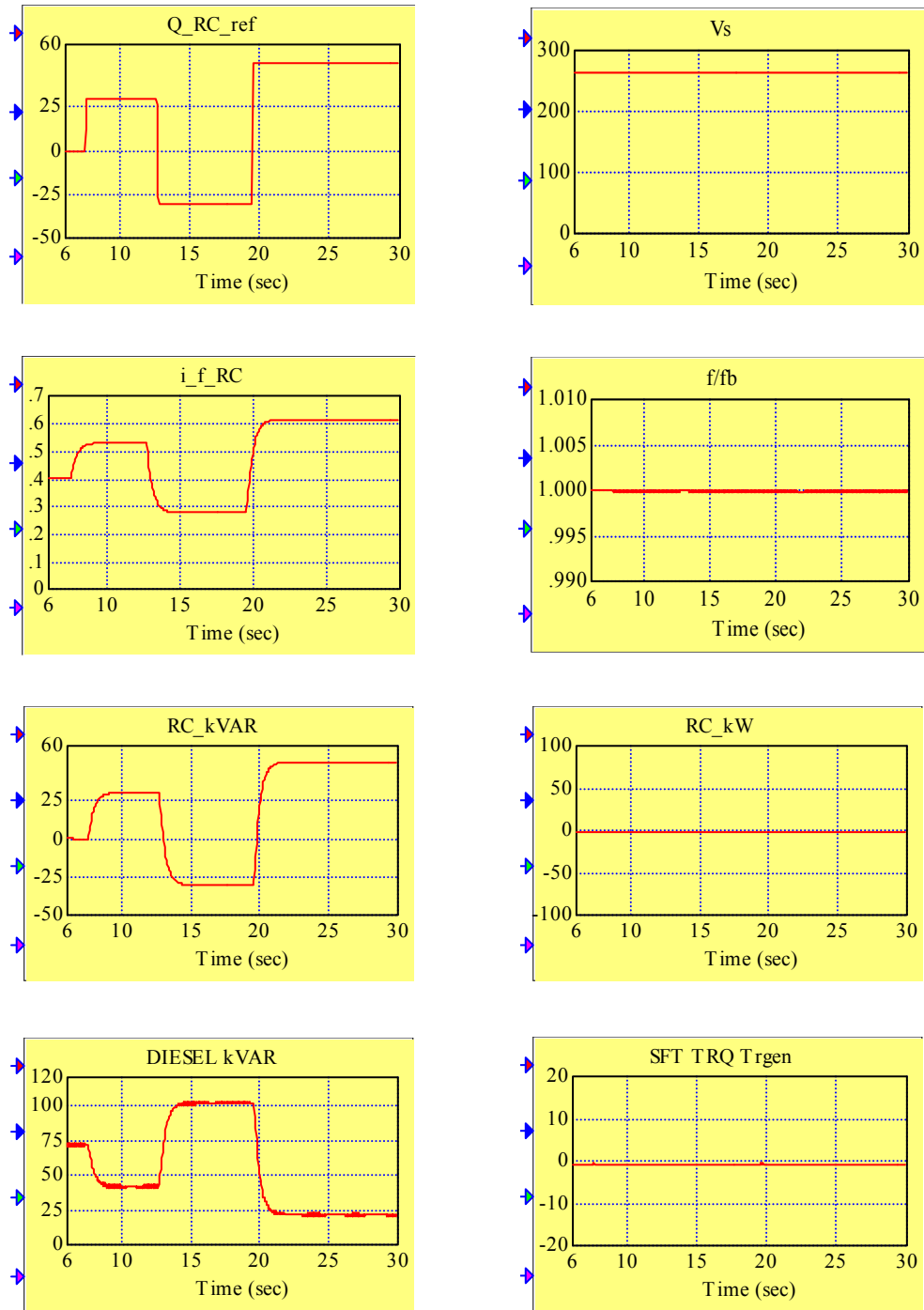


Figure 9.13 Responses to the step-wise changes in the commanded (reference) reactive power of the synchronous condenser

DC MOTOR

The DC motor/generator is a part of the rotary converter and its field current i_{f_DC} is used to control the power provided by the battery to the system (during the discharging process) or absorbed by the battery (during the charging process). Therefore, it is important to test the operation of the DC motor with the field current as an independent variable. To perform this test, we isolated the DC motor from the model of the rotary converter replacing the field current controller (shown in Figure 5.8) by the field-current source as shown in Figure 9.14(a). The DC motor armature compound block shown in Figure 9.14(a) is expanded in Figure 9.14(c). To perform the open-armature circuit test, we added a binary variable generated by the button. When the button is ON, we have normal operation, i.e., the armature current $I_{DC} \neq 0$, and when the button is OFF, $I_{DC} = 0$. For the purpose of testing, we added the calculation of the armature voltage V_t .

The compound block Parameters is expanded in Figure 9.14(b). It contains parameters of the 125 HP Reliance Electric DC motor. As explained in Chapter 5, the conversion coefficient K_{f_Lf} is calculated with the consideration of the field saturation effect, i.e., it is calculated for every value of the field current.

The test results presenting the responses of the armature current, DC power output and shaft torque to the field current changed linearly with time, as DC voltage and shaft rpm remain constant are shown in Figure 9.15. The rated velocity of 1800 rpm was assumed for this test. The test results are as expected. An alternative presentation of the results shown in Figure 9.15 is given in Figure 9.16.

The responses of the same variables to the step changes (step-up and step-down) of the field current are shown in Figure 9.17.

In Figure 9.18, we show the open-circuit armature voltage as a function of the field current.

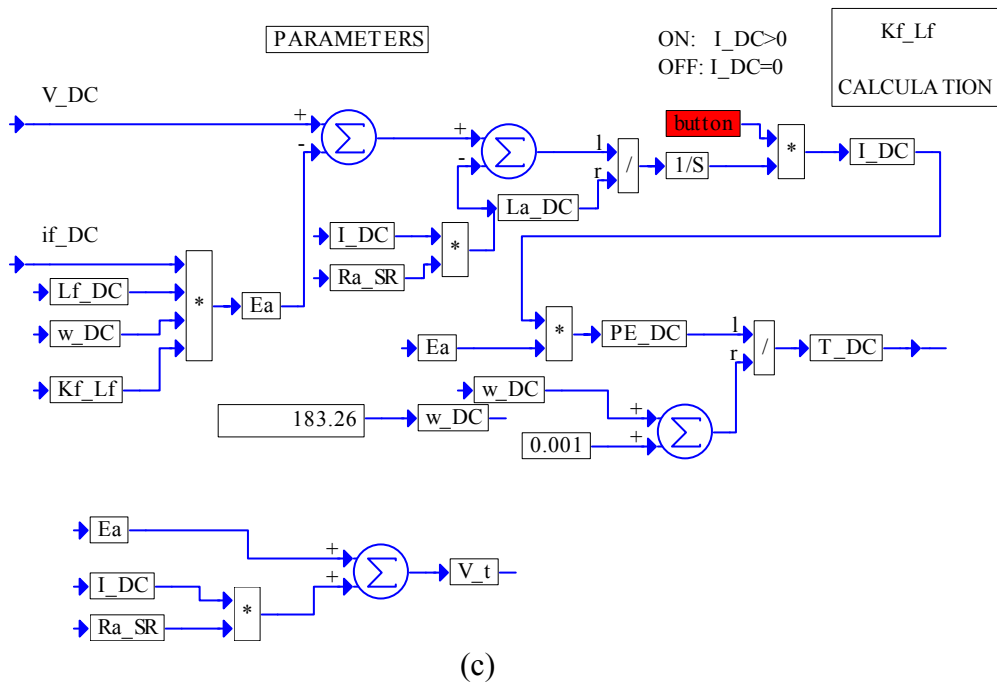
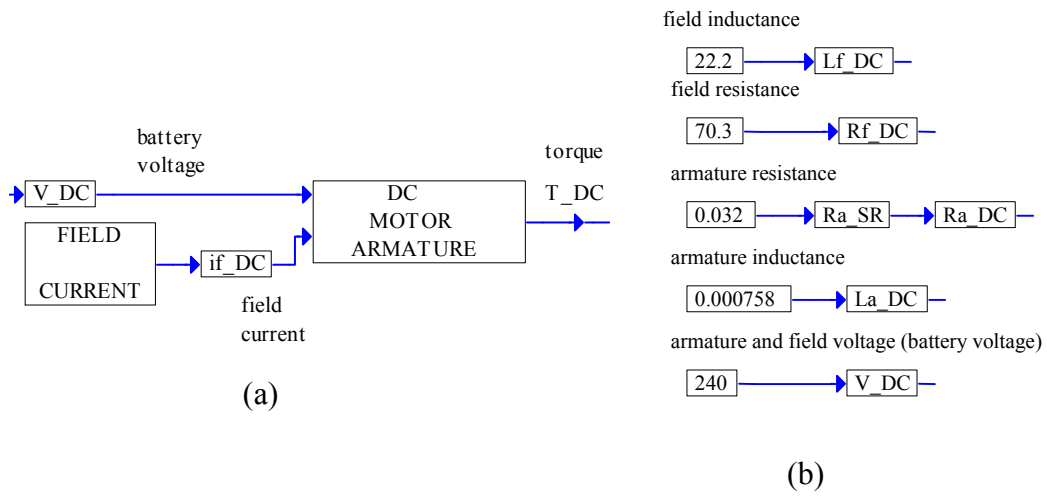


Figure 9.14 Simulation diagram of the tested DC motor

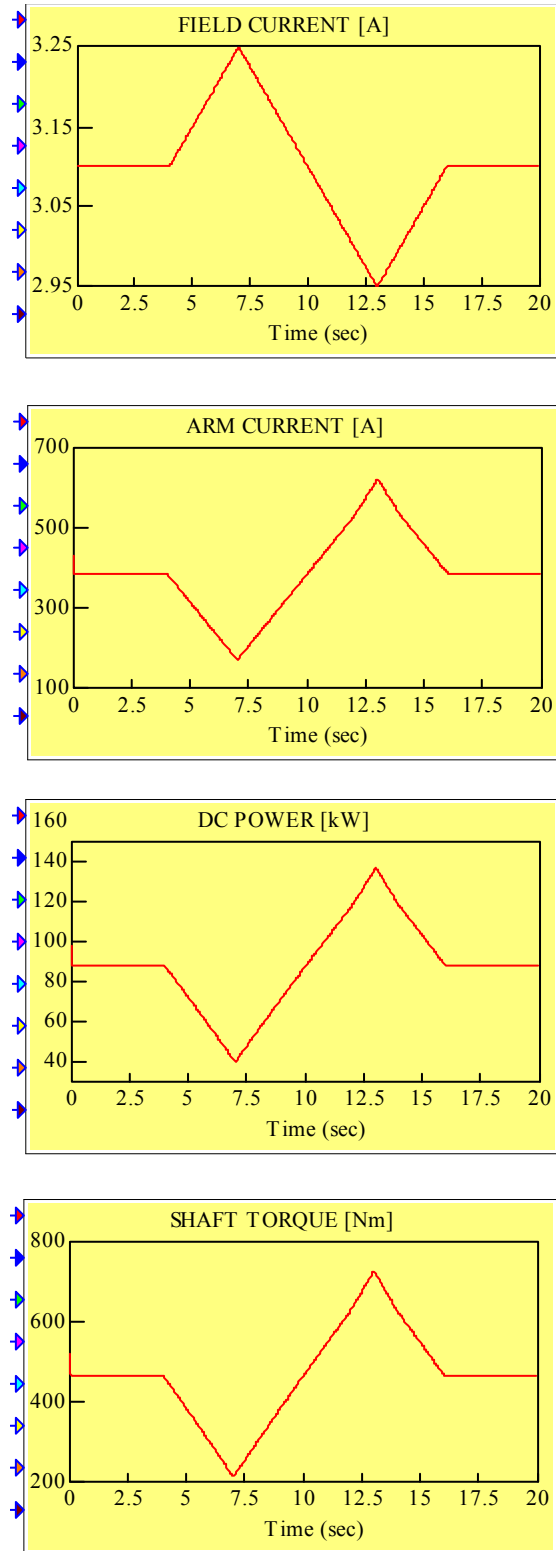


Figure 9.15 Responses of the armature current, DC power output and shaft torque to the field current changing linearly with time, as DC voltage and shaft rpm remain constant

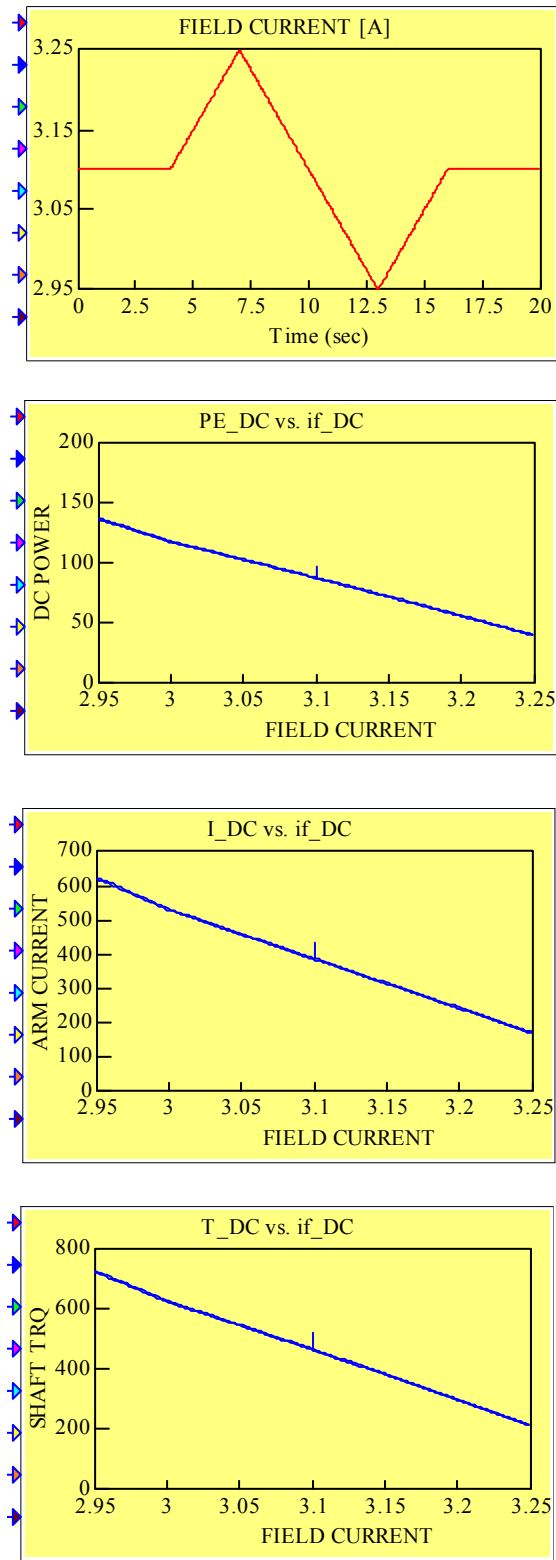


Figure 9.16 Alternative presentation of the test results shown in Figure 9.15

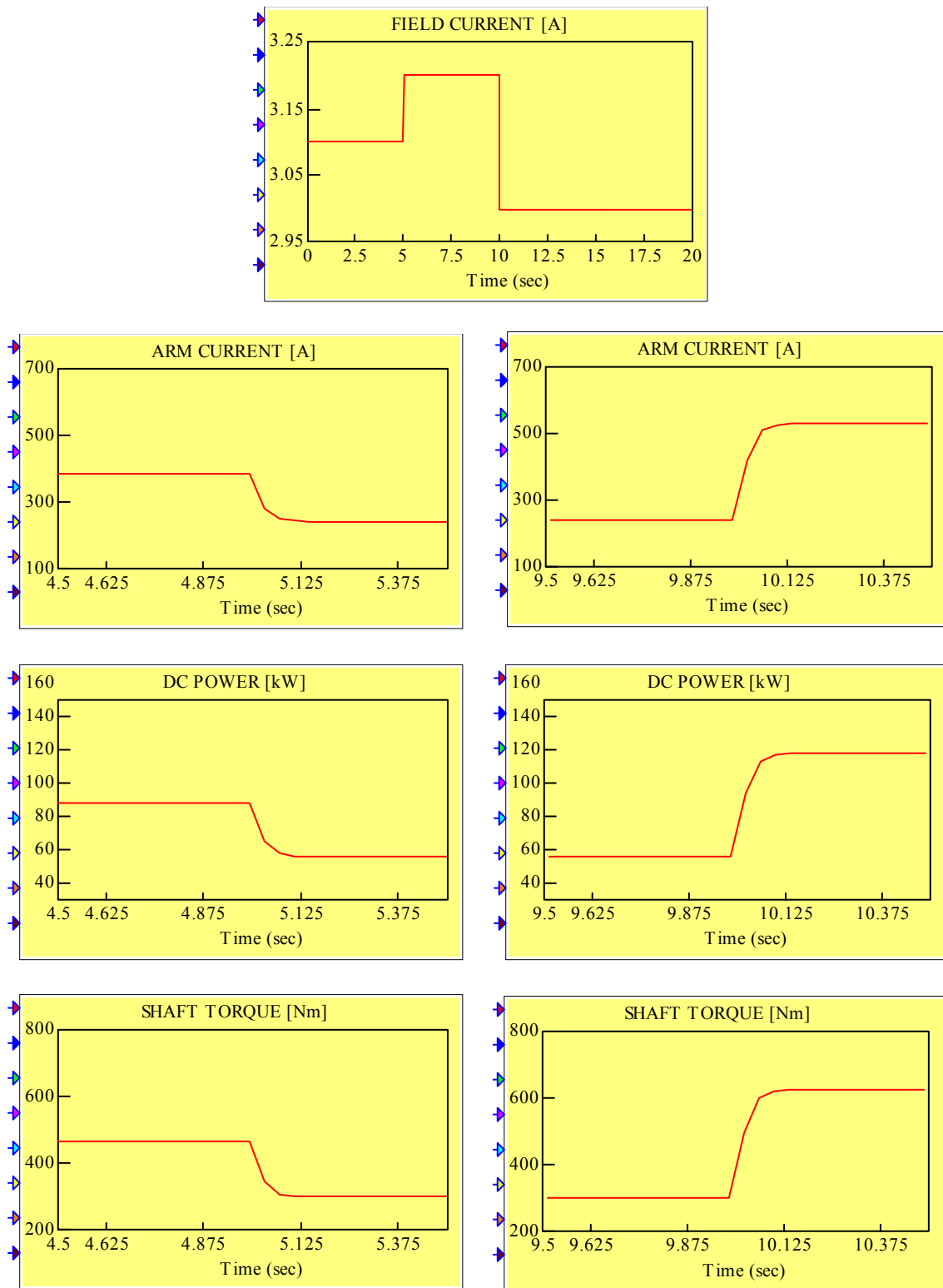


Figure 9.17 Responses of the variables of interest to the step changes of the field current

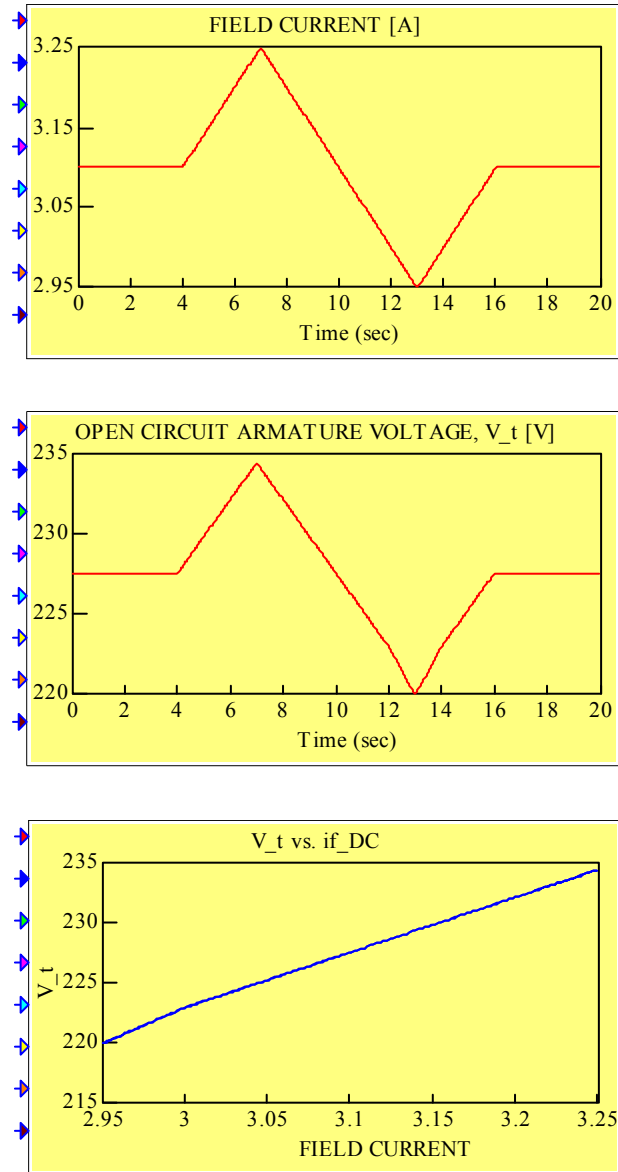


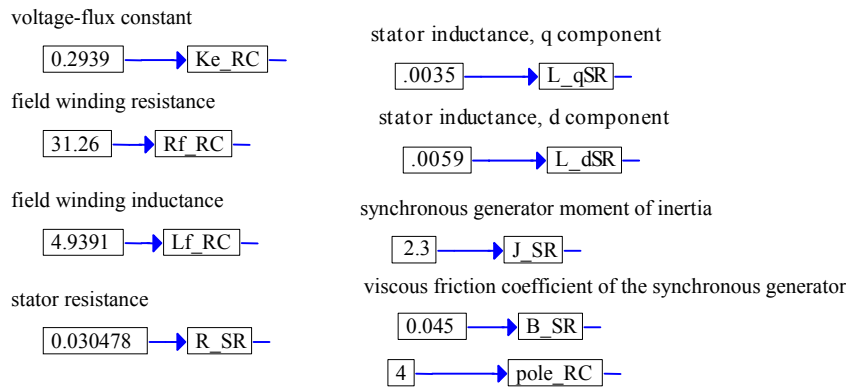
Figure 9.18 Open-circuit armature voltage as a function of the field current

SYNCHRONOUS GENERATOR

The synchronous generator is a part of the rotary converter and diesel generator. We tested a model of the 125 kW KATO synchronous machine. In the test performed, we look at its power output and its armature current as a function of the shaft torque. In this test, we keep the AC voltage and frequency constant. Before we applied a variable shaft torque, we brought the machine to a steady state corresponding to the shaft torque of 600 Nm and the nominal full load field current of 1 A. This value of the field current remained constant for both static and dynamic tests. It can best be seen from Figure 9.20 that at this initial steady state the armature current has a value of 177 A, the real power generated is 110 kW and the reactive power is 98 kVAR.

The results of a “quasi-static” test are presented in Figure 9.19. “Quasi-static” means that the load torque was varied continuously, i.e., we did not wait after a small change for the steady state to be reached. This non-ideal testing is responsible for the hysteresis seen in the plots presented. In other words, the inertia seen in the step responses, shown in Figure 9.20 is responsible for this hysteresis.

The following are the parameters of the machine used in the simulation:



Some of these parameters had to be calculated from the manufacturer’s data. Let us show these calculations. The manufacturer specifies d and q components of the reactance of the armature as per unit values. We need them in henries. We have to find the unit, which is calculated as follows:

$$Z_{base} = \frac{V_s}{I_{a rated}} = \frac{480/\sqrt{3}}{188} = 1.4741\Omega, \quad \text{and } V_s = 277.1281$$

We know that $\omega = 377$ rad/s. Now we can calculate

$$L_{qSR} = \frac{X_q}{\omega} = \frac{0.89 \times 1.4741}{377} \approx 0.0035 \text{ H}, \quad L_{dSR} = \frac{X_d}{\omega} = \frac{1.504 \times 1.4741}{377} \approx 0.0059 \text{ H}$$

The armature resistance for the star connection is

$$R_{SR} = \frac{0.060956}{2} = 0.030478.$$

For the field winding the manufacturer specifies $R_f = 31.26 \Omega$ and the time constant $T_d' = 0.158 s = \frac{L_f}{R_f}$, which results in $L_f = 4.9391$ H. Now, we shall find the voltage-flux constant K_e as defined by the following relation:

$$K_e = \frac{E}{\omega L_f i_f},$$

where i_f is the full load field current specified by the manufacturer to be 1 A. The only unknown in this equation is E . To find E , we must consider the phasor diagram. The power factor is specified to be 0.8, which corresponds to the angle $\theta = 0.644501$ rad. Therefore, the phasor diagram is represented by the following relation:

$$\hat{E} = \hat{V}_s + R_{SR} \hat{I}_a + \hat{I}_a (jX_s),$$

where

$$\hat{V}_s = 277.1281 \angle 0$$

$$\hat{I}_a = 188 \angle -\theta.$$

Finally, we obtain $E = |\hat{E}| = 547.3163$ V, from which we find the voltage-flux constant $K_e = 0.2939$.

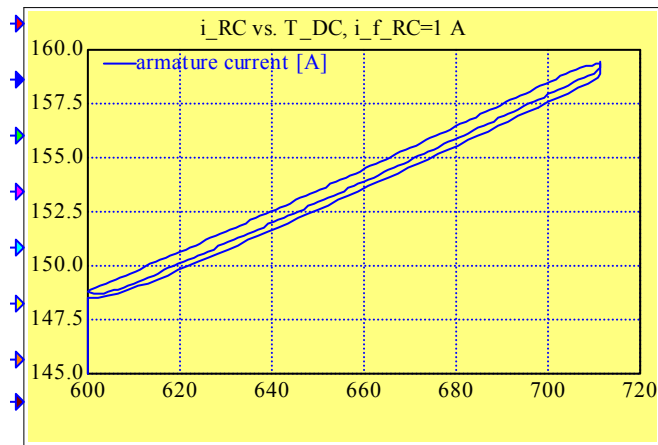
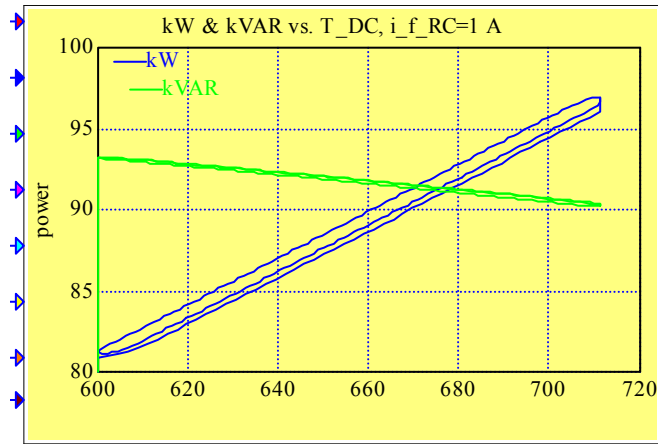
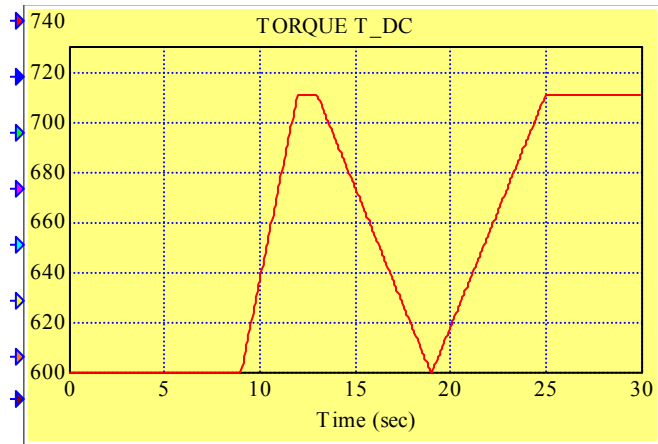


Figure 9.19 Results of a static test of the synchronous generator

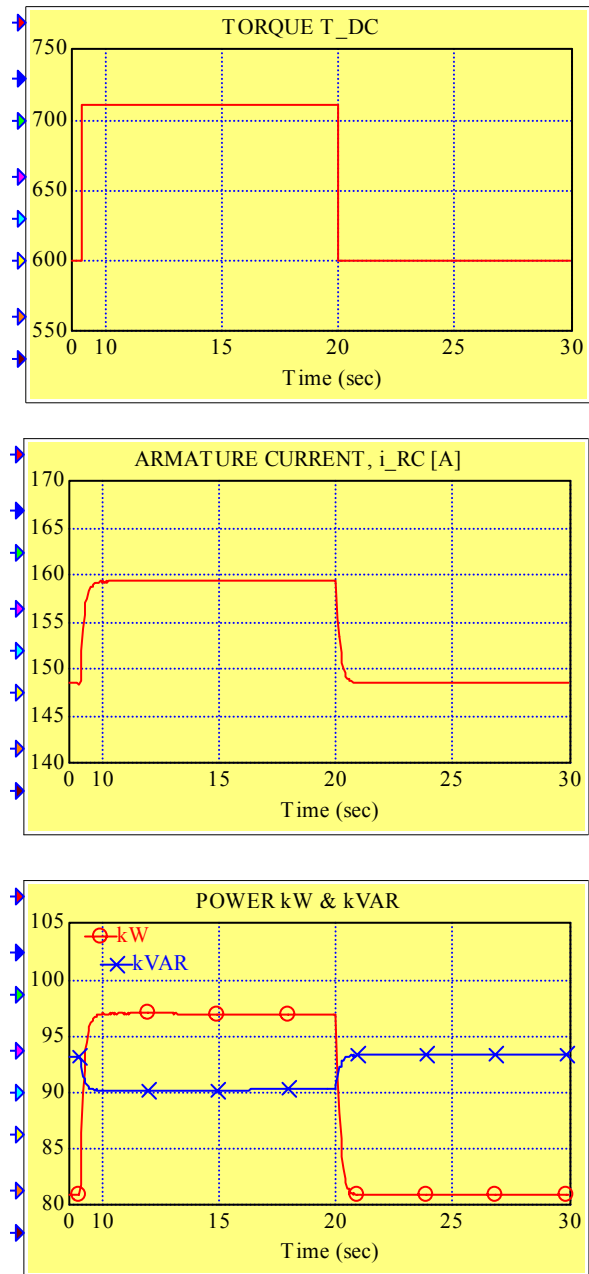


Figure 9.20 Results of a dynamic test of the synchronous generator

INDUCTION GENERATOR

The induction generator is a part of the wind turbine generator. For the purpose of testing, it was isolated from the model of the wind turbine generator. The top view of the simulation diagram used in the test is shown in Figure 9.21. The independent variable is the asynchronous generator shaft rpm. In this test, we hold constant the line voltage V_s and the frequency ω . This is clearly shown in Figure 9.21. As shown in Figure 9.22, we used the shaft torque and the armature current as dependent variables in this test. First, the shaft velocity is ramped to 1800 rpm, i.e., the synchronous generator passes initially through the phase of motoring as in the normal operation. At this state, the armature current assumes its minimum value, the shaft torque is 0, and no power is generated. In this state we start to increase and then to decrease the shaft rpm linearly with time. Initially, the torque and the armature current increase, which corresponds to the power generation. As the rpm decreases and passes through the synchronous speed, the shaft torque reverses sign, i.e., below the synchronous speed the machine starts to operate as a motor.

In the standard model, the shaft velocity is the solution of the torque equation. In other words, we do not have mechanical inertia in this test. This is apparent from the step responses shown in Figure 9.23.

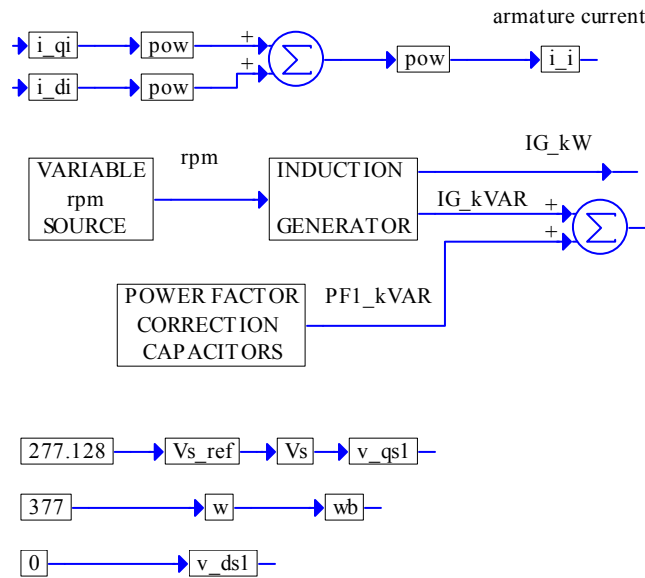


Figure 9.21 Top-view of the simulation diagram used in the test performed

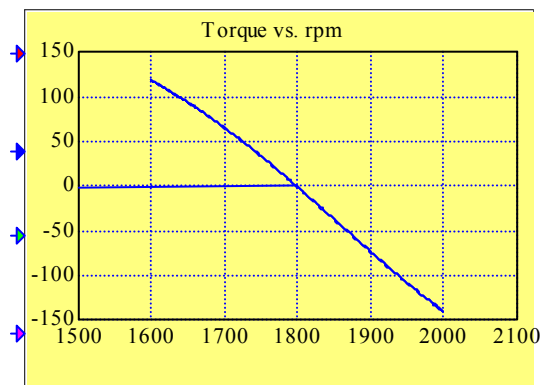
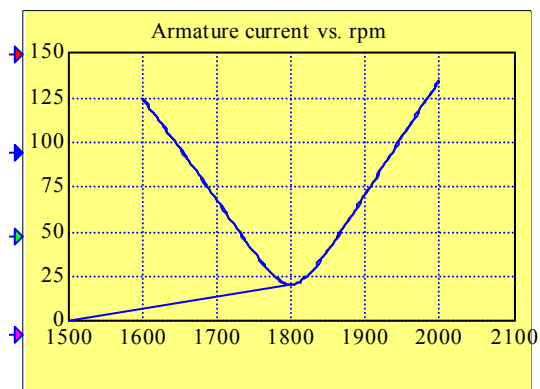
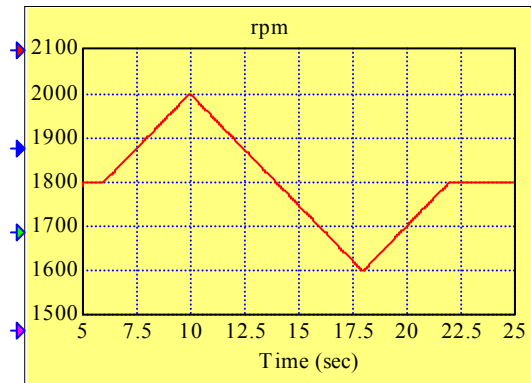


Figure 9.22 Steady-state test of the asynchronous generator: armature current and shaft torque versus shaft rpm (varied linearly around the synchronous speed of 1800 rpm) at a constant frequency and AC voltage

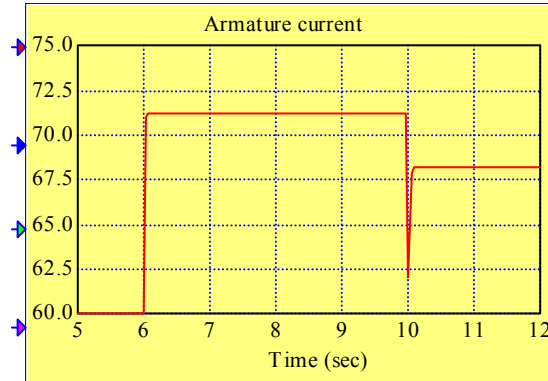
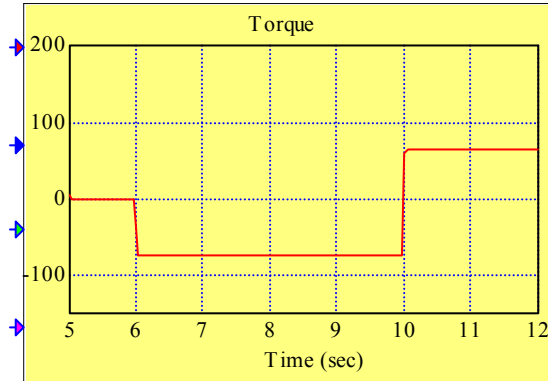
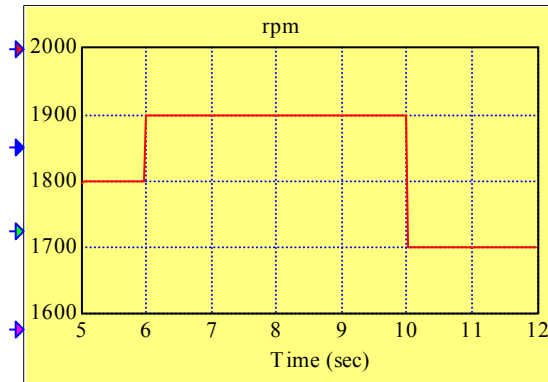


Figure 9.23 Responses of the torque and armature current to step changes in the shaft velocity

ROTARY CONVERTER

The model of the rotary converter tested consists of the models of the 125 kW KATO synchronous machine and the 125 HP Reliance Electric DC motor. The simulation diagram is shown in Figure 9.24. As shown in this diagram, we keep constant the line voltage and frequency, and the DC (battery) voltage. The synchronous machine field current is set at the nominal full load value of 1 A. The DC motor field current is an independent variable. We plot the AC output power and the rotary converter efficiency as a function of the DC motor field current. There are two ranges of the DC field current: one corresponds to battery discharging or power generation (output power positive) and the other one corresponds to battery discharging or power absorption (output power negative). Depending on the range of operation, we calculate the efficiency accordingly (as shown in Figure 9.24). In both ranges of operation, there is a value of the DC motor field current for which the efficiency assumes its maximum value.

In Figure 9.25, we show the plots of efficiency and power generated by the rotary converter versus DC motor field current (discharging battery). In Figure 9.26 we present the efficiency and power absorbed by the rotary converter versus the DC motor field current (charging battery). All plots are as expected.

In Figure 9.27, we show the response of the power generated by the rotary converter to a step change in the DC motor field current (while discharging the battery). In Figure 9.28, we present the response of the power absorbed by the rotary converter to a step change in the DC motor field current (while charging the battery).

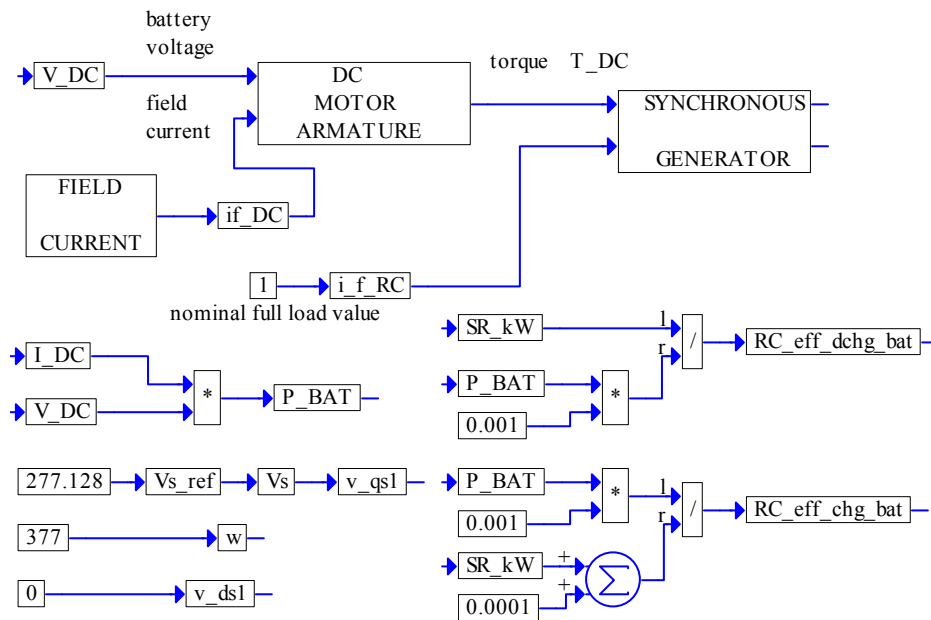


Figure 9.24 Top-view of the simulation diagram used in the test performed

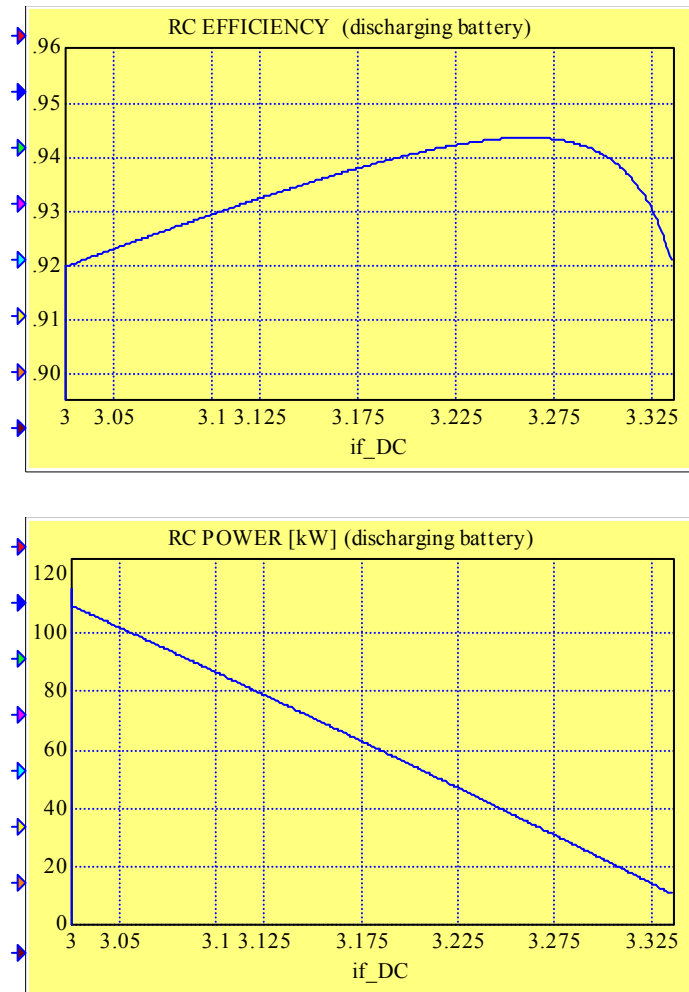


Figure 9.25 Efficiency and power generated by the rotary converter versus the DC motor field current (discharging battery)

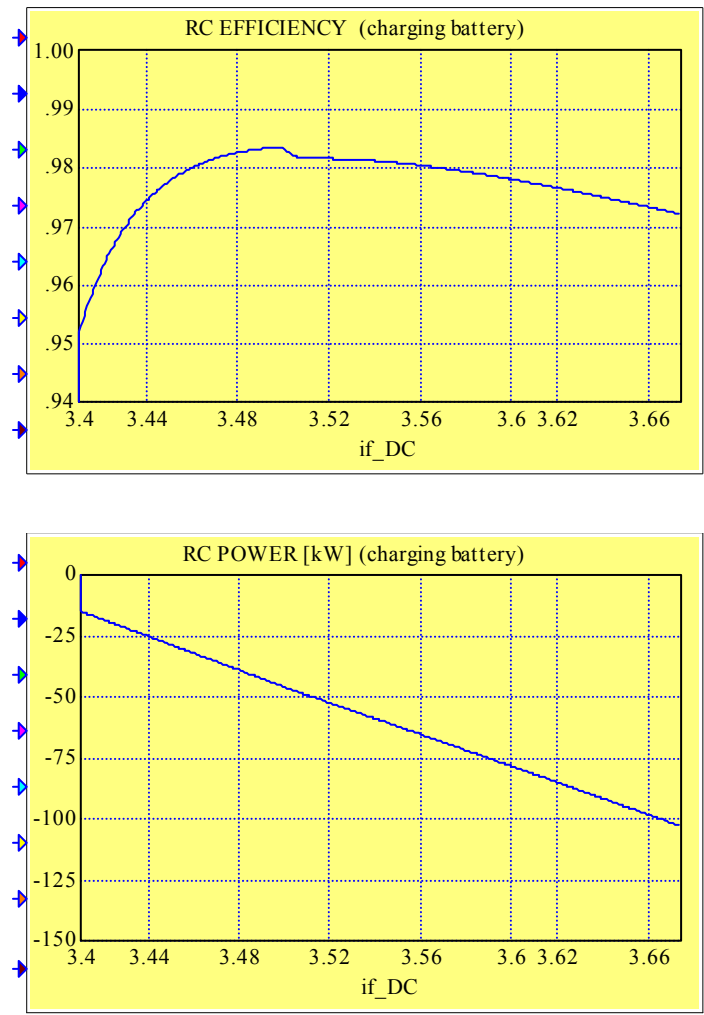


Figure 9.26 Efficiency and power absorbed by the rotary converter versus the DC motor field current (charging battery)

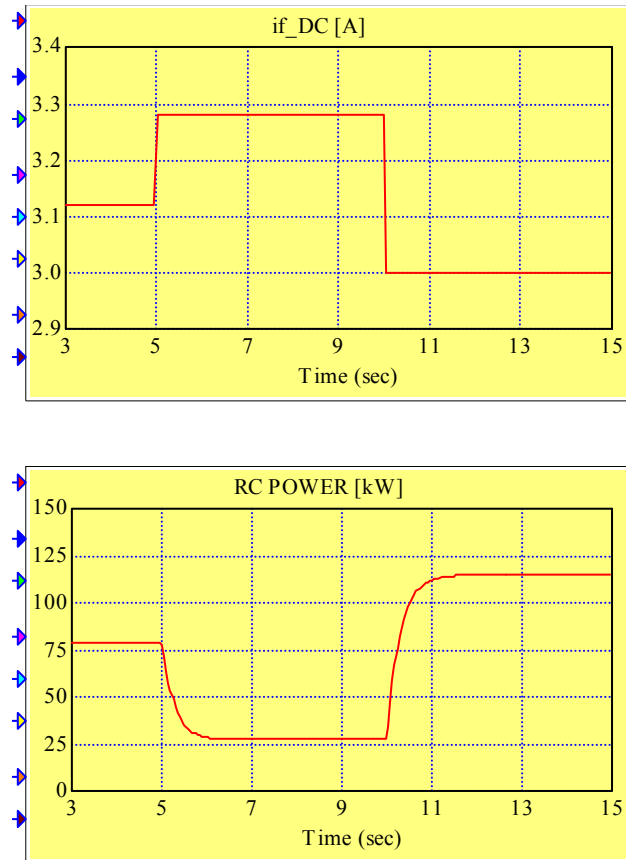


Figure 9.27 Response of the power generated by the rotary converter to a step change in the DC motor field current (while discharging the battery)

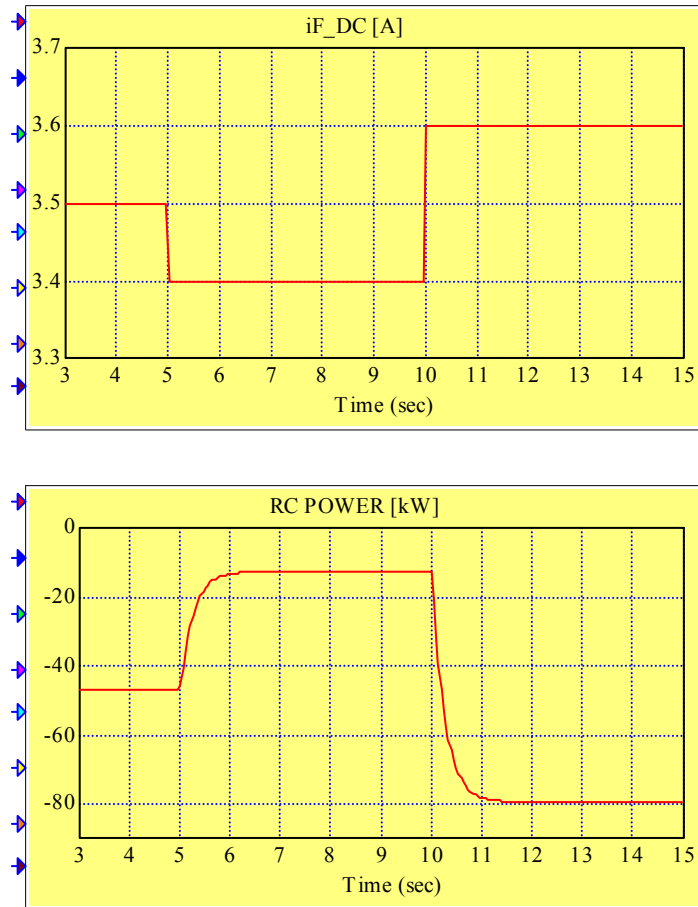


Figure 9.28 Response of the power absorbed by the rotary converter to a step change in the DC motor field current (while charging the battery)

Validation Tests at the System Level

In this chapter, we report the results of the validation tests performed at the system level using the data recorded from the Hybrid Power Test Bed (HPTB) at the National Renewable Energy Laboratory. The power system included: a diesel

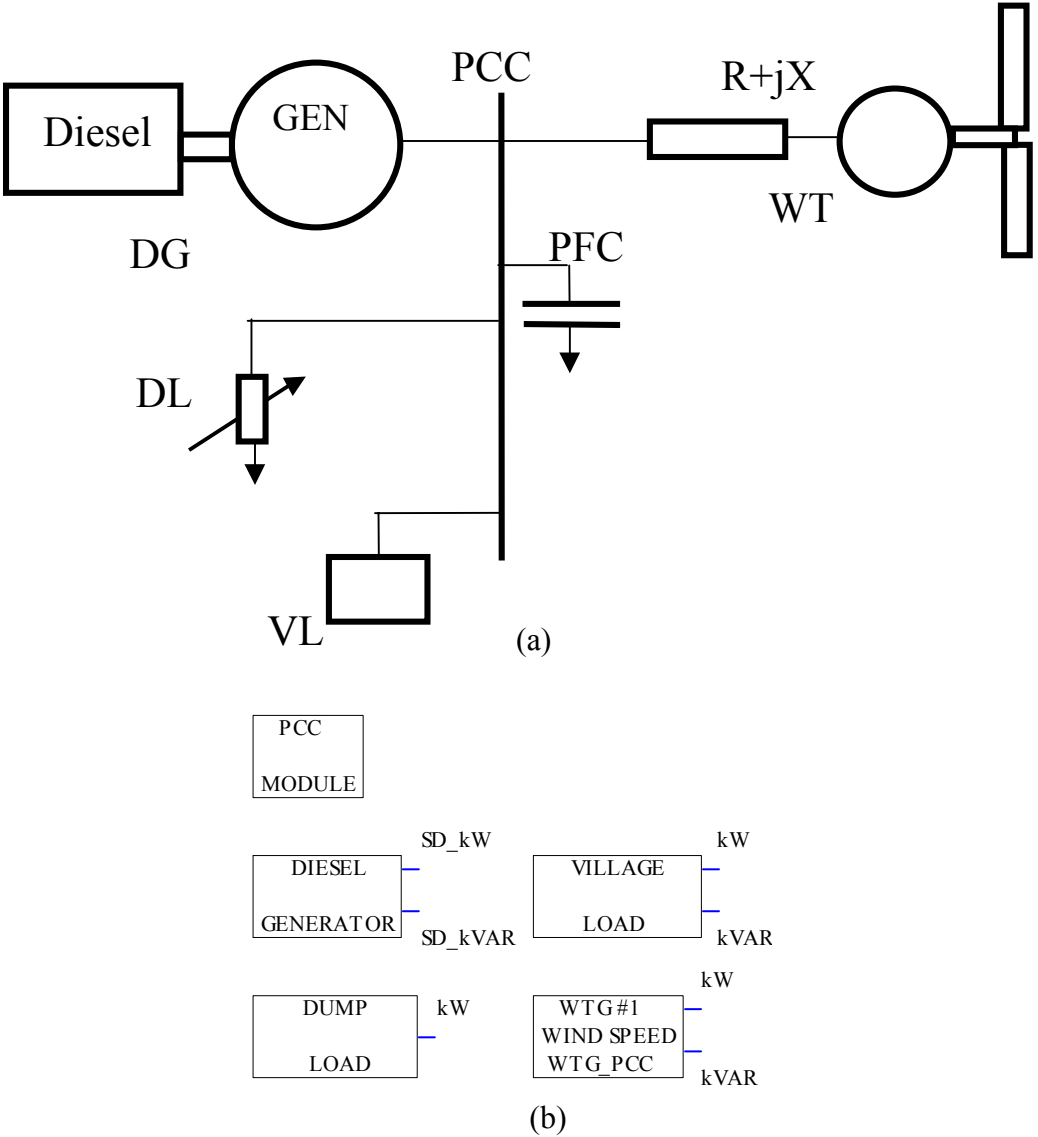


Figure 10.1 Power system composed of diesel generator (DG), AC wind turbine (WT), dump load (DL) and village load (VL): (a) single-line diagram, (b) Top-view of the RPM-SIM simulation.

generator (DG), an AOC wind turbine (WT), a dump load (DL), and a village load (VL). A power system with this configuration is presented in Figure 10.1, where we show both the single line diagram and the top-view RPM-S_{IM} simulation diagram. We were provided with data sets for five runs with the following names assigned: case A, case B, AOC start-up, step-in load, and AOC shutdown. The synchronous generator Model E7201L1 data sheet, attached as Appendix 2, was used to determine the parameters of the diesel generator model. These parameters (as they appear in the parameter block of the simulated model) are shown in Figure 10.2.

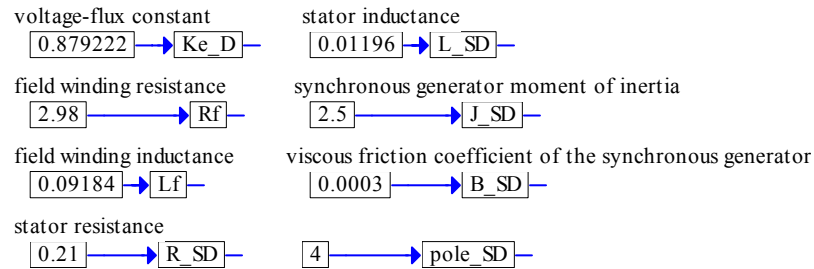


Figure 10.2 Parameters of the diesel generator

The data recorded over the interval of 10 s with a sampling period of 0.01 s included real and reactive power files for all these modules as well as the line-to-line voltage file and frequency file. The wind speed was not measured. To use these sets of data for partial validation of the simulator, we could use only the diesel generator block and PCC block in the original RPM-S_{IM} format. We had to modify the other blocks involved, so that they could work with power files as their inputs. These modified blocks also have real and reactive power as their outputs, which are calculated using the voltage generated in the simulated system. Consequently, the simulated power traces follow closely the traces recorded after approximately 2 seconds, which is the start-up time of the diesel generator. The traces involved are shown in the following figures:

- Figure 10.3 Simulation results for the case A data
- Figure 10.4: Simulation results for the case B data
- Figure 10.5: Simulation results for the AOC start-up data
- Figure 10.6: Simulation results for the step-in load data
- Figure 10.7: Simulation results for the AOC shutdown data.

Considering a slight oscillatory power imbalance of the recorded data (shown in each figure) and the smoothing involved in the measuring system, there is a very good agreement of the traces recorded with those obtained from the simulation.

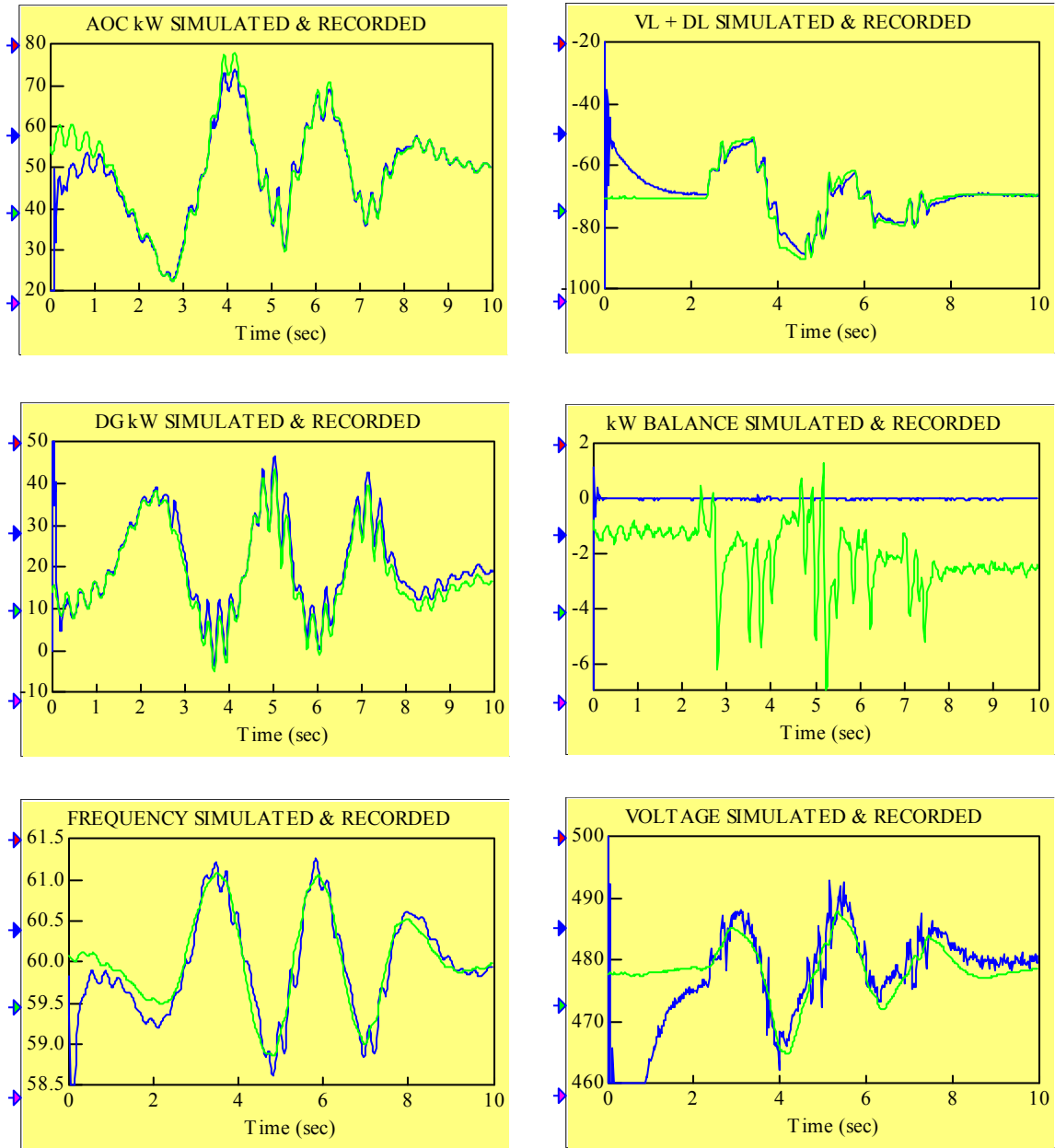


Figure 10.3 Simulation results for the case A data: the dark line is used for traces simulated and the light line is used for traces recorded

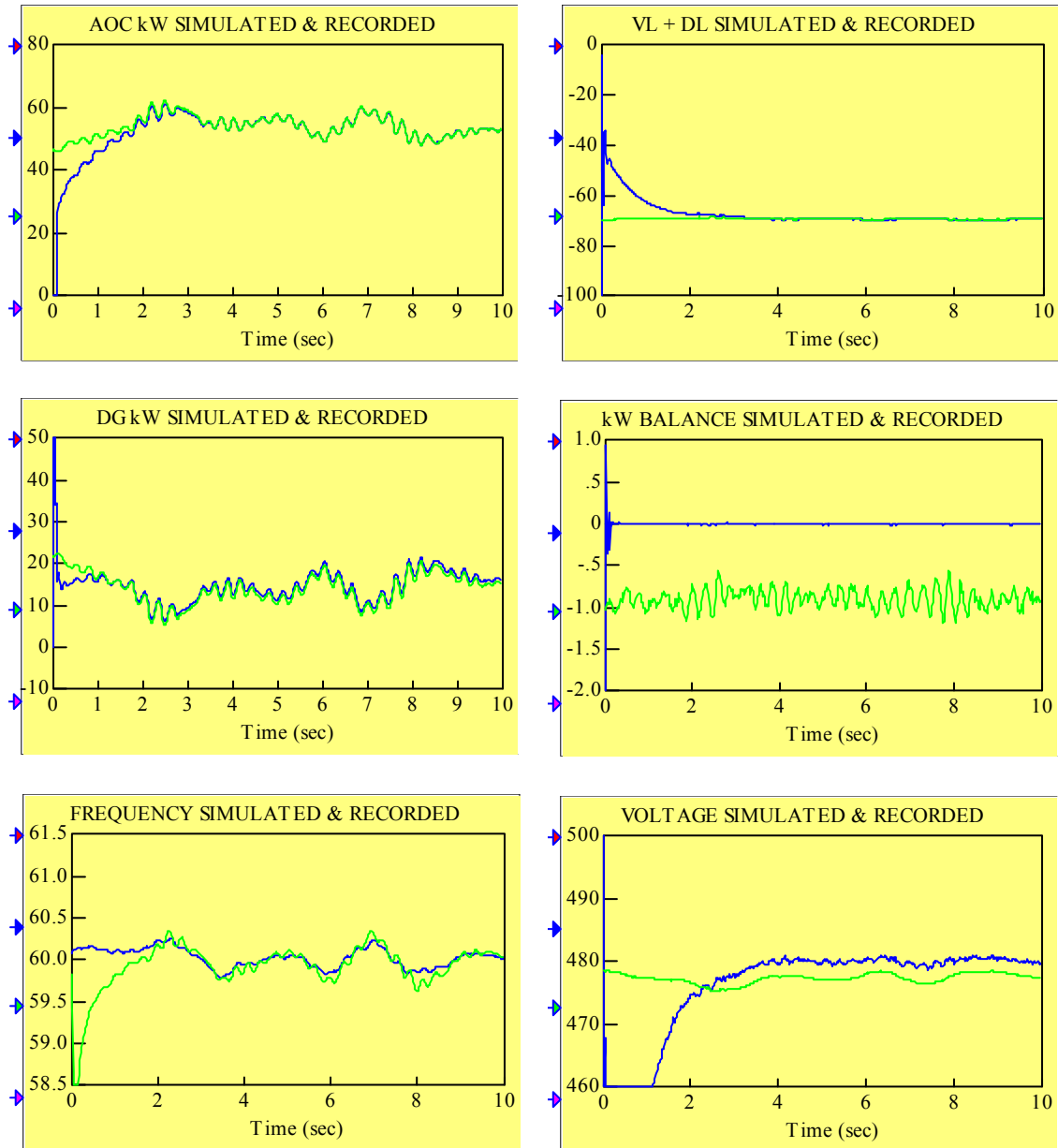


Figure 10.4 Simulation results for the case B data: the dark line is used for traces simulated and the light line is used for traces recorded

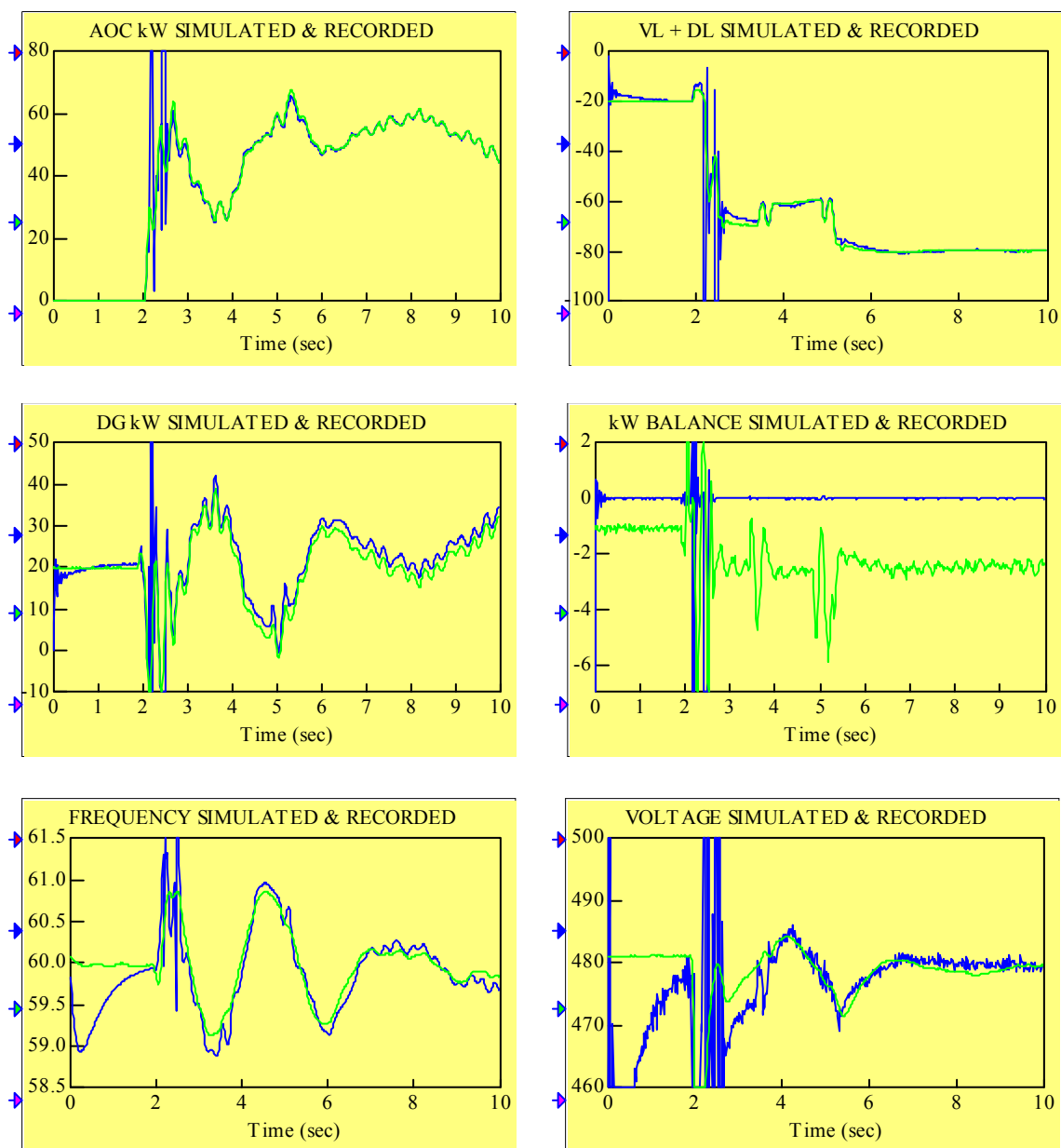


Figure 10.5 Simulation results for the AOC start-up data: the dark line is used for traces simulated and the light line is used for traces recorded

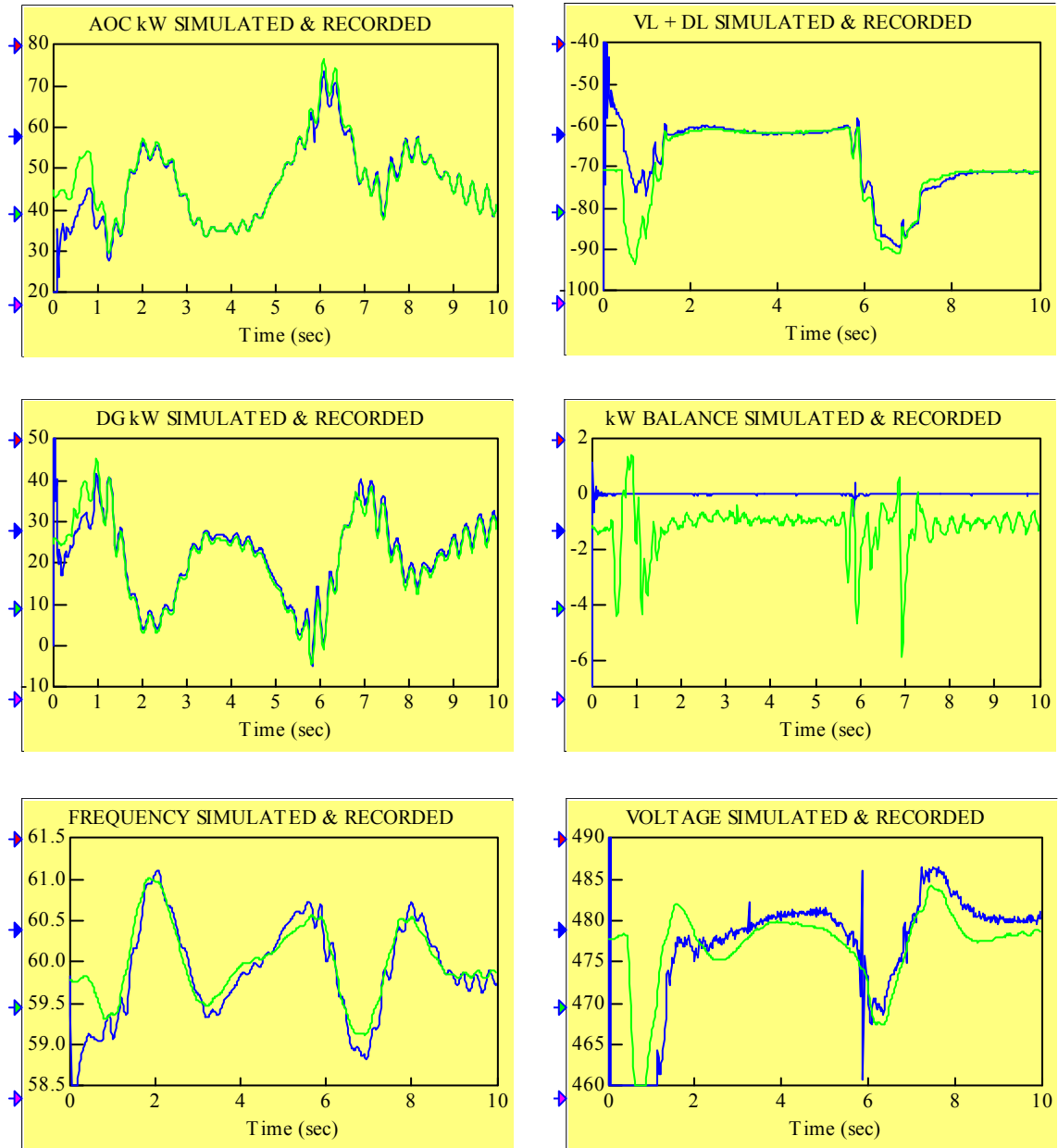


Figure 10.6 Simulation results for the step-in load data: the dark line is used for traces simulated and the light line is used for traces recorded

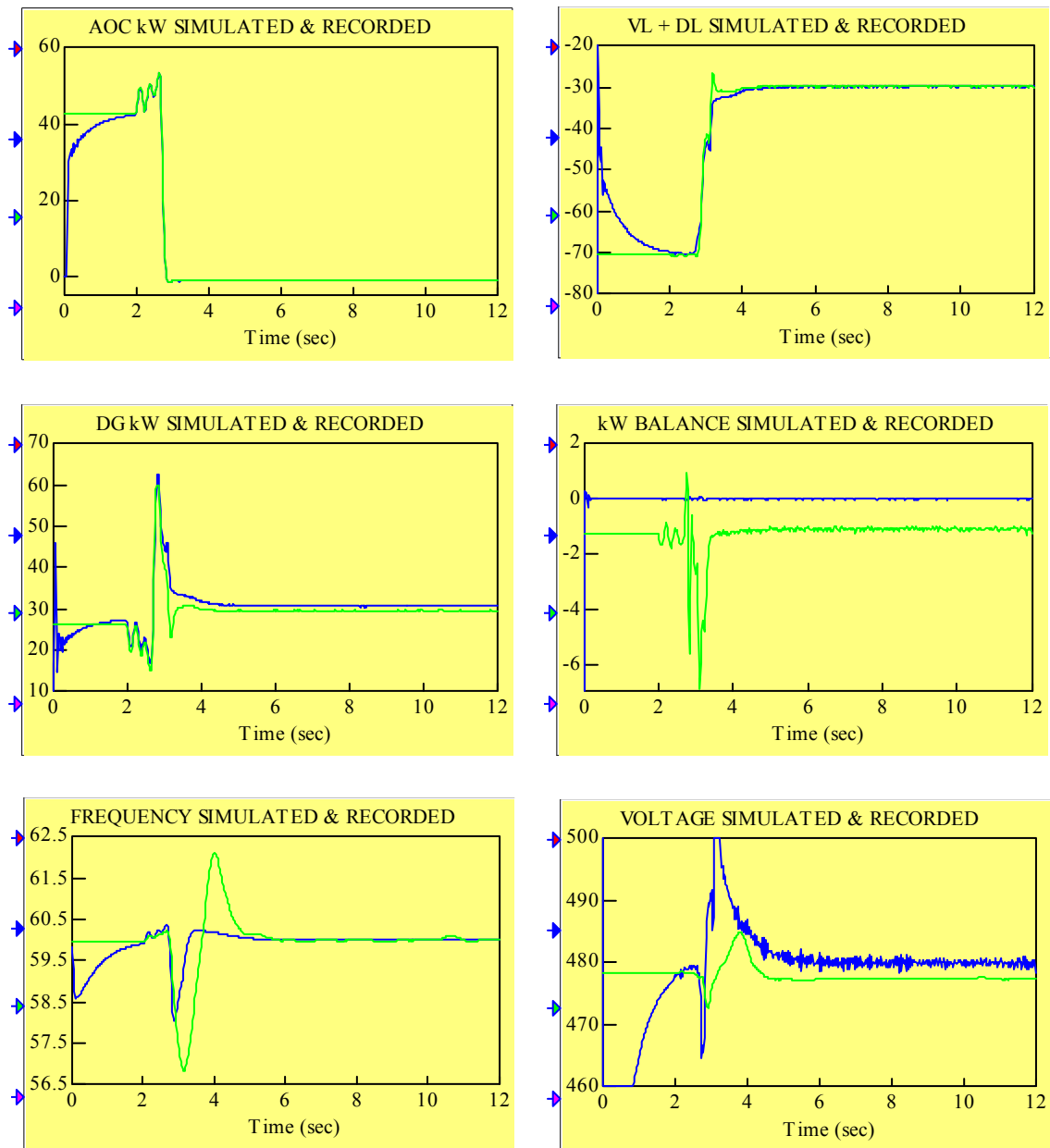
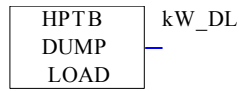


Fig10.7 Simulation results for the AOC shutdown data: the dark line is used for traces simulated and the light line is used for traces recorded

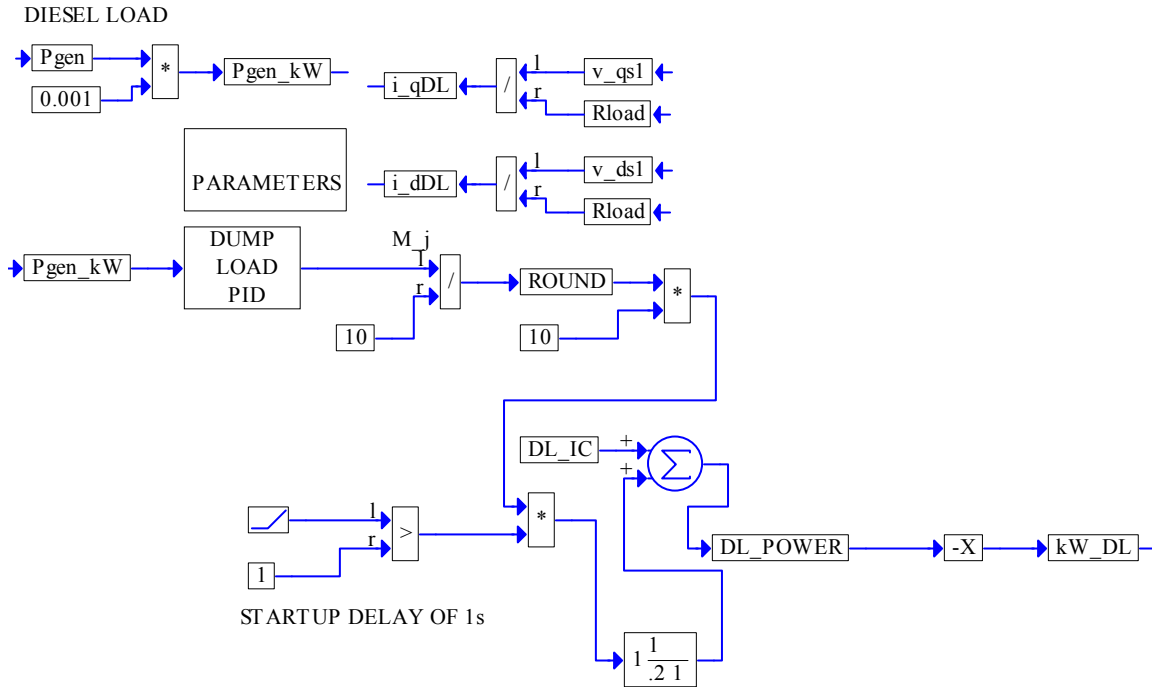
We also validated the RPM-S_{IM} simulator using the same data and, in addition to the real diesel generator model, we included the model of the real dump load block with the Wales Control System Dump Load Dispatch used at the HPTB. It was implemented according to the description given in Appendix 3 and is shown in Figure 10.8. In addition, its parameters are shown in Figure 10.9. The traces involved appear in the following figures:

- Figure 10.10: Simulation results for the case A data
- Figure 10.11: Simulation results for the AOC start-up data
- Figure 10.12: Simulation results for the step-in load data
- Figure 10.13: Simulation results for the AOC shutdown data

A good agreement of the traces recorded with those obtained from the simulation can be observed.



(a)



(b)

Figure 10.8 Dump load block with the Wales Control System Dump Load Dispatch used at the HPTB: (a) top-level view, (b) first level expansion.

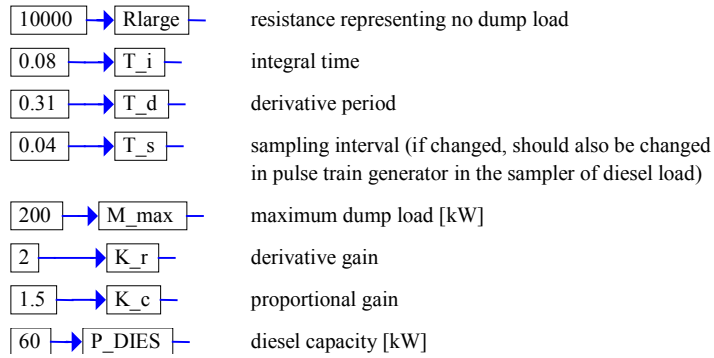


Figure 10. 9 Expansion of the PARAMETERS block

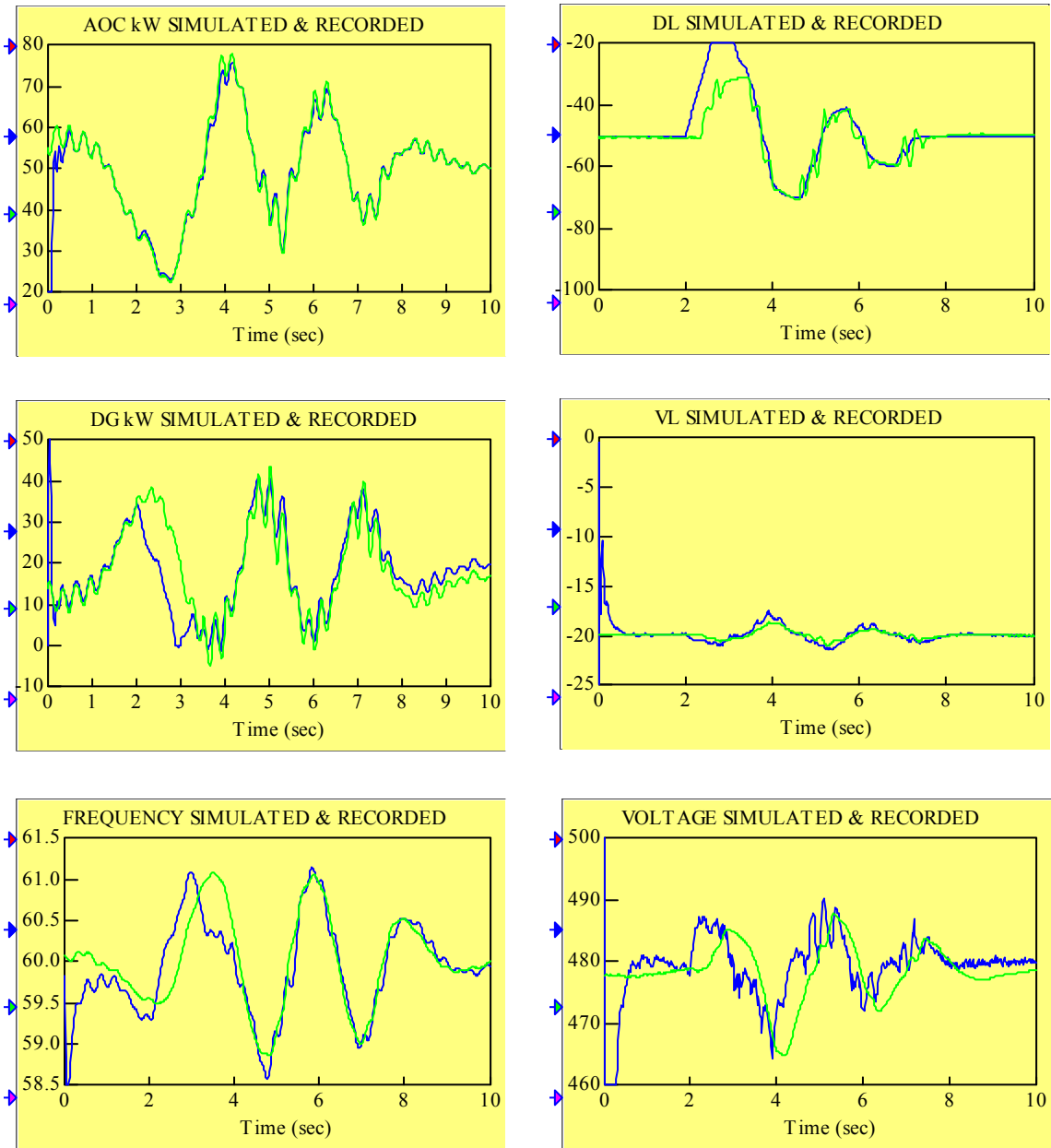


Figure 10.10 Simulation results for the case A data with a real dump load model included: the dark line is used for traces simulated and the light line is used for traces recorded

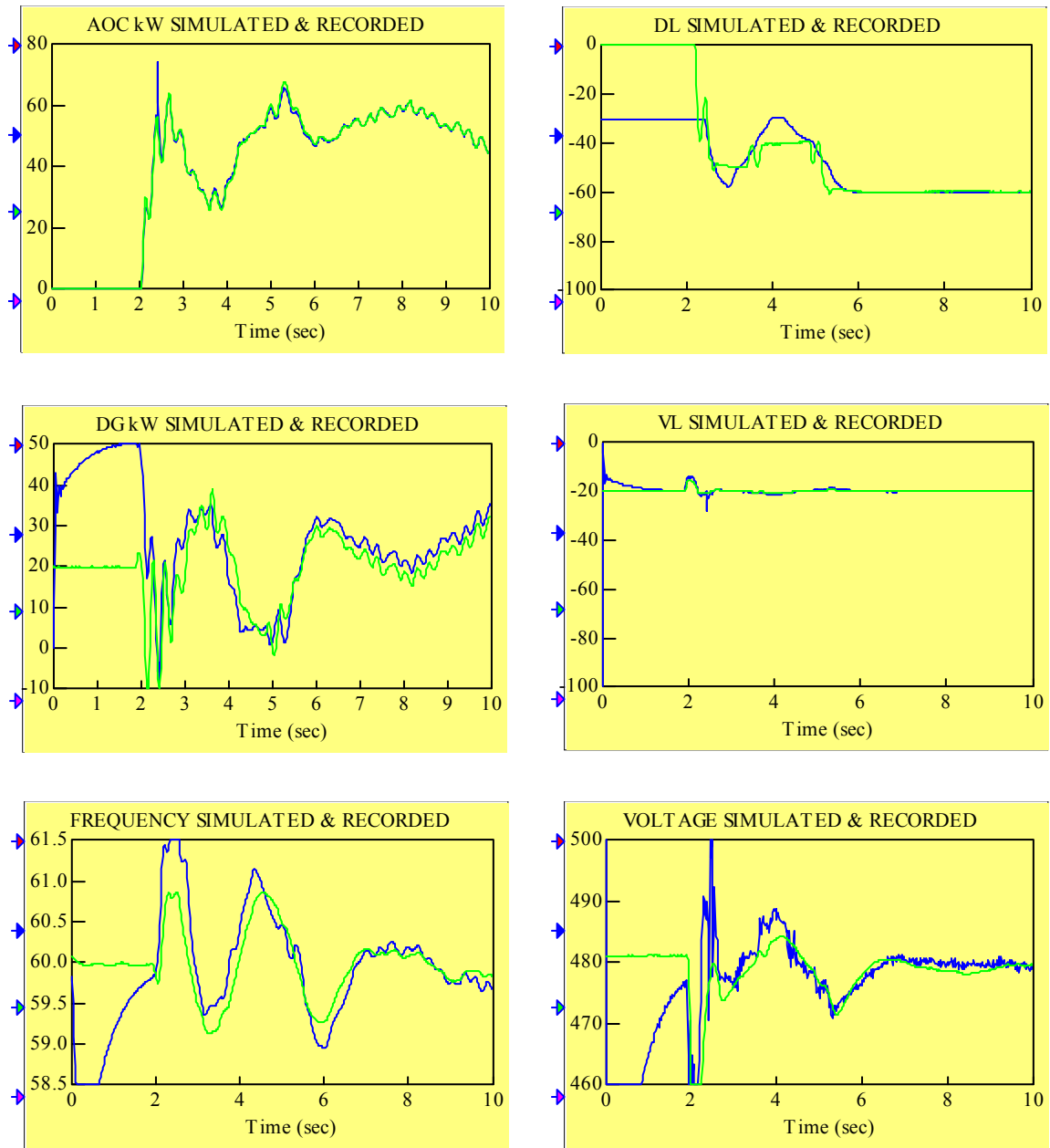


Figure 10.11 Simulation results for the AOC start-up data with a real dump load model included: the dark line is used for traces simulated and the light line is used for traces recorded

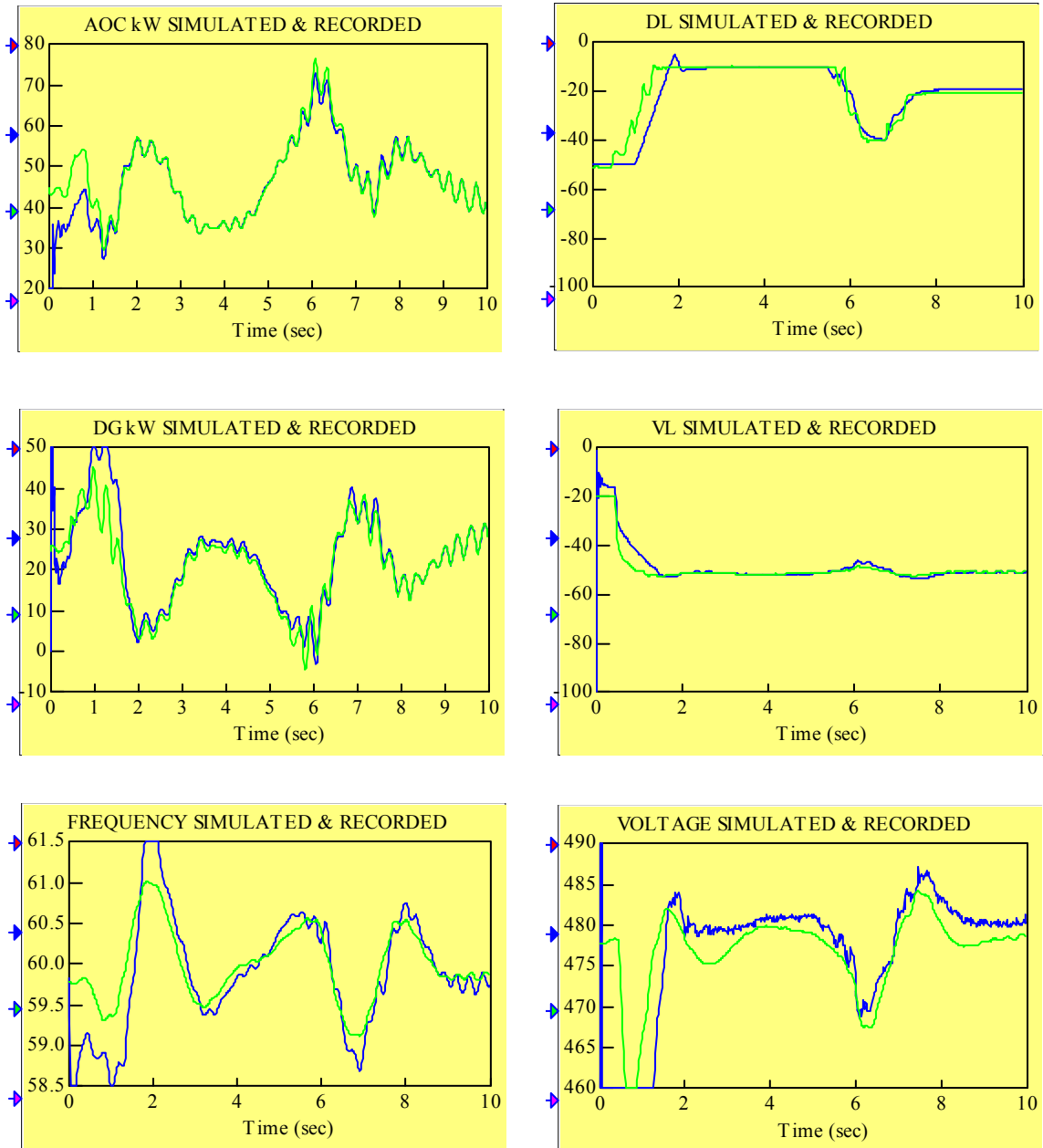


Figure 10.12 Simulation results for the step-in load data with a real dump load model included: the dark line is used for traces simulated and the light line is used for traces recorded

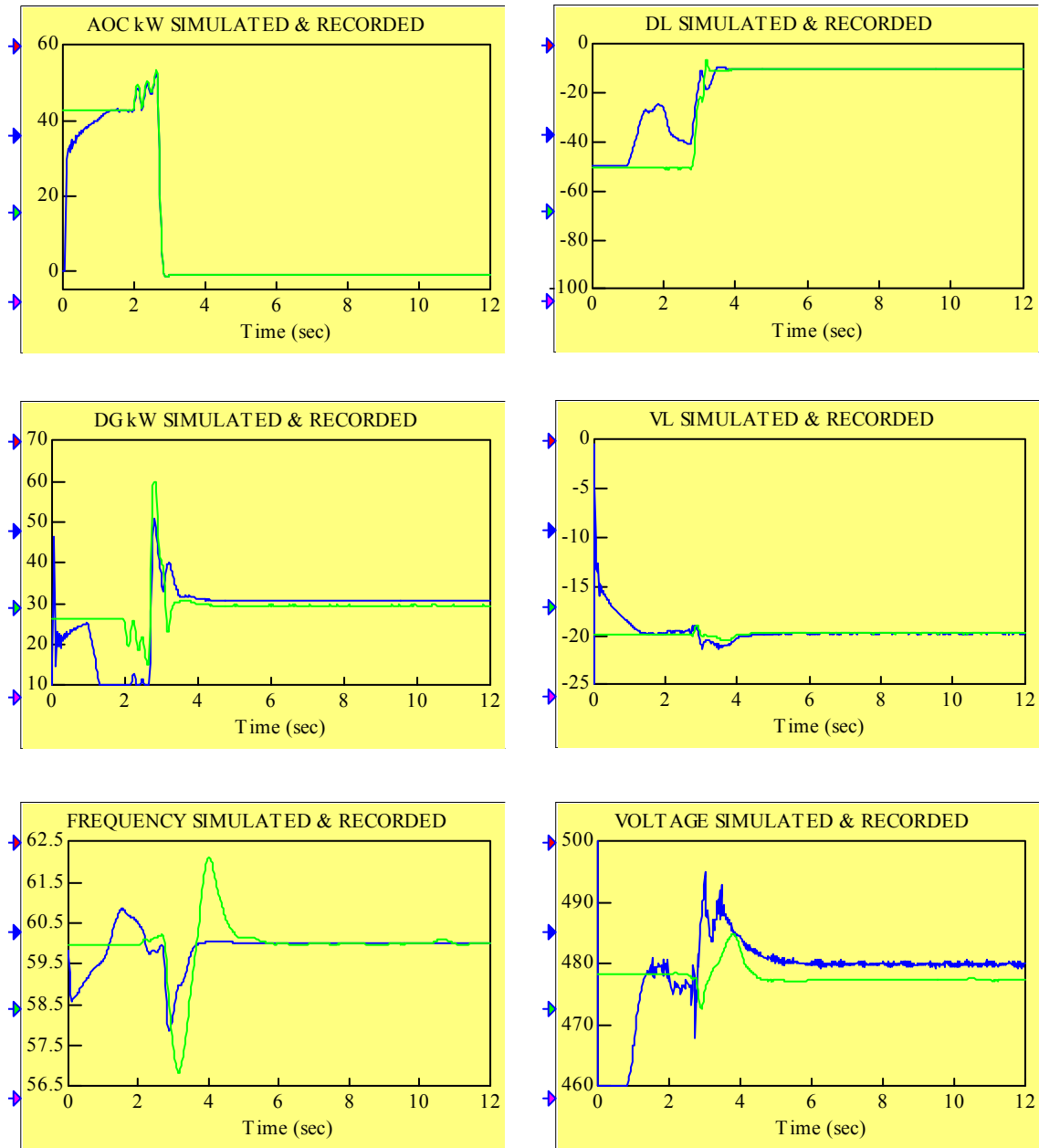


Figure 10.13 Simulation results for the AOC shutdown data with a real dump load model included: the dark line is used for traces simulated and the light line is used for traces recorded

Appendix 1

How to Set-up and Run the Simulation

To demonstrate a step-by-step procedure on how to setup and run the simulation, we use the Case Study 3 presented in Chapter 8. For the convenience of the user, we repeat here Figure 8.5 showing the configuration of the power system considered in a form of single-line diagram and top-view of the RPM-SIM simulation.

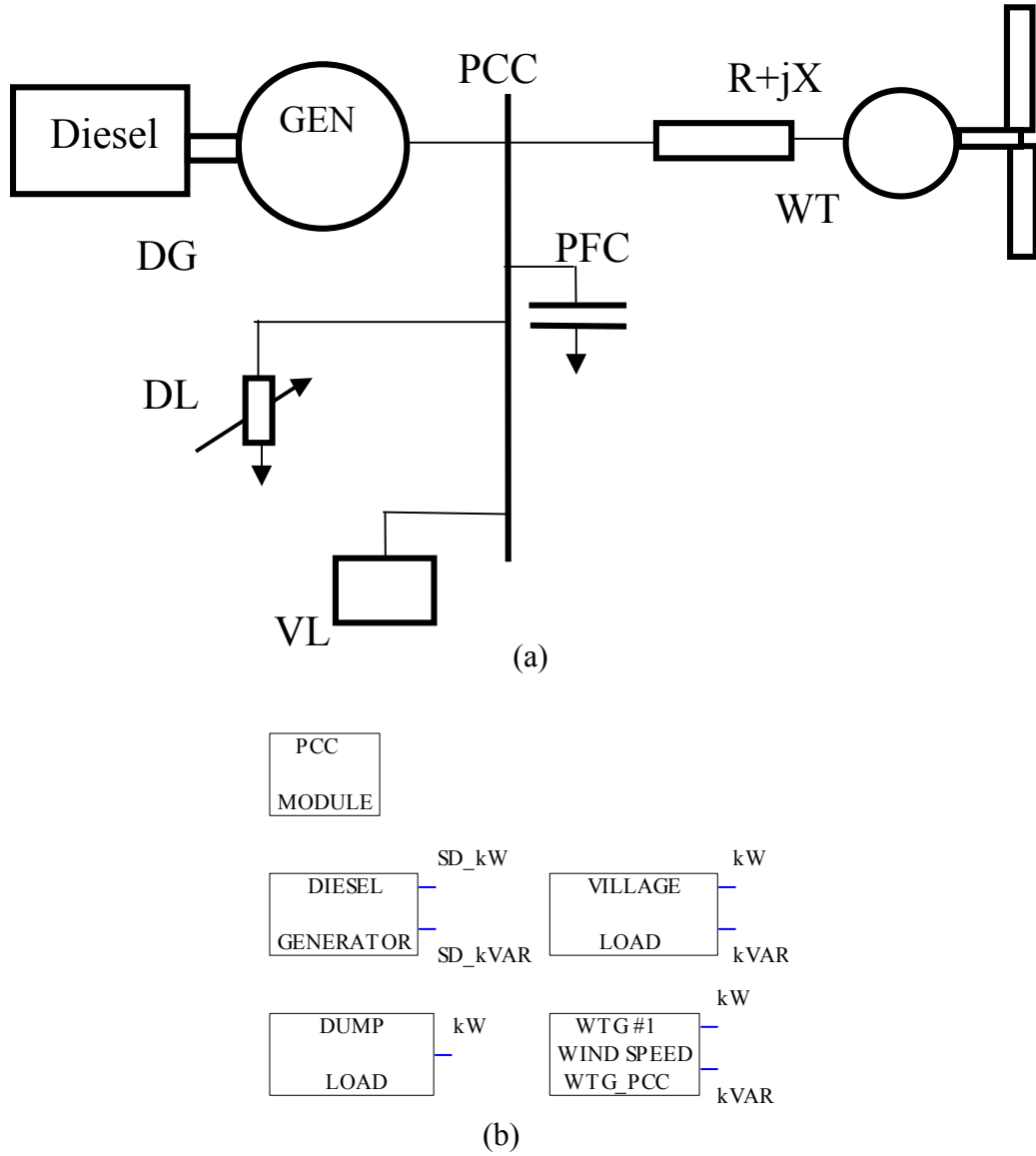


Figure 8.5 Power system composed of diesel generator (DG), AC wind turbine (WT), dump load (DL) and village load (VL): (a) single-line diagram and (b) top-view of the RPM-SIM simulation.

First, copy the directory RPMSim_DST from CD-ROM and paste it as a subdirectory of Vissim4 directory.

To setup the simulation you must do the following:

1. Click on the VisSim icon to obtain the simulation screen.
2. Use **Save As** command from the File menu to assign the file name and directory for your simulation.
3. Add RPM-SIM modules involved in the power system you would like to simulate. Recall that the PCC module must be included in every simulation diagram, and add this module first performing the following steps:
 - Click on **Add** command in the File menu to obtain Add File dialog box; select directory c:\Vissim4\RPMSim_DST, and the list of RPM-SIM files will appear. Find PCC.vsm file and double click on it.
 - You will see a green rectangle (with the cursor of the mouse attached) in the simulation screen. Click the mouse and the green rectangle will turn into a RPM-SIM block named PCC MODULE.
 - Recall the multilevel/compound block simulation concept of VisSim and explore the contents of this module. Click on the block with the right button of the mouse to see the top-view diagram of the PCC as shown in Figure 2.2. For the description and exploration of the compound blocks shown in this diagram, refer to Chapter 2.
 - The values of the parameters included in the PARAMETER MODULE block can be changed by opening this block (clicking the right button of the mouse on it) and clicking the right button on the parameter value. As a result of this action, the Setup Block dialog box opens and makes the change possible.
 - To move up one simulation level you point the mouse cursor to empty space in the simulation screen and click the right button.

Repeat the same steps for each module involved when adding their files to the simulation screen. For Case Study 3 you must add DG.vsm, VL.vsm, DL.vsm, and wtg_base.vsm. While moving up and down the simulation hierarchy of a particular module, refer to the proper chapter of this manual. This will help you to understand what you see, and you will find out which parameters can be changed to represent your system.

As a result of this step, you will see the simulation diagram shown in Figure 8.5(b). You can move any element of the simulation diagram or a selected group of elements by dragging it with the mouse.

4. To monitor your system variables of interest, you will use a VisSim display block (for numerical value) or plot block (to plot your variable as a function of time). Both are available with a click of the mouse in the VisSim menu Blocks\Signal Consumers. These monitor blocks can be directly connected with mouse to a particular variable on the simulation diagram. Alternatively, the variable to be monitored can be replicated (using the Variable block available in the VisSim menu

Blocks\Annotation, and setting its name as desired in the associated dialog box) and connected to the display or plot block. You can connect up to eight variables (VisSim 4.0) to a single plot block. The unused connectors of the plot block can be removed with the **Remove Connector** command in the Edit menu. Double clicking (on the plot block) with the left mouse button opens Plot Setup dialog box. The options available are self-explanatory. Consult the VisSim manual if needed.

Both the display block and the plot block can be added to any simulation level.

5. Open the Simulate menu and click on **Simulation Setup** command. The dialog box appears. Choose adaptive Bulirsh-Stoer integration algorithm to maintain stability. To specify a step size do the following:
 - (a) In the Step Size box under Range Control, enter the size that represents the maximum length of the interval. The practical value is 0.0001. If you make this value larger, the algorithm will attempt to use it. This will result in oscillations of your variables, which do not reflect the behavior of the real system (to see this effect try the value of 0.01). This effect is illustrated in Figure A1.1. It may even result in simulation instability leading to the over-flow error, and stop the simulation right after the start (to see this effect chose the value of 0.05).
 - (b) In the Min Step Size under Integration Algorithm menu, enter a size that represents the minimum length of the interval. The default value of 1e-006 is a good choice.

Setup the simulation range choosing the Range Start and Range End parameters.

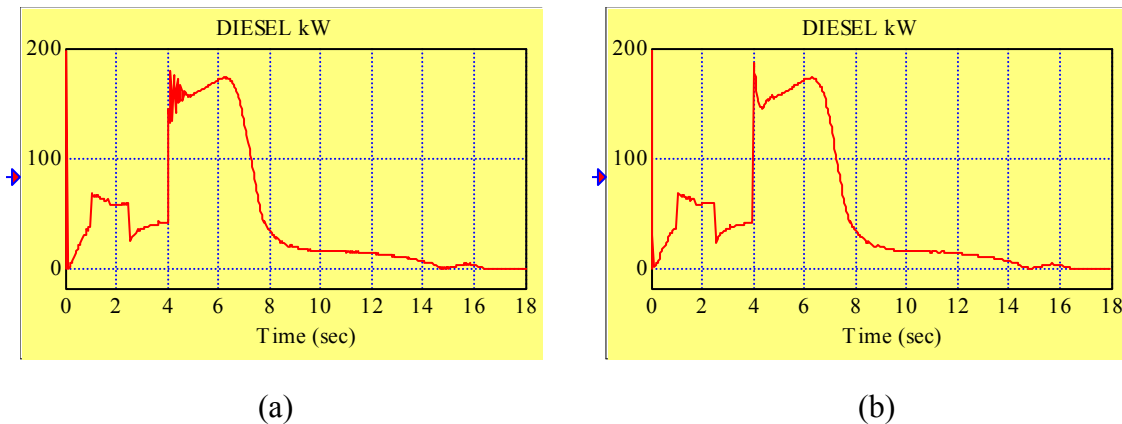


Figure A1.1 The effect of the maximum step size of integration interval: (a) visible oscillations for the maximum step size of 0.01, (b) smooth curve for the maximum step size of 0.0001

To control the simulation, i.e., to start, stop, and continue, you can use the commands from the Simulate menu or from the simulation Control Panel, or the pushbuttons from the toolbar. Consult the VisSim manual for more details.

Appendix 2

Synchronous Generator Model E7201L1 Data Sheet



GENERATOR DATA SHEET

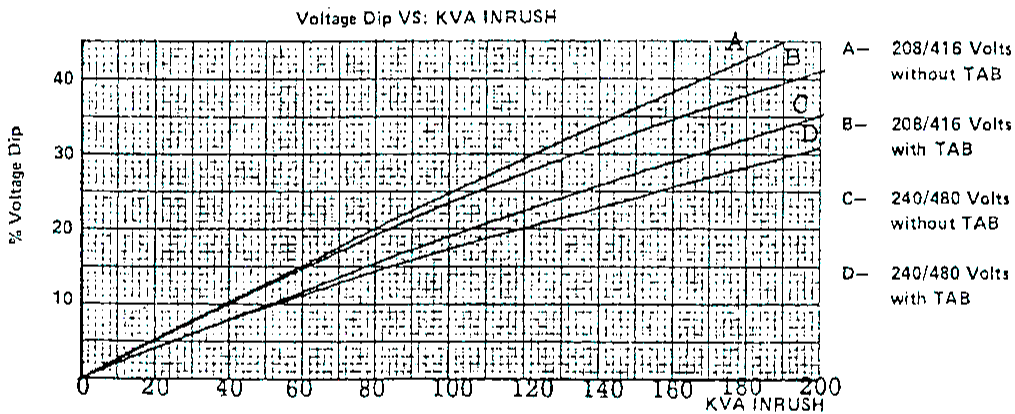
MODEL NUMBER

E7201L1

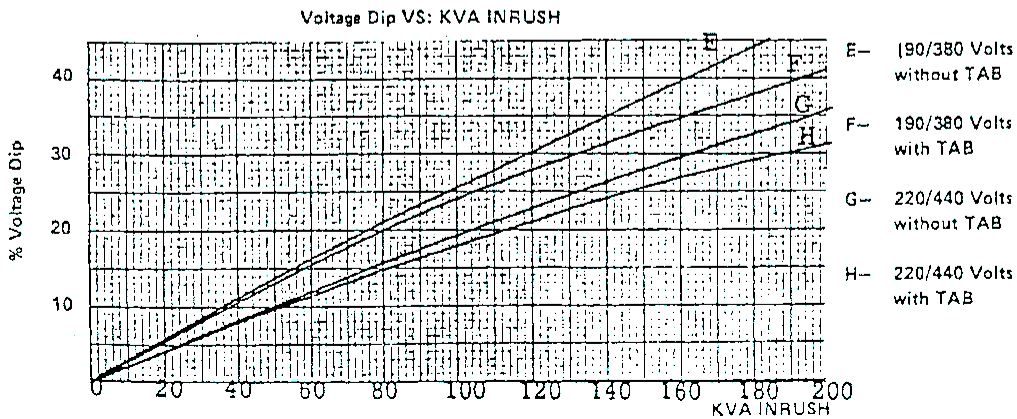
60 KW 208-240/416-480 Voltage 1800RPM, 60 Hz, 0.8 P.F.
 Amps 208-180/104-90 Weight 825
 40 °C Ambient, Dim Code Engine 4-53
 12 Leads

	Duty	HZ	KW	Voltage	NOMINAL EFFICIENCY			.8 P.F. FULL LOAD ON*
					Full Load	3/4 Load	1/2 Load	
NAME PLATE RATING	CONT	60	50	208/416	85.2	84.9	82.9	11.2
			50	240/480	85.7	85.0	82.4	8.4
	STAND BY	60	60	208/416	84.5	84.7	83.3	13.5
			60	240/480	85.3	85.1	83.1	10.1
MAXIMUM RATING PER NEMA MG 1 SPECIFICATIONS	CONT	60		208/416				
				230/460				
				240/480				
		50		190/380				
				200/400				
				220/440				
	STAND BY	60		208/416				
				230/460				
				240/480				
		50		190/380				
				200/400				
				220/440				

1800 RPM Motor Starting (Taken on Constant Speed Driver*)



1500 RPM Motor Starting (Taken on Constant Speed Driver*)



*Engine Droop will effect Voltage Dip

PERFORMANCE PARAMETERS
AT NAMEPLATE RATING
EXCEPT WHERE NOTED

DESCRIPTION	VOLTAGE	MAX. TOTAL (%)		MAX. INDIVIDUAL (%)	
		DELCO	NEMA	DELCO	NEMA
HARMONIC CONTENT No Load L-L	208/416		No Limit		No Limit
	240/480	1.71	No Limit	1.54	No Limit
WAVE FORM DEV. FACTOR No Load L-L	208/416		10 Max.		
	240/480	4.14	10 Max.		

TELEPHONE INFLUENCE
FACTOR-TIF 39.6

Symbol	Machine Constant @ 480 Volts	Value
X _d	Direct Axis Sync Reactance	1.81 P.U.
X' _d	Direct Axis Transient Reactance	.191 P.U.
X'' _d	Direct Axis Sub Trans. Reactance	.084 P.U.
X _q	Quadrature Axis Sync. Reactance	1.12 P.U.
X'' _q	Quadrature Axis Trans. Reactance	.238 P.U.
X _a	Zero Sequence Reactance	.040 P.U.
X ₂	Negative Sequence Reactance	.161 P.U.
T' _{do}	Open Circuit Time Constant	.967 Sec.
T' _d	Short Circuit Time Constant (Transient)	.061 Sec.
T'' _d	Short Circuit Time Constant (Sub Transient)	.018 Sec.
Z _d	Synchronous Impedance	1.81 P.U.

Resistances (Ω) at 25°C	
Exciter Fld	50.5
Exciter Arm	.43
Rotating Fld	2.98
Stator	.21

12 Volt Battery Test @ 1800 RPM	
Connected For	
Low Voltage	High Voltage
187	374

TAB Model #	H3801RCDA	
Resistor Setting	10 Ohms	
Tap Selection	4-9 & 10-3	
SHORT CIRCUIT DRIVE		
	208/240	416/480
Three Phase	636.8 Amps	318.4 Amps

EXCITATION REQUIREMENTS			
Load	Operating Voltage	Exciter Fld. Amp.	TAB Voltage
No Load	208/416	.242	-1.45
	240/480	.338	-1.5
Full Load	1.0 P.F. 208/416	.504	14.7
	240/480	.532	9.8
Load	.8 P.F. 208/416	.798	19.6
	240/480	.813	13.0

CFM Heat Rejection at Max. Nameplate Rating 37,563 BTU/Hr.
WR² Dwg # XB-203800-612
Outline Drawing # 2800795

A. C. GEN. DATA <i>E720111</i>				SER. NO.	
Type <i>NEMA</i>	KVA <i>75</i>	Volts <i>208 - 240</i> <i>416 - 480</i>	Amps. <i>208 - 180</i> <i>104 - 90</i>	Phase <i>3</i>	Cycles <i>60</i>
Frame <i>#2 B.H.</i>	Temp. - <i>AMB.</i> <i>40°C MAX.</i>	P.F. <i>80%</i>	Poles <i>4</i>	Duty <i>CONTINUOUS</i>	RPM. <i>1800</i>
Generator					
1	Direct Axis Synchronous Reactance (Unsaturated)			Xd	<i>1.81 PER UNIT</i>
2	Quadrature Axis Synchronous Reactance (Unsaturated)			Xq	<i>1.12 " "</i>
3	Direct Axis Transient Reactance (Rated Voltage)			X'd	<i>.191 " "</i>
4	Direct Axis Subtransient Reactance (Rated Voltage)			X''d	<i>.084 " "</i>
5	Quadrature Axis Subtransient Reactance			X''q	<i>.238 " "</i>
6	Zero Sequence Reactance			Xo	<i>.040 " "</i>
7	Negative Sequence Reactance			X2	<i>.161 " "</i>
8	Direct Axis Transient Open Circuit Time Constant			T'do	<i>.967 SECOND</i>
9	Short Circuit Transient Time Constant			T'd	<i>.061 " "</i>
10	Short Circuit Sub Transient Time Constant			T''d	<i>.018 " "</i>
11	Synchronous Impedance			Zs	<i>1.81 PER UNIT</i>
12					
13	Field Resistance @ 25° C				<i>2.98 OHMS</i>
14	Field Current @ F/L, Rated PF				<i>20.4 AMPS</i>
15	Field Current @ N/L, Rated Voltage				<i>8.0 " "</i>
16	Field Current @ N/L, 550 Volts				<i>13.2 " "</i>
17	Continuous Duty Field Voltage				<i>90.5 VOLTS</i>
18	Inherent Regulation				<i>26.0 %</i>
19	Recommended Field Discharge Resistor <i>N/A</i>				
20	Wave Form Deviation, No Load Line-Line		<i>4.14 %</i>	Line-Neutral	<i>2.13 %</i>
21	Wave Form Deviation, Full Load Line-Line		<i>3.06 %</i>	Line-Neutral	<i>2.73 %</i>
22					
23					
Exciter - Type <i>BRUSHLESS</i> Rpm <i>1800</i> Ser.#					
1	<i>2.5 KW</i>		<i>100</i> Volts	<i>25</i> Amp.	
2	Field Res. @ 25° C			<i>50.5</i> Ohms.	
3	Recommended Rheostat:		—	Plate(s)	Ohms. Amps.
4	Curve No. <i>C-6505-A</i>				

Appendix 3

Wales Control System Dump Load Dispatch at the HPTB

Wales Control System Dump Load Dispatch at the HPTB

I. DUMP LOAD HARDWARE

The dump load at the HPTB can be modelled as (20) 10-kW elements.

II. DIESEL ON DUMP LOAD DISPATCH

A. Purpose: If there is at least 1 diesel on-line, the diesel generator's own controls (speed control and voltage regulator) control system frequency and voltage. The Wales Control System PLC will dispatch dump load elements in order to maintain a minimum load on the diesels.

B. Method: The Wales Control System dispatches dump load elements to maintain instantaneous diesel load values (as read by the PLC every scan) within a certain range defined by maximum and minimum diesel load values. The algorithm uses a modified PID loop to determine the dump load kW required, subtracts the dump load kW currently on to determine the delta dump load kW required, and divides this value by the dump load step size and rounds to determine the number of dump load elements to add or remove. There are several modifications to a standard PID loop: 1) instead of trying to maintain the process value (diesel load) around one setpoint value, we are trying to maintain the process value between an upper and lower setpoint (max and min diesel load values), so the actual setpoint used to calculate the loop error term depends on whether the process value is greater than the upper setpoint, less than the lower setpoint, or in between; 2) the proportional and derivative terms are combined into one by using a predicted error term; and 3) the derivative term is modified in two ways: a) since there is a large deadband during which the error equals zero, the derivative term is based on the derivative of the process value rather than the derivative of the error term (we can do this because the setpoints are constant), and b) the derivative term is also based on a 310 ms interval rather than the PID loop sample rate to account for the 3-per ripple imposed on the diesel kW values by a 3-bladed turbine. The PID Loop algorithm is defined below.

PID Loop Algorithm:

$$M_j = K_c \times PE_j + K_c \times \frac{T_s}{T_i} \times ES_{j-1}$$

M_j = Control Output (Dump Load Required) [kW] for sampling period j

PE_j = Predicted Error [kW] for sampling period j

E_j = Error [kW] for sampling period j

ES_j = Error Sum [kW] for sampling period (See below) j

K_c = Proportional Gain: 1.50

T_s = Sampling Interval: 40 ms

T_i = Integral Time: 80 ms

Limit Control Output if it goes out of bounds:

$$\begin{aligned}M_j &= M_j \text{ if } 0 < M_j < M_{\max} \\ &= 0 \text{ if } M_j \leq 0 \\ &= M_{\max} \text{ if } M_j \geq M_{\max}\end{aligned}$$

M_{\max} = Maximum Control Output Allowed (Total DL kW Available): 200 kW

Error Term Definition:

$$\begin{aligned}E_j &= SP_L - PV_j \text{ if } PV_j \leq SP_L \\ &= SP_H - PV_j \text{ if } PV_j \geq SP_H \\ &= 0 \text{ if } SP_L < PV_j < SP_H\end{aligned}$$

PV_j = Process Value (Diesel Load) [kW] for sampling period j

SP_L = Lower Setpoint (Minimum Diesel Load) [kW]

= 10% of current diesel capacity on line

SP_H = Upper Setpoint (Maximum Diesel Load) [kW]

= 50% of current diesel capacity on line OR 34 kW, whichever is greater

Predicted Error Term Definition:

$$\begin{aligned}PE_j &= SP_L - PPV_j \text{ if } PPV_j \leq SP_L \\ &= SP_H - PPV_j \text{ if } PPV_j \geq SP_H \\ &= 0 \text{ if } SP_L < PPV_j < SP_H \\ PPV_j &= PV_j + K_r \times \left[\frac{PV_j - PV_{j-310ms}}{T_d} \right] \times T_s\end{aligned}$$

PPV_j = Predicted Process Value (Predicted Dsl Load) [kW] for sampling period j

$PV_{j-310ms}$ = Process Value (Predicted Dsl Load) [kW] 310 ms BEFORE time of sampling period j

T_d = Derivative Period: 310 ms

K_r = Derivative Gain: 2.00

Error Sum Definition:

Freeze Error Sum if last Control Output (before limiting) was out of bounds:

$$\begin{aligned}ES_j &= ES_{j-1} + E_j \text{ if } 0 < M_j < M_{\max} \\ &= ES_{j-1} + \text{MAX}(E_j, 0) \text{ if } M_j \leq 0 \\ &= ES_{j-1} + \text{MIN}(E_j, 0) \text{ if } M_j \geq M_{\max}\end{aligned}$$

Appendix 4

Documentation for RPM-SIM on CD-ROM

Documentation for RPM-SIM

developed at the NREL's National Wind Technology Center

This CD-ROM contains two directories and this 'readme.wri' file. Its structure is shown in Figure A4.1.

Directory RPMSim_DST has the following simulator modules/components:

BB_RC.vsm
DG.vsm
DL.vsm
PCC.vsm
VL.vsm
WIND_SPEED.vsm
WTG.vsm
wtg_base.vsm

Directory RPMSim_LIB has the structure shown in Figure A4.2 and contains the following subdirectories:

- C_stds

contains executable VisSim files for all case studies presented in the manual. The file names used are self-explanatory. These are the following files:

C_Sn.vsm with $n=1,2,\dots,7$
C_S8_rc_HPTB_AOC_Mode1.vsm
C_S8_rc_HPTB_AOC_Mode2.vsm
C_S8_rc_HPTB_AOC_Mode3.vsm

- Comp_Valid

contains executable VisSim files for all component validations described in the manual. They were used to obtain characteristics presented in the manual and their names contain the acronym of the particular RPM-SIM module or component and refer to the number of the figure. Thus the file names are self-explanatory. These are the following files:

DC_FIG9_15&16.vsm
DC_FIG9_17.vsm
DC_FIG9_18.vsm
DG_FIG9_2.vsm
DG_FIG9_3.vsm

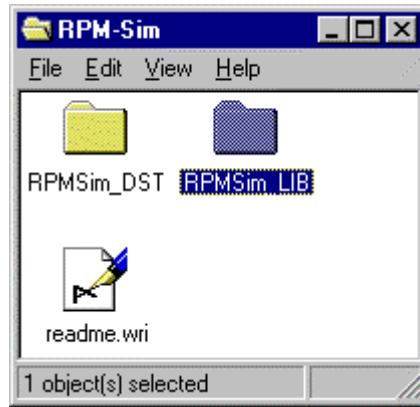


Figure A4.1 Structure of the documentation for RPM-SIM

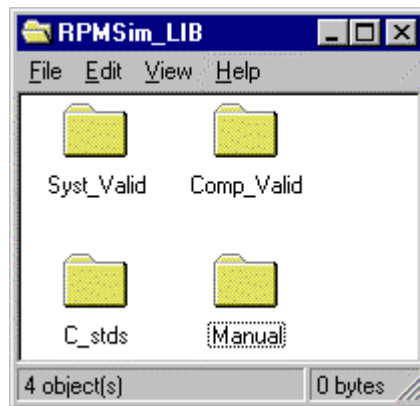


Figure A4.2 Subdirectories of the directory RPMSim_LIB

IG_FIG9_22&23.vsm
RC_FIG9_25&27.vsm
RC_FIG9_26&28.vsm
SC_FIG9_11&12.vsm
SC_FIG9_13.vsm
SG_FIG9_19&20.vsm
WTG_FIG9_5.vsm
WTG_FIG9_9.vsm

- Syst_Valid

contains executable VisSim files for system validations described in the manual. These are the following files:

hybrid_casea.vsm	used to obtain Figure 10.3
hybrid_caseb.vsm	used to obtain Figure 10.4
hybrid_stup.vsm	used to obtain Figure 10.5
hybrid_stld.vsm	used to obtain Figure 10.6
hybrid_s-shd.vsm	used to obtain Figure 10.7
dl_casea_mod.vsm	used to obtain Figure 10.10
dl_stup_mod.vsm	used to obtain Figure 10.11
dl_stld_mod.vsm	used to obtain Figure 10.12
dl_shd_mod.vsm	used to obtain Figure 10.13

- Manual

contains the RPM-SIM manual in a form of Microsoft Word files.

NOTE :

All executable files are ready to run under Professional VisSim 4.0 available from Visual Solutions, Inc., 487 Groton Road, Westford, MA 01886, phone 978 392 0100, fax 978 692 3102. Web site www.vissim.com.

REPORT DOCUMENTATION PAGE			Form Approved OMB NO. 0704-0188	
Public reporting burden for this collection of information is estimated to average 1 hour per response, including the time for reviewing instructions, searching existing data sources, gathering and maintaining the data needed, and completing and reviewing the collection of information. Send comments regarding this burden estimate or any other aspect of this collection of information, including suggestions for reducing this burden, to Washington Headquarters Services, Directorate for Information Operations and Reports, 1215 Jefferson Davis Highway, Suite 1204, Arlington, VA 22202-4302, and to the Office of Management and Budget, Paperwork Reduction Project (0704-0188), Washington, DC 20503.				
1. AGENCY USE ONLY (Leave blank)	2. REPORT DATE October 1999	3. REPORT TYPE AND DATES COVERED Technical Report		
4. TITLE AND SUBTITLE Renewable Energy Power System Modular Simulator			5. FUNDING NUMBERS WE001710	
6. AUTHOR(S) Jan T. Bialasiewicz, Eduard Muljadi, R. Gerald Nix, Stephen Drouilhet				
7. PERFORMING ORGANIZATION NAME(S) AND ADDRESS(ES) National Renewable Energy Laboratory 1617 Cole Boulevard Golden, Colorado 80401-3393			8. PERFORMING ORGANIZATION REPORT NUMBER TP-500-25951	
9. SPONSORING/MONITORING AGENCY NAME(S) AND ADDRESS(ES) U.S. Department of Energy 1000 Independence Ave. Washington, D.C. 20585			10. SPONSORING/MONITORING AGENCY REPORT NUMBER	
11. SUPPLEMENTARY NOTES				
12a. DISTRIBUTION/AVAILABILITY STATEMENT National Technical Information Service U.S. Department of Commerce 5285 Port Royal Road Springfield, VA 22161			12b. DISTRIBUTION CODE	
13. ABSTRACT (Maximum 200 words) Using the VisSim™ visual environment, researchers developed a modular simulation system to facilitate an application-specific, low-cost study of the system dynamics for wind-diesel hybrid power systems. This manual presents the principal modules of the simulator and, using case studies of a hybrid system, demonstrates some of the benefits that can be gained from understanding the effects of the designer's modifications to these complex dynamic systems.				
14. SUBJECT TERMS			15. NUMBER OF PAGES	
			16. PRICE CODE	
17. SECURITY CLASSIFICATION OF REPORT	18. SECURITY CLASSIFICATION OF THIS PAGE	19. SECURITY CLASSIFICATION OF ABSTRACT	20. LIMITATION OF ABSTRACT	